+

ADDIS ABABA UNIVERSITY

SCHOOL OF GRADUATE STUDIES

ADDIS ABABA INSTITUTE OF TECHNOLOGY (AAiT)

ELECTRICAL AND COMPUTER ENGINEERING DEPARTMENT

Analysis and Evaluation of Diversity-Multiplexing Tradeoff for Multiple-Antenna systems in Ultra Wideband (UWB-MAS) and Rake Receiver

By

Gebremariam Hailu

Advisor

Dr.-Ing Getahun Mokuria

A Thesis Submitted to the School of Graduate Studies of Addis Ababa University in Partial Fulfillment of the Requirements for the Degree of Masters of Science in Electrical Engineering

July, 2012

Addis Ababa, Ethiopia

ADDIS ABABA UNIVERSITY

SCHOOL OF GRADUATE STUDIES

ADDIS ABABA INSTITUTE OF TECHNOLOGY (AAiT)

ELECTRICAL AND COMPUTER ENGINEERING DEPARTMENT

Analysis and Evaluation of Diversity-Multiplexing Tradeoff for Multiple-Antenna systems in Ultra Wideband (UWB-MAS) and Rake Receiver

Gebremariam Hailu

Approval by Board of Examiners

_____ _____

Chairman, Dept. Graduate Committee — Signature

Dr.-Ing Getahun Mokuria _____

Advisor — Signature

_____ _____

Internal Examiner — Signature

_____ _____

External Examiner — Signature

Declaration

I, the undersigned, declare that this thesis is my original work, has not been presented for adegree in this or any other university, and all sources of materials used for the thesis have been fully acknowledged.

Gebremariam Hailu _____

Name Signature

Place: Addis Ababa

Date of Submission: July 2012

This thesis has been submitted for examination with my approval as a university advisor.

Dr.-Ing Getahun Mokuria _____

Advisor's Name Signature

Analysis and Evaluation of Diversity-Multiplexing Tradeoff for Multiple-Antenna systems in Ultra Wideband (UWB-MAS) and Rake Receiver

Gebremariam Hailu

Addis Ababa Institute of Technology (AAiT)

July 2012

Abstract

Ultra wide-band (UWB) systems have recently attracted much research interest owing to their appealing features in short-range wireless communications. These features include high data rates, low power consumption, multiple access communications, and precise positioning capabilities.On the other hand, multiple antenna systems (MAS) and space-time coding (STC) techniques, such as space time block coding (STBC) are well known for their great potential to play a significant role in the design of the next-generation broadband wireless communications. Multiple-Input Multiple-Output (MIMO) system extends the link reliability (spatial diversity (SD)) and increase throughput,(spatial multiplexing (SM)).However, there is a fundamental tradeoff(DMT) between how much of each type of gain in any coding scheme can extract.

In this thesis the approach for multi-antenna system is to obtain tradeoff between SD and SM gains for UWB technology. Atheoretical analysis is conducted to enlighten the DMTfor UWB-MAS (UWB-MISO/SIMO) and therefore; performance enhancements provided by the proposed scheme compared to the classic single link scheme is evaluatedat finite signal-to-noise ratios (SNRs).The tradeoff curves provide a characterization of achievable SD and SM for a given space-time code at SNR's encountered in practice. A Rake receiver is employed that captures energy from sequences transmitted from N transmit antennas at M receive antennas in a subset of the resolvable multipath components. Exact diversity gain expressions are determined for orthogonal space–time block codes (OSTBC). It is shown that the asymptotical diversity gain has an infinite valueeven with single-antenna systems and the multi-antenna techniques can be very beneficial in the practical range of signal-to-noise ratios. Comparisons are also provided with DMT results in the literature and found thatcodes that are not optimal over the Rayleigh fading channels are also not optimal over the UWB channels.

Key words: DM, DMT, Finite signal-to-noise ratio (SNR), MAS, OSTBC, outage probability, SM, UWB.

Acknowledgments

I would like to first and foremost express my gratitude to my supervisor, Dr:-Ing Getahun Mokuria for giving me the opportunity to be astudent in his department. I am thankful to him for providing meguidance, encouragement and constructive feedback in my work. His direction and suggestions have been instrumental in the completion of this thesis.

I would also like to thank to the late Dr:-Ing Hailu Ayele, His direction and supervision were invaluable to the success of this work. May his soul rest in peace.

Finally, I would like to thank all classmates at the department for making anice and friendly atmosphere. My heartfelt thanks also expressed to all my friends for their priceless help.

Contents

List of figures

List of Tables

List of Acronyms

AWGN	additive white Gaussian noise
BPAM	binary pulse amplitude modulation
BPSK	Binary Phase Shift Key
BW	Bandwidth
cdf	cumulative density function
CM1~ CM4	standard UWB channel
CIR	channel impulse response
CSI	channel state information
dB	Deci Bell
DMT	Diversity –Multiplexing gains tradeoff
DS	direct sequence
EGC	Equal Gain Combining
FCC	Federal commission for communication
IEEE	Institute of Electrical and Electronics Engineers
EIRP	equivalent isotropically radiated power
FFT	fast Fourier transform
IFFT	inverse fast Fourier transform
IR	impulse radio
IFI	inter frame interference
ISI	Intersymbol interference
LOS	line-of-sight
LST	Layered Space Time
MAI	multiple access interference
MB	Multiband
MISO	multiple-input single-output
MIMO	multiple-input multiple-output
ML	maximum likelihood
MPC	multipath components
MRC	maximum ratio combiner,
MUI	multiuser interference
NBI	narrow band interference

NLOS	non-line-of-sight
OFDM	orthogonal frequency-division multiplexing
OOk	On Off keying
OSTBC	orthogonal space time coding
PAM	pulse-amplitude modulation
Pdf	probability density function
PPM	pulse position modulation
PR	Pseudo Random sequence
PN	Pseudo Random
PSD	power spectral density
RF	radio frequency
ROD	real orthogonal design
SD	Spatial Diversity
SIMO	single-input multiple-output
SISO	single-input single-output
SM	spatial multiplexing
SNR	signal-to-noise (power) ratio
SS	spread spectrum
STC	space –time coding
S-V	Saleh – Valenzuela
TDL	tapped delay line
TH	time hopping
UWB	ultra wideband
VBLAST	vertical Bell Laboratory layered space – time
WLAN	wireless local area network
WPAN	wireless personal area network
WUSB	Wireless universal serial bus
ZF	zero-forcing

Chapter 1

Introduction

High data-rate wireless communications, nearing 1Gb/s transmission rates, are of interest in emerging wireless local area networks (WLANs) and in home audio/video network applications [8, 9, 13]. People will be sharing photos, video, data and voice among networked consumer electronics throughout their digital homes and offices. Network technologies should meet the needs of wireless connectivity among these devices that require high bandwidth for connection and media exchange. This introduces an urgent need of a new wireless technology that is able to support multiple high data rate streams, consume very low power, and maintain low implementation cost. Ultra-wideband (UWB) is one of the emerging technologies that can fulfill these requirements. The enormous bandwidths available, the potential for high data rate, and the potential for very low cost operation makes UWB technology a viable candidate for current and future wireless applications. But to reach the target of high data rate such as 1Gb/s, more advanced techniques should be used. The combination of ultra-wideband (UWB) spectrum with Multiple-Input Multiple-Output (MIMO) system techniques show great promise for developing very high bandwidth wireless networks suchas wirelesspersonal area networks (WPANs). Nevertheless, to realize these expectations, UWB research and development has to cope with several design challenges that limit the performance and coverage range of UWB systems.

In this chapter, we first present an introduction of UWB and explain why UWB is considered as an emerging technology for short-range wireless communications. The general Overview for UWB is presented. The advantages, the applications as well as the challenges of UWB technology are discussed. Then, we provide objectives, problem statement as well as literature review. Finally, the outline of the thesis is given and the contents of each chapter are presented.

1.1Overview of UWB

The term Ultra Wideband (UWB) usually refers to signals or systems that both have a large relative or absolute bandwidth. The enormous bandwidths available, the wide scope of the data rate /range tradeoff, and the potential for very low-cost operation which couldlead to large-scale usage, are all present unique opportunity for UWB to impact the way people interact with communications systems [3, 4, 5].

The concept of UWB was developed in the early 1960s through research in time-domain electromagnetics where impulse measurement techniques were used to characterize the transient behavior of a certain class of microwave networks [1]. In the late 1960s, the impulse measurement techniques were applied to the design of wideband antenna elements, leading to the development of short pulse radar and communications systems. Through the late 1980s, UWB was referred to as baseband, carrier-free, or impulse technology. The term ultra-wideband was first started to be used in approximately 1989 by the US Department of Defense. By 1989, UWB theory, techniques and many implementation approaches had been developed for a wide range of applications such as radar, communications, automobile collision avoidance, positioning systems, etc. However, much of the early work in the UWB field occurred in the military funded by the US Government under classified programs, in late 1990s. For further interesting and informative review of UWB history, the interested reader is referred to [1, 3].

A dramatic change in the study happened in 2002, when the US FCC issued the regulation on the spectral mask of UWB radios rulings that provided the first radiation limitations for UWB transmission, and also permitted the operation of UWB devices on an unlicensed basis [2]. According to the FCC rulings, UWB is defined as any transmission scheme that occupies a fractional bandwidth of greater than 0 .2, or a signal bandwidth of more than 500 MHz.The fractional bandwidth a UWB transmission system, by definition is [3, 5, 10, 20]

$$B_f = 2\frac{f_H - f_L}{f_H + f_L} \quad (1.1)$$

Where; f_H=the highest -10 dB frequency point of the signal spectrum

f_L=The lowest -10 dB frequency point of the signal spectrum

UWB systems with $f_c = \frac{f_H + f_L}{2}$ >2.5GHz need to have a -10 dB bandwidth of at least 500 MHz, whereas UWB systems with fc < 2 .5GHz need to have fractional bandwidth of at least 0.2. The US FCC has mandated UWB radio transmission can legally operate in the range from 3.1 GHz to 10.6 GHz, with the power spectral density (PSD) satisfied a specific spectral mask assigned by the US FCC as shown in fig.1.1.

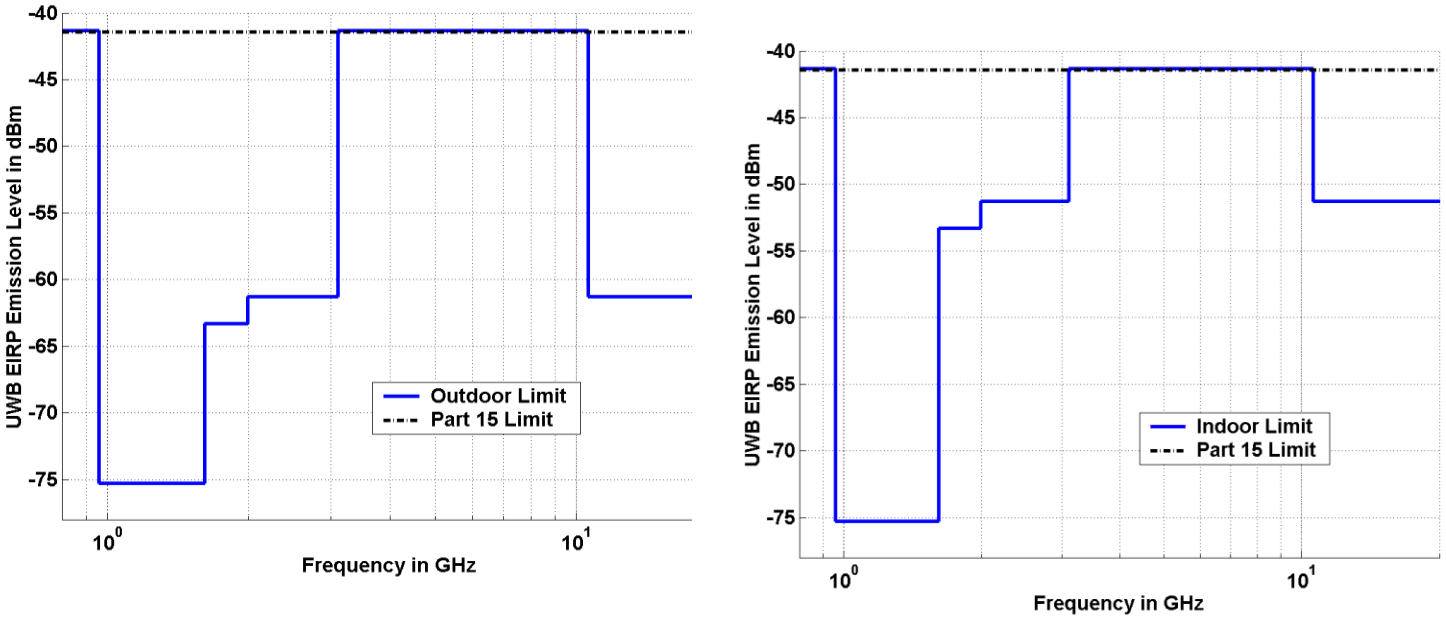

Fig.1.1 UWB spectral mask for outdoor and indoor communication systems

According to the spectral mask, the PSD of UWB signal measured in 1 MHz bandwidth must not exceed -41.3dBm, which complies with the FCC of US Part 15 general emission limits to successfully control radio interference.As depicted in Fig.1.2, such ruling allows the UWB devices to overlay existing narrowband systems, while ensuring sufficient attenuation to limit adjacent channel interference.

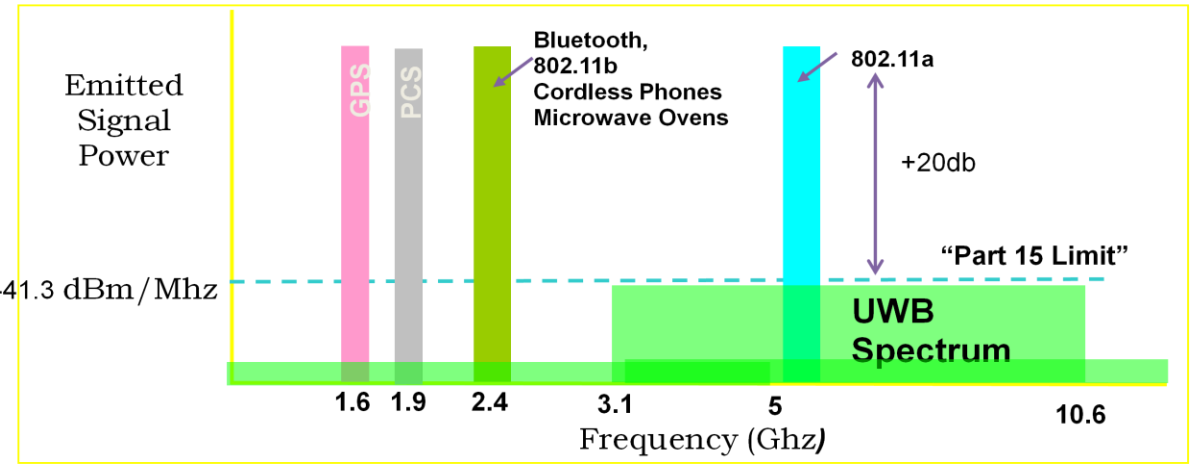

Fig.1.2 Spectrum of UWB and existing narrowband systems

1.1.1 Advantages and benefits of UWB

Due to the ultra wideband nature, UWB radios come with unique advantages and benefits overnarrowband technologies and are tabulated below [5].

Table 1.1 Advantages and benefits of UWB communication

Advantage	Benefits
Coexistence with current narrowband and wideband radio services	Avoids expensive licensing fees
Huge data rate	High bandwidth can support real-time high definition video streaming
Low transmit power	Provides low probability of detection and intercept.
Resistance to jamming	Reliable to hostile environments
High performance in multipath channel	Delivers higher signal strengths in adverse conditions
Simple transceiver architecture	Enables ultra-low power, smaller form factor at a reduced cost

The extremely large bandwidth occupied by UWB gives the potential of very high theoretical capacity, yielding very high data rates. This can be seen by considering Shannon's capacity equation [5, 7]. Shannon's capacity limit equation shows capacity increasing as a function of bandwidth(Bw) faster than as a function of SNR (signal to noise ratio).

$$\mathrm{C} = Bw * \log_2(1 + \mathrm{SNR}) \tag{1.1}$$

Where; C = Channel Capacity (bits/sec) $SNR = P/N0$

Bw = Channel Bandwidth (Hz) P = Received Signal Power (watts)

SNR = Signal to noise ratio. $N0$= noise power

The above Shannon's equation illustrates that increasing channel capacity requires a linear increase in bandwidth while similar channel capacity increases would require exponential

increases in power. This is why UWB technology is capable of transmitting very high data rates using very low power. It is important to notice that UWB can provide dramatic channel capacity only at limited range as shown in Fig.1.3.

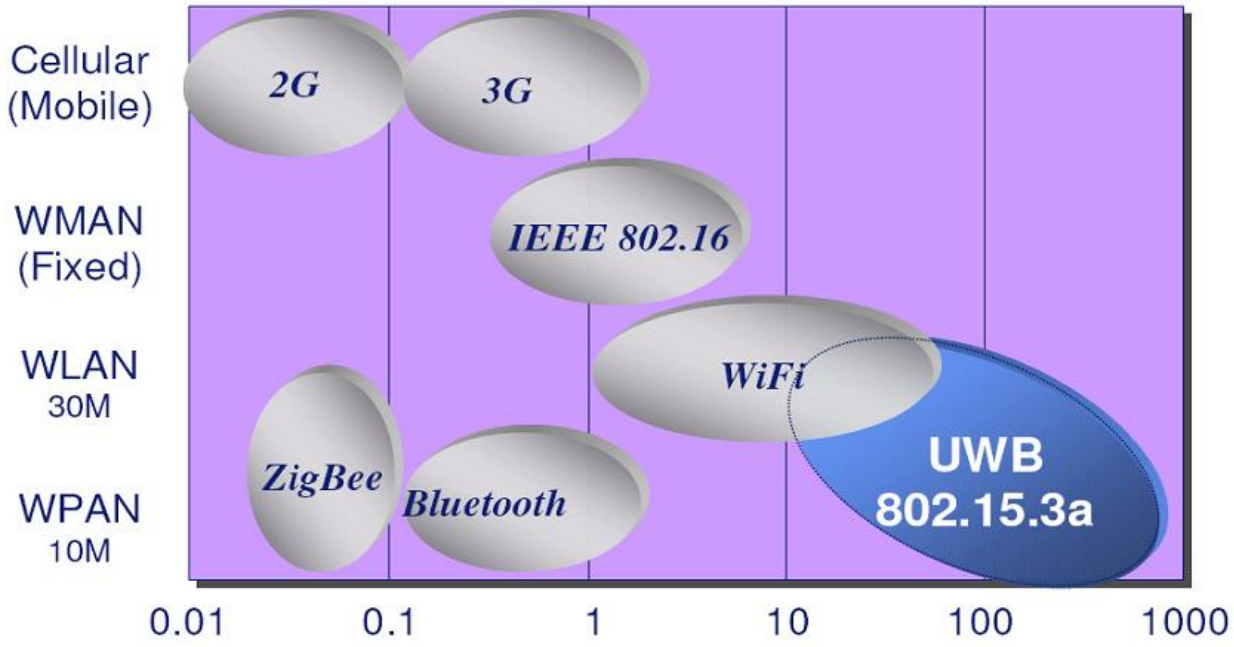

Fig.1.3 Range Vs Data rate (Source WiMedia)

The ultra-short duration of UWB waveforms gives rise to a fine resolution of reflected pulses at the receiver and resolves many paths.Therefore it is rich in multipath diversity.

1.1.2 UWB application

For wireless communications the use of UWB technology under the FCC of U.S.A guidelines [2] offers significant potential for the deployment of two basic communications systems [4, 5, 17]:

- High-data-rate short-range communications: high-data-rate wireless personal area networks
- Low-data-rate and location tracking: sensor, and positioning identification networks.

UWB enables various WPAN applications, such as high-speed wireless universal serial bus (WUSB) connectivity for personal computers (PCs) and PC peripherals, high-quality real-time video and audio transmission, file exchange among storage systems, and cable replacement for home entertainment systems.

Recently, IEEE 802.15.3 standard task group has established the 802.15.3a study group [6] to define physical layer concept for high-data-rate applications for indoor WPAN transmissions. The effort for the IEEE 802.15.3a standard is to provide a higher-speed physical layer standardizedchannel model for applications that involve imaging and multimedia.

IEEE also established 802.15.4 study group to define a physical layer concept for low-data-rate applications utilizing UWB technology. The study group addressed new applications which require only moderate data throughput but long battery life, such as low-rate wireless personal area networks, sensors, and small networks [3].

1.1.3 Challenges of UWB

While UWB has many reasons to make it an exciting and useful technology for future wireless communications and many other applications, it also has some challenges which must be overcome for it to become a popular and ubiquitous technology such as multi-access code design, multiple access interference (MAI) cancellation, narrowband interference (NBI) detection and cancellation, synchronization of the receiver to extremely narrow pulses, low-power transceiver design [3, 4, 5, 17].

1.2 Problem Statement

UWB provides great potential for increasing data transmission rates according to the Shannon theorem. However, owing to the strict power regulations imposed by the regulatory bodies the power spectral density of the transmitted UWB signal is rather strictly limited. All applications within spread the necessary energy over a wide frequency range to radiate below the limit. This poses significant design challenges for any UWB systems such as limiting data transmission rates and complicating the design and implementation of UWB receiver.Currently, the coverage of UWB-IR Physical Layer is designed to provide data rates of about 110 Mbps, 200 Mbps and (optionally) 480 Mbps at 20mt, 10mt and 2-3mt, respectively [31]. Such small coverage may be inadequate for some indoor applications. To fully exploit the benefits of UWB technology, it is therefore significantly necessary to develop efficient techniques such as space time codingfounded on introducing joint processing in time as well as in space via the use of multiple spatially distributed antennas.

The usage of multiple antennas is an important option in order to cope with the challenging power restriction and enables features like exploitation of spatial diversity, beam forming, and

spatial multiplexing.Aconsiderable number of multi antenna coding methods have been proposed, for example, in [22-29]. Space–time-coded systems such as space time block coding (STBC)are well known for their effectiveness at improving system performance under multipath fading scenarios[26, 28, 29].Naturally, the rich scattering multipath channel in UWB indoor environment provides an ideal transmission scenario for multi antenna systems (MAS) implementation. In addition, the GHz center frequency of UWB radio relaxes the requirements on the spacing between antenna array elements. Consequently, the combination of UWB and MIMO technology will become a viable and cost efficient method to achieve the very high data rate requirement for future short range wireless applications.

MIMO system can generallyoffer two types of gains: spatial diversity gain and spatial multiplexing gain. One may focus on designing schemes to extract either maximal diversity gain or maximal spatial multiplexing gain. However, maximizing one type of gain may not necessarily maximize the other. This makes it difficult to compare the performance between diversity-based and multiplexing-based schemes. Given a MIMO channel, both gains can in fact be simultaneously obtained, but there is a fundamental tradeoff between how much of each type of gain any coding scheme can extract. The Diversity-Multiplexing gains tradeoff (DMT) framework bridges the two endpoints of pure diversity gain or pure multiplexing gain. The tradeoff curve of a given space-time code enables one to determine the set of diversity and multiplexing gains that can be obtained simultaneously in a given scheme. Characterizing this tradeoff in the finite SNR regime (non-asymptotic or operational region), for UWB-MAS is crucial because it needs to work at low power regiondue to power mask. Diversity gain at each SNR is obtained from the slope of the outage probability versus signal to noise ratio (SNR) curve. The significance is that diversity gain at a particular operating SNR provides an indication of the additional power required to decrease the error probability by a specified amount.

In this thesis, we will focus on a general MIMO coding framework for UWB communications, and provide performance analysis to quantify spatial diversity (SD) and spatial multiplexing (SM) trade off for UWB-MAS systems for a given STBC scheme.

1.3. Objective of the Thesis.

The goal of this thesis is to develop MIMO systems coding framework for UWB impulse radio and investigate the performance improvement by analyzing, simulating and evaluating the diversity and multiplexing gains trade off in the finite SNR (non-asymptotic) /power/ region for the dense multipath UWB IEEE.802.15.3a standard channels model.

Specifically

- Analyzing the capacity/ performance improvement of MIMO in UWB.
- Analyzing and evaluatingoutage formulation for the multi-antenna in UWB using space time coding and modulated signals in a given range of signal-to-noise ratios.
- Analyzing, evaluating and simulating the tradeoff between the two different gains for a range of finite SNR where the UWB needs to operate to maximize reliability as well as the rate.
- Compare and contrast the tradeoff with the conventional narrow band wireless communication systems for the given SNR region.

1.4. Literature Review

So far many researchers have conducted on different aspects of narrow band/UWB-MIMO wireless communication systems.Some of the researches are reviewed here.

In [24]L.Yang and G. B.Giannakis, an analog STC scheme for the analog multi antenna UWB systems under frequency-nonselectiveRayleigh fading environments was developed.This is inspired by ST code that has been considered in narrowband wireless system standards in Peer-to-peer scenario. As confirmed, there isa considerable increase in bit-error rate performances.It hasalso shown the STC multi antenna schemes increase the *diversity order* compared toincreasing the number of Rakefingers.

In [57] the performance of UWBMIMO systems using spatial orthogonality and correlation properties has been studied. The *increase in system capacity,*compared to that of a single UWB link, has been acknowledged experimentally for 3x3 UWB-MIMO channels.

[31] EnzoBaccarelli et.al, develop a family ofMIMO UWBImpulse-Radio (UWB-IR) transceivers for Orthogonal PPM-modulated (OPPM) coded transmissions over (baseband)multipath-faded MIMO channelstransceivers. They prove that the family of Space-Time OPPM(STOPPM) is able to attain *full diversity*in the considered multipath affected application scenarios.

[41]Huaping Liu, the error performance of an ultra-wide-band (UWB) system with a hybrid pulse amplitude and positionmodulation (PAPM) scheme where input data ismodulated onto both the pulse amplitudes and pulse positions over indoor lognormal fading channels is analyzed. The receiver employs Rake fingers to combine energy contained in theresolvable multipath components. A closed-form *error rate expression* of the system under lognormal fading channels is derived. The sum of independent lognormal random variables (RVs) isapproximated by F-Wilkinson's methodwhere the average SNR per bit is a Random Variable.The proposed PAPM scheme can provide a higher throughput than the binary pulse amplitude or pulse position modulation scheme.

In [55]John D.et.al.et.al, the analytical error performance of MIMO systems over highly a frequency-selective UWB log-normal fading channel is formulated. A zero-forcing (ZF) scheme is used to separate the spatially multiplexed data on a path-by-path basis. A Rake receiver employing maximal ratio combining (MRC) is applied to the ZF paths to form the decision statistics.The *probability of detectionerror* is derivedas a function of $Eb/N0$. For$N$number of transmit, Mreceive antennas, and Lnumber of resolvable paths combined; a diversity order of $L(M-N\ +1)$ is achieved for each data stream when LM is large.

W. Siriwongpairat, et.al [36]evaluates the performance of UWB-MIMO systems employing various modulation and multiple access schemes, and quantify the performance merits of UWB Space-Time systems. ForEach modulation scheme, a framework that enables to compare UWB MIMO systems with conventional UWB single-antenna systems in terms of *diversity and coding*gain has been introduced.The result shows that the combination of ST coding and Rake receiver is capable of exploiting*spatial diversity* as well as *multipath diversity*, richly inherent in UWB environments.

Zheng and Tse showed an elegant formulation of diversity-multiplexing Tradeoff to provide a better understanding of the asymptotic interplay between transmission rate, error probability and signal-to-noise ratio in block fading MIMO channels [25]. The paper showed that both diversity and multiplexing gains can be simultaneously obtained but there is a tradeoff between how much of each type of gain any MIMO scheme can extract. They derive the fundamental trade-off curve achievable by any scheme at high SNR region .Thus for N transmit and M receive antennas, maximum diversity $d_{max}(r) = (M - r)(N - r)$where risthe multiplexing gain. But this asymptotic DMT overestimates the finite-SNR one. For frequency selective, Pedro Coronel and Helmut Bolcskei have characterized Diversity-Multiplexing Tradeoff at high SNR region(56), and find that $d_{max}(r)=(LP-r)(Q-r)$ *where* $P=max(M,N)$, $Q=min(M,N)$.

Ravi Narasimhan et.al,[38] using the recent results on the asymptotic (in the number of antennas) and in view of outage capacity distribution, theyderive and analyze the finite-SNR DMT. They haveanalyzed over Space-Time Block Codes,of Rayleighflat fading channel. This formulation is of course the generalization of DMT given in [25] but used to analyze in operational SNR region. The paper showed the asymptotic DMT cannot be used at realistic SNR values.

Most literatures were focused on making use of only one approach, either to maximize the rate through spatial multiplexing or reliabilitythrough spatial diversitycomputed from the theory of error exponents (detection error). Since maximizing one scheme may not necessarily mean maximizing the other, current researches, however, try to combine both schemes trading one for the other based on the channel stateitself especially for narrow band as in the last two literatures.To fully exploit the benefits of space time codes systems in UWB technology, it is therefore greatly necessary to make analysis and evaluation on diversity- Multiplexing gains tradeoff for IR-UWB multiantenna systems by exploiting the spatial properties of the *scalar fading channel itself* and develop a simple approach, based on the outage capacity formulationinstead of using the machinery of the error exponent theory.

1.5 Outline of the Thesis

In Chapter 2, first, we provide the fundamental of UWB wireless communications, some basic mathematical background representations. We begin with the background of UWB radios with emphasis on physical layer issues includingsignal modeling, Modulation Techniques, channel modeling and transceiver design.We describe the characteristics of UWB channels and establish a mathematical signal representation for the analysis in subsequent chapters.

In Chapter 3, a general background for multi antenna systems & space time block codinghas been described.We present an adaptation of the multi antenna technique to single-band UWB(UWB-IR) communications, basic mathematical backgroundand a comprehensive analysis of the system. We present a general framework to analyze MIMOsystems in UWB.

In chapter 4, Diversity-Multiplexing Tradeoff analysis for UWB-MAS systems has been stated. Mathematical analysis for OSTBC and RODsystemsmodeling, channel capacity analysis and outage formulation has been introduced for MIMO systems. We provide performance analysis and represent the diversity as well as the multiplexing advantages of UWB-MASunder lognormal channel fading. The diversity gain as a function of finite SNR and multiplexing gain is derived here based on the outage formulation of the effective channel.

Chapter 5 deals about Simulation Results and Discussion of Diversity-Multiplexing Tradeoff analysis for UWB-MAS. Simulation parameters and assumption considered has been presented.

Chapter 6 is all about conclusion and recommendation for future works.

Chapter 2

Communication Systems Modeling to UWB

2.1. UWB transmission schemes

A traditional UWB technology is based on single-band systems making use of carrier-free or impulse radio communications.Generally, UWB transmission approaches can be categorized into two main approaches, namely single-band and multiband approaches [4, 5]. This subsection explains both single-band and multiband transmission approaches.

2.1.1 Single-Band (IR) Approaches

Single-band UWB signal is implemented by directly modulating a sequence of impulse-like waveforms that occupies several gigahertz bandwidths. The band width is mainly determined by the pulse duration. Inorder to minimize potential interference from UWB transmissions and to make UWB spectrum more noise-like, TH and DS randomizing technique is applied. The main advantage of IR-based UWB systems is the simplicity in the transceiver structure. No up- and down-mixers are needed. Drawback oftheIR-based UWB system is large number of multipaths, typically on the order of several tens to a hundred more for a normal office environment[6, 31]. This causes a big challenge for the synchronizer design with reasonably quick acquisition time and rake receiver implementation with sufficient fingers to capture enough energy. IR-UWB pulse waveform can be any function which satisfies the spectral mask regulatory. A very common pulse shape is however a Gaussian waveform and its series of derivatives. The basis Gaussian pulse given by [3]

$$w_g(t) = \frac{1}{\sqrt{2\Pi}\sigma} e^{-1/2\left(t-\mu/\sigma\right)^2} \qquad (2.1)$$

2.1.2 Multiband Approaches (MB)

The basic idea behind multiband schemes is to split the total available bandwidth into multiple frequency bands for efficient utilization of the UWB spectrum by transmitting multiple signals at different frequenciesoppositeto single-band approach. By partitioning the spectrum into smaller chunks, a better co-existence with other wireless technologies can be achieved. In multiband based approach information data are multiplexed into sub-frequency bands in the entire band or a

part of it with each sub-band having 528 MHz bandwidthsatisfying the FCCpower mask. Each 528MHz band comprises 128 carriers modulated using QPSK on OFDM tones [5].In MB-OFDM, the UWB spectrum is divided in to 14 bands of528MHz each (Fig 2.1).

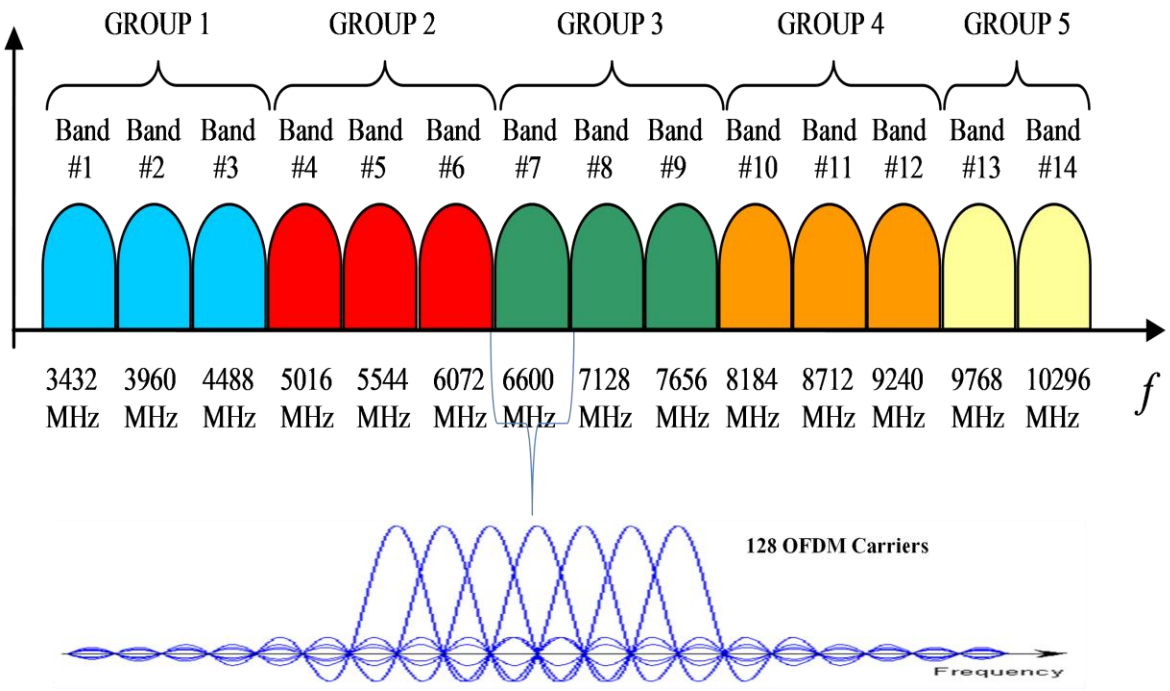

Fig 2.1 MB-OFDM system

The three lower bands are used for standard UWB communications (mandatory) and the rest of the bands are allocated for optional use or future expansion [46]. The main advantage of MB-based UWB systems is that OFDM technique is already mature for deployment in market.High spectral efficiency, inherent resilience to radio-frequency (RF) interference, robustness to multipaths, and the ability to efficiently capture multipath energy, are other nice properties.The Drawback of MB-based UWB systems is complexity involved in implementing up- and down-mixers and OFDM. OFDM requires Fast Fourier Transform (FFT) and inverse FFT (IFFT) algorithms at the receiver and transmitter sides respectively [4]. This is not preferable in typical UWB applications. Currently, it is controversial about which technology will dominate the future market, due to the various pros and cons in each technology. However, the IR-based UWB technology is finding its place in some applications such as indoor wireless communication and localization [31, 32]. The interest of this thesis is on IR-based UWB systems.

2.2 Single-Band Transmitted Signal Model

Since the transmit power is rather low due to the power mask, one information symbol is generally spread over multiple N_f monocycles to achieve a processing gainalong with reducing noise and interference [10].These need a generation of a series of very short duration pulses over a designated period of time (pulse duration) and repeat the transmission at intervals of time. Each pulse has a very wide spectrum that must adhere to the spectral mask requirements. A general block diagram of UWB wireless communication systems isin Fig.2.2consists of three main blocks; transmitter, channel and receiver, which might also be common for any communication system.

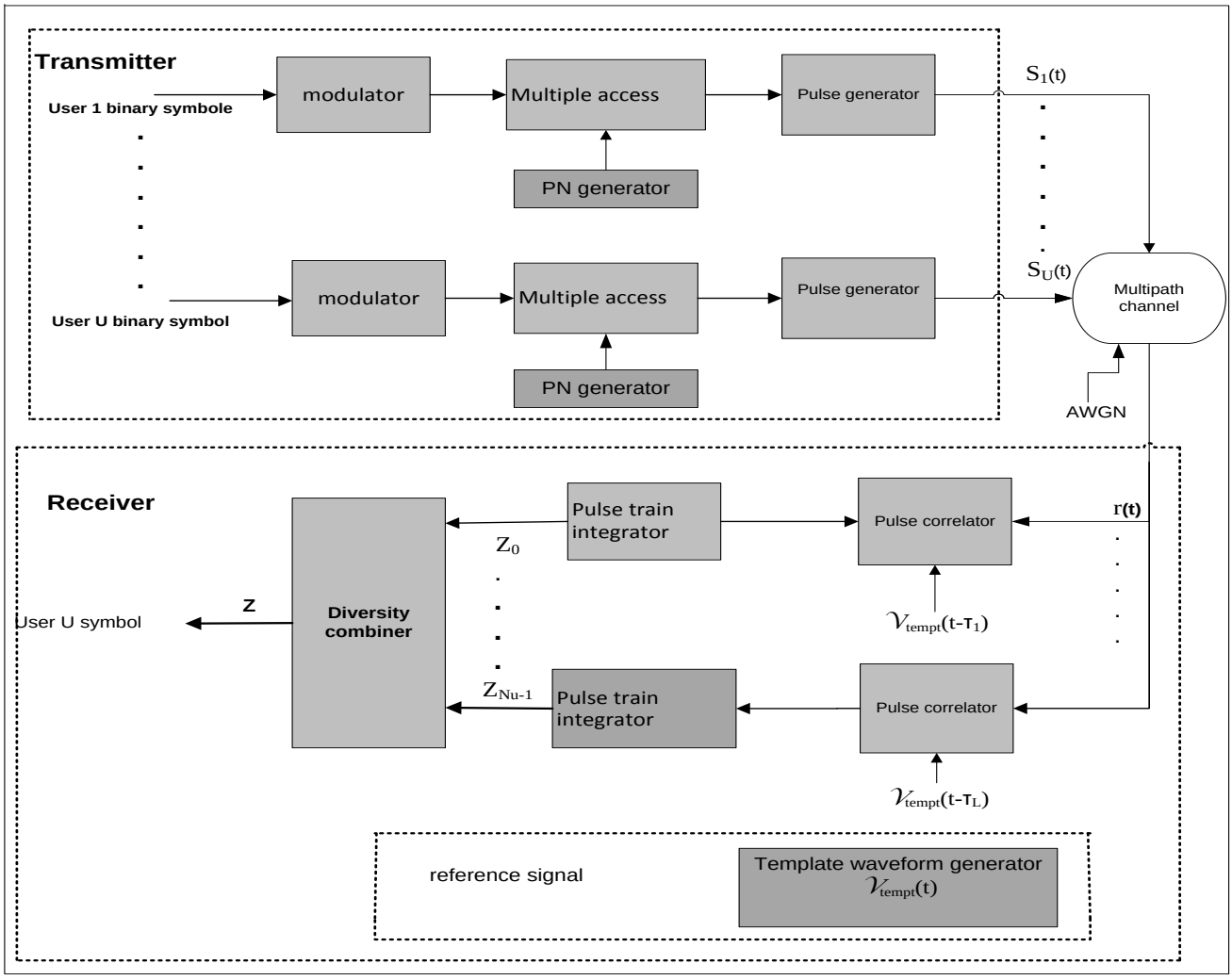

Fig.2. 2 Block diagram of UWB communication system model

2.2.1 UWB Signal representation.

In UWB impulse radios, every information symbol istransmitted using N_f pulses over N_f frames (one pulse per frame of duration T_f). The transmitted waveform at the i^{th} frame can be described as [3].

$$\tilde{S}(t) = w_{tr}\left(t - iT_f\right) \tag{2.2}$$

The basic model for unmodulated IR-UWB train of pulses can be thus written as

$$S_{tr}(t) = \sum_{i=0}^{N_f-1} A_i w(t - iT_f)\ , \qquad i = 0, 1 \ldots\ldots N_f - 1 \tag{2.3}$$

where$A_i$the amplitude of the pulse, $w(t)$is the pulse shape with normalized energy and T_f is the frame duration. UWB pulses waveform $w(t)$can be any function that satisfies the spectral mask regulatory requirements.

Gaussian, Laplacian, and Rayleigh or Hermitean pulses are Common pulse shapes. Typically the first and the second derivative of a Gaussian pulse are most widely used waveforms due to their simplicity and feasibility [3, 5].The derivatives can be generated by filtering the Gaussian pulse since filtering can be modeled by the derivative function.Higher- order derivatives can be generated by successive filtering. The second derivative of the Gaussian pulse is often used in impulse radio systems [3] and we consider in this thesis as well.

A Gaussian pulse is described analytically as [3]

$$w_g(t) = \frac{1}{\sqrt{2\Pi}\sigma} e^{-1/2\left(t-\mu/\sigma\right)^2} \tag{2.4}$$

Where μ is the centre of the pulse and σ relates to the width of the pulse. Note that Gaussian pulse also contains a DC term making it impractical for use in wireless systems. However, higher order derivatives do not contain such a term and are therefore applicable [3].

The first derivative of the Gaussian pulse is defined as [3]

$$w'(t) = \frac{-(1/2)(t-\mu)}{\sqrt{2\Pi}\sigma^{3/2}} e^{-1/2\left(t-\mu/\sigma\right)^2} \quad (2.5)$$

The time and frequency domain representation of the second derivative Gaussian can be analytically represented by, $W_{tr}(t), W_{tr}(f)$, respectively [3, 4]:

$$w'' = W_{tr}(t) = \frac{1}{\sqrt{2\Pi}\sigma}\left[1 - \left(\frac{t-\mu}{\sigma}\right)^2\right] e^{-\frac{1}{2}\left(\frac{t-\mu}{\sigma}\right)^2} \quad (2.6)$$

$$W_{tr}(f) = (2\Pi\sigma f)^2 e^{-\frac{1}{2}(2\Pi\sigma f)^2} e^{-j2\Pi f\mu} \quad (2.7)$$

The effective time duration,T_p for the Gaussian monocycle is $T_p = \zeta * \sigma$ with the centre of the pulse; $\mu = m * \sigma$ where ζ and m are constants. Mostly$T_p = 7\sigma \; and \;\; \mu = 3.5\sigma$ [3, 4].

First derivatives Gaussian pulse has a single zero crossing in the time domain, whilst higher-order derivatives have additional zero crossings. Therefore, higher-order Gaussian pulses yield waveforms with lower relative bandwidths and higher centre frequencies.

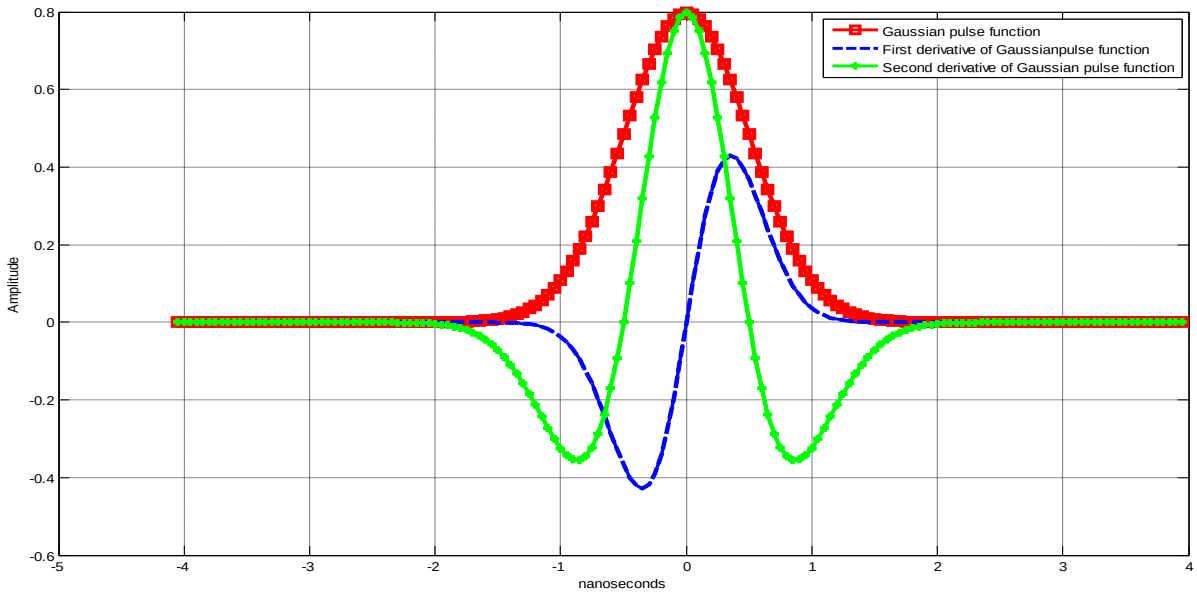

Fig 2.3atime domain Gaussian pulse, 1st derivativeand2nd derivative.

2.2.2. UWB Modulation Techniques

In order to transmit information, additional processing is needed to modulate the monocycle pulse sequence [7, 10]. Several modulation techniques can be used to create UWB signals, where some are more efficient than others. Although numerous modulation techniques are used with impulse-radio UWB: Pulse Amplitude Modulation (PAM), Pulse Position Modulation (PPM), On-Off Keying (OOK) or Antipodal Modulation (BPSK) are common schemes often found in research papers and journals.

2.2.2.1Pulse Amplitude Modulation

PAM works by separating the "large" and the "small" amplitude pulses i.e. the information in a PAM signal is conveyed in the amplitude of pulses. By varying the amplitude the receiver can tell the difference between "1" and "0" and thereby decode the data from the received signal. Specifically, an M-ary PAM signal comprises a sequence of modulated pulses with M different amplitude levels. The PAM signal can be modeled as

$$S(t) = \sum_{i=-\infty}^{\infty} A_i w_{tr}\left(t - iT_f\right) \qquad (2.8)$$

where: A_i is the amplitude of the i[th]pulse

$w_{tr\,(t)}$is the second derivative Gaussian pulse

$T_f$is the pulse repetition period

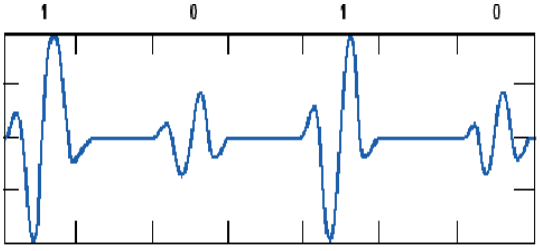

Fig.2.1a PAM modulation

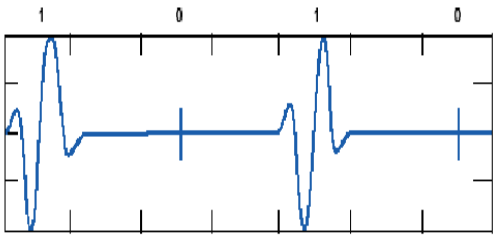

Fig 2.1bOOk modulation

PAM generation is simple because it requires pulses with only one polarity to represent data. Although PAM pulses are less sensitive to noise than OOK-modulated pulses, attenuation

in wireless channels can convert them to theOOK case. Due to that, the receiver will need the attenuation gain control.

2.2.2.2. On-Off Keying (OOK)

On-off keying (OOK) is the simplest form of pulse modulation, in which a "1" is a pulse and an absence of a pulse is a "0".

Actually, it is a special case of PAM where the amplitude of zero represents a "0". The baseband representation of OOK signal can be modeled as

$$S(t) = \sum_{i=-\infty}^{\infty} m_i w_{tr}(t - iT_f) \qquad (2.9)$$

where: $m_i \epsilon [\mathbf{0}, \mathbf{1}]$ is the amplitude of the i[th] pulse $m_i = \begin{cases} 1\,. & i = 1 \\ 0\,, & i = 0 \end{cases}$

$w_{tr\,(t)}$ is the second derivative Gaussian pulse

T_f is the pulse repetition period(is the frame period (seconds))

The main advantages of OOK are simplicity and low implementation cost. The OOK transmitter is quite uncomplicated; a simple RF switch can be turned on and off to represent data. This way, OOK modulation allows the transmitter to idle while transmitting a bit 0 and thus save power. OOK is highly sensitive to noise and interference: an unwanted signal can be detected as a false data bit 1.

2.2.2.3. Pulse Position Modulation (PPM)

In PPM, all pulses (both "1"s and "0"s) are of the same amplitude. The receiver distinguishes between a "1"or a "0" by its time of arrival, or the time lag between pulses. Signals are pseudo randomly encoded based on the position of the transmitted pulse trains by shifting the pulses in a predefined window in time. A PPM represents a data bit 0 by a pulse with no shift with respect to a specific reference point in time and it represents a data bit 1 by a shifted pulse with respect to a specific reference point in time. The M-ary PPM signal can be modeled as

$$S(t) = \sum_{i=-\infty}^{\infty} w_{tr}(t - iT_f - m_i\delta) \quad (2.10)$$

where$m_i$is the i[th] pulse M-ary symbol
$w_{tr\,(t)}$is the second derivative Gaussian pulse
$T_f$is the pulse repetition period
$\delta$is the modulation delay

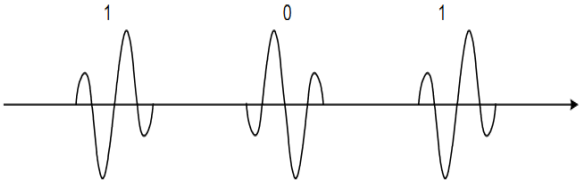

Fig.2.2 a PPM modulation scheme Fig2.2b BPSK modulation scheme

Compared to OOK and PAM, PPM has its advantages on synchronization and good ability against attenuation effects. But because the transmitted information is contained in the time lag, a higher timing accuracy is required for the system to avoid catastrophic collisions that are caused by multiple-access channels.

2.2.2.4. Binary Phase Shift Keying (BPSK).

In BPSK, the polarity of the pulse changes to represent digital data bits. A binary "1" is represented by a positive pulse and binary "0" is represented by a negative pulse. There is a 180 degrees polarity shift between pulses of "0" and "1".

A BPSK signal can be modeled as

$$S(t) = \sum_{i=-\infty}^{\infty} d_j\, w_{tr}\,(t - iT_f) \qquad (2.11)$$

where$d_i \boldsymbol{\epsilon} [-\mathbf{1}, \mathbf{1}]$is the polarity of the modulated pulse
$w_{tr\,(t)}$is the second derivative Gaussian pulse
$T_f$is the pulse repetition period

This type of modulation scheme is less susceptible to distortion because the difference between the two pulse levels is twice the pulse amplitude. Another advantage of BPSK is that the change in polarity can remove the discrete spectral lines in the pulse's PSD, because changing the polarity of pulses produces a zero mean.

2.2.3 Randomizing and Multiple-Access Techniques

On the one hand, continuous-pulse generation implies spectral lines in the transmitted signal that may create interference with other communication systems [3, 10, 45]. On the other hand, as with most of the wireless communication systems, UWB is designed for data transmission between several users at the same time. Therefore, UWB communications require robust randomizing and multiple-access techniques. Until now, Time Hopping (TH) and Direct Sequence (DS) have proven to be the two most popular of these techniques for UWB systems [4, 5, 36].

2.2.3.1. Time Hoping (TH)

In TH-based systems [4, 14, 36,], the information is sent with a time offset for each pulse determined by the TH sequence. Time-hopping can be applied to all of the modulation schemes, where each user is assigned a time-hopping sequence. This sequence reduces collisions in the communication system by assigning each user a unique time shift pattern. Each receiver can detect a signal during its own unique hopping pattern, mitigating interference. The mathematical representation of signal for TH-UWB system can be modeled as [3, 4,]

$$s(t) = \sum_{i=0}^{N_f-1} w_{tr}\left(t - iT_f - C_i^u T_c\right) \qquad (2.12)$$

where: w_{tr} is the transmitted baseband pulse waveform

T_f is the pulse repetition time

C_i^u is the time-hopping sequence

T_c is the duration of the time delay bins

N_f is the number of impulses transmitted for each information symbol

Basically, each frame interval duration is divided into multiple smaller segments and only one of these segments carries the user's transmitted pulse. The TH sequence is assigned to each user to specify which segment in each frame interval is used for transmission. In TH-UWB systems, the frame interval T_f is divided into N_c segments of T_c seconds such that $N_c T_c \leq T_f$. The

TH sequence is denoted byC_i, $0 \le C_i \le N_c - 1$. It provides an additional time shift of $N_c T_c$ seconds to the i^{th} monocycle to allow multiple access without catastrophic collisions. By combining the TH technique with the various modulation options discussed in section 2.2.2 different transmitted signal formats can be generated. A typical TH-PAM-UWB and TH-PPM-UWB format basebandrepresentation of the u^{th} user signal for a transmission of N_s symbolsis writtenrespectively as: [3, 5]

$$S^u(t) = \sqrt{\frac{\epsilon_u}{N_s}} \sum_{j=0}^{N_s-1} \sum_{i=0}^{N_f-1} a_i^u w_{tr}\left(t - jTs - iT_f - C_i^u T_c\right) \quad (2.13)$$

$$S^u(t) = \sqrt{\frac{\epsilon_u}{N_s}} \sum_{j=0}^{N_s-1} \sum_{i=0}^{N_f-1} w_{tr}\left(t - jTs - iT_f - C_i^u T_c - m_j^u \delta\right) \quad (2.14)$$

Where $\sqrt{\frac{\epsilon_u}{N_s}}$ is an energy normalization term.

2.2.3.2. Direct Sequence (DS)

In DS spreading systems [3, 5, 44], the data are carried in multiple pulses whose amplitudes are modulate based on a certain spreading code. It employs a train of pulses whose polarities follow pseudorandom code sequences. Specifically, each user in the system is assigned a Pseudo Random (PR) sequence that controls pseudorandom inversions of the UWB pulse train. DS is commonly used with impulse-radio UWB, although it is typically limited to OOK and biphase modulation schemes. At the receiver, the waveform is demodulated using the same PR sequence, which is unique at the time of communication. Therefore, a minimal amount of interference occurs with other users.Since PPM is intrinsically atime-hopping technique, it is not used for DS-UWB transmission. The expression characterizing the DSspreading approach in the case of PAM and OOK modulations for the information signal $s(t)$and the u^{th} user can be presented as [3]

$$s^u(t) = \sqrt{\frac{\epsilon_u}{N_s}} \sum_{j=0}^{N_s-1} \sum_{i=0}^{N} w_{tr}(t - jT_s - iT_C) C_i^u a_j^u \quad (2.15)$$

Where a_j^u is the jth data bit (modulated data symbols for the uth User)

$C_i^u \epsilon[-1,1]$is the i[th] chip of the PR code (the spreading sequence)

w_{tr} is the transmitted baseband pulse waveform

N is the number of pulses per data bit

$T_c$is the chip Length

The transmitted DS-BPSK signal model for a given information symbol for the u^{th}user can be described as

$$s^u(t) = \sqrt{\frac{\epsilon_u}{N_s}} \sum_{j=0}^{N_s-1} d_j^u \sum_{n_c=0}^{N_c-1} C_j^u w_{tr}(t - jT_s - n_c T_C) \qquad (2.16)$$

Where $d_j^u \epsilon[-1,1]$ is the modulated binary data

$\{C(c_n)\}_{n_c=0}^{N_c-1} \epsilon[-1,1]$is the pseudorandom code or spreading sequence

$T_C \geq T_W$denotes the hop period and total $\sqrt{\frac{\epsilon_u}{N_s}}$ normalizing factor.

2 .3 Single-Band UWB Channel Models

The propagated radio signals undergo attenuation by objects and the multipath components are characterized by different delays and attenuations.Because of the reflection, refraction and scattering, the signal arrives at the receiver through different paths having different amplitudes withdelayed and attenuated echoes of each transmitted pulse.

For narrowband signal the multipath components arrive continuously, and severe multipath fading can be observed. Whena large number of multipath components are observed at the receiver within its resolution time, the central limit theorem is commonly call upon to model the amplitude of the received signal as Rayleigh distributed. The Rayleigh fading is therefore extensively used for channel models in many narrowband systems.

In UWB systems, the ultra large bandwidth of a UWB waveform considerably increases the ability of a receiver to resolve a variety of reflections. As a result, the signal received contains a significant number of resolvable multipath components. This characteristic of UWB systems can give rise to two main effects which make UWB channels different from that of narrowband systems [3, 4].

I. The number of multipath components (MPCs) arriving at the receiver within the period of an ultra short waveform. Consequently, the channel fading is not as severe as that in narrow-band channels, and Rayleigh fading may not perfectly match to the amplitude of the received signal.

II. Since multipath components can be resolved on a very fine time duration, time of the multipath components may not be continuous. Consequently it is possible to have time intervals during which no significant amount of energy exist between the arriving multipath components. In other words several MPCs arrive shortly one after the other (in clusters), then after a pause, another group of MPCs arrive. Particularly, due to the very fine resolution of UWB waveforms, different objects or walls in a room could contribute different clusters of multipath components.

Three main channel models in standard for indoor short range UWB radio channels are as follows.

2.3.1 Tap-delay line fading model

A simple model for characterization of a UWB channel is the tap-delay-line fading model [4] in which the signal received is a sum of the replicas of the signal transmitted. Such a tap-delay-line fading model allows frequency selectivity of UWB channels to be taken into consideration. Under the tap-delay-line fading model, the channel impulse response can be described as [4]

$$h(t) = \sum_{l=0}^{L-1} \alpha_l \delta(t - \tau_l) \qquad (2.17)$$

where $h(t)$ is the channel impulse response (CIR), α_l is the multipath gain coefficient of the l^{th} path, Ldenotes the number of resolvable multipath components, δ is the Dirac delta function, and $\tau_l$represents the path delay of thel^{th} path. The statistics of $|\alpha_l|$ are typically modelled by the Nakagami distribution [31] or lognormal distribution [41, 43].

- **Lognormal distribution** is described by

$$f_{|\alpha_l|}(x) = \frac{20/ln10}{x\sqrt{2\Pi\Omega_l}} exp\left\{-\left[\frac{[10\ log_{10}(x^2) - \mu_l]^2}{2\Omega_l}\right]\right\} \qquad (2.18)$$

whereμ_l and$\Omega_l$are the mean and the variance of$|\alpha_l|$ in dB. The lognormal distribution has the advantage that the fading statistics of the small-scale statistics and the large-scale variations have the same form; the superposition of lognormal variables can also be well approximated by a lognormal distribution [40, 42].

Log-normal distribution is the single-tailed probability distribution of any random variable whose logarithm is normally distributed. If x is a random variable with a normal distribution, then $y = exp(x)$ has a log-normal distribution; likewise, if y is log-normally distributed, then $ln(y)$ is normally distributed [42]

For x being a log normal random variable, the cumulative distribution function is described as

$$F_x(x,\mu,\sigma) = \Phi\left(\frac{\ln(x)-\mu}{\sigma}\right) \tag{2.19}$$

where$\Phi(.)$is the cumulative distribution function (CDF) of standard Normal Gaussian distribution and μ,σ are the mean and standard deviation of the normal random variable.

Thus:[7pp 84]

$$F_x(x,\mu,\sigma) = P(X<x) = \Phi\left(\frac{\ln(x)-\mu}{\sigma}\right) \tag{2.20}$$

$$\Phi(x) \triangleq \frac{1}{2\Pi}\int_{-\infty}^{x} e^{\frac{-t^2}{2}}dt = \frac{1}{2}\left(1+erf\left(\frac{\ln(x)-\mu}{\sigma\sqrt{2}}\right)\right),\ \ erf$$

$$= \frac{2}{\sqrt{\Pi}}\int_{0}^{\infty} e^{-t^2}dt \tag{2.21}$$

From the property of standard Normal Gaussian Cumulative Distribution $\Phi(x)$, the complementary CDF is given by

$$\widetilde{\Phi}(x) = 1-\Phi(x) \triangleq Q(x), \qquad Q(x) = \frac{1}{\sqrt{2\Pi}}\int_{x}^{\infty} e^{\frac{-t^2}{2}}dt = \frac{1}{2}\left(1-erf\left(\frac{x}{\sqrt{2}}\right)\right), \quad x \geq 0$$

$$\text{erf}(-x) = -\text{erf}(x), \qquad \frac{d}{dx} erf(x) = \frac{2}{\sqrt{\Pi}} e^{-t^2} \tag{2.22}$$

$Q(x)$represents the upper tail property of the Gaussian distribution, e.i the probability that standard Normal Gaussian random variable X is greater than x.

Additionally,$Q(x) = 1 - Q(-x)$, thus $\Phi(x) = Q(-x)$.

Also Let y be a normally distributed RV with mean m_y and standard deviation σ_y such that $y = 10log10\ (\alpha)$; Thenm_y = cm_α and σ_y = $c\sigma_\alpha$, where $c = 10/\ ln\ (10)$.
Several approximation solutions to the probability distribution of a sum of independent lognormal RV's have been reported, including Wilkinson's, Schwartz-Yeh's, and Farley's methods [40, 43]. For interested readers one can refer to the references.

- **Nakagami distribution:** amplitude of multipath coefficient can be modeled by $Nakagami - m$ distribution as

$$f_{|\alpha_l|}(x) = \frac{2}{\Gamma(m)} \left(\frac{m}{\Omega_l}\right)^m x^{2m-1} exp\left\{-\frac{m}{\Omega_l} x^2\right\} \tag{2.23}$$

where$\Gamma(.)$is the Gamma function, $m \geq 1/2$ is the Nakagami fading parameter, and Ω_l is the mean-square value of the fading amplitude.The fading parameter, describes the severity of the fading. The smaller is m, the more severe the fading will be. With$m = 1$ and $m = \infty$ corresponds to the Rayleigh fading and non-fading channel, respectively. The advantage of Nakagami- $m$statistics is that a wide range of fading conditions can be modeledby adjusting their fading parameters. In fact, Nakagami- m distributions with large value m are similar to the log-normal distributions [4].

In conventional narrowband systems, it is well established that the amplitude of the l^{th}path, $|\alpha_l|$ is modeled as a Rayleigh random variable with a probability density function (pdf)

$$f_{|\alpha_l|}(x) = \left(\frac{x}{\Omega_l}\right) exp\left\{-\frac{x^2}{\Omega_l}\right\} \tag{2.24}$$

where$\Omega_l = E[|\alpha_l|^2]$ denotes the average power of the path l^{th}.

Although the tap-delay line fading model is able to capture the frequency selectivity, it does not reflect the clustering characteristic of UWB channels. Two mathematical models that reflect this clustering is the Δ- K model and the Saleh-Valenzuela (S-V) model.

2.3.2 $\Delta - K$ Model

The Δ- Kmodel defines two states, state X where the arrival rate of paths isλ, and state $Y$where the rate is $\nu\lambda$. The model starts in state$X$. If a path arrives at time t, then a transition is made to state $Y$for a minimum of timeλ. If no path arrives during that time, the model reverts to state$X$; otherwise, it remains in state$Y$.The number of clusters and the duration of the clusters become random variables in this model. The number of clusters is a random variable, whose realization is determined by how often system enters into state Y.To capture the clustering property, the multipath arrival times τ_l can be characterized by a Poisson process with a constant arrival rate λ¸ as

$$P(\tau_l - \tau_{l-1} > t) = \exp(-\lambda t) \qquad (2.25)$$

The inter-arrival time of multipath components is exponentially distributed, i.e., given a certain arrival time $\tau_{l-1}$for the previous time, $pdf$for the arrival of path l can be written as [10].

$$P(\tau_l/\tau_{l-1}) = \lambda_1 \exp\left[-\lambda_1(\tau_l - \tau_{l-1)}\right], \qquad l > 0 \qquad (2.26)$$

2.3.3 Saleh-Valenzuela (S-V) model

This is the most common statistical model for the discrete indoor channel impulse response. The basic assumption behind this model is that the multipath components arrive in clusters. The cluster arrivals are described by a Poisson process, and thus, the cluster inter-arrival times are described by exponential random variables as in eqns (2.25, 2.26).The multipath arrivals are grouped into two different categories: a cluster arrival and a ray arrival within a cluster. The S-V model requires four main parameters, namely, the cluster arrival rate, the ray arrival rate within a cluster, the cluster decay factor, and the ray decay factor.

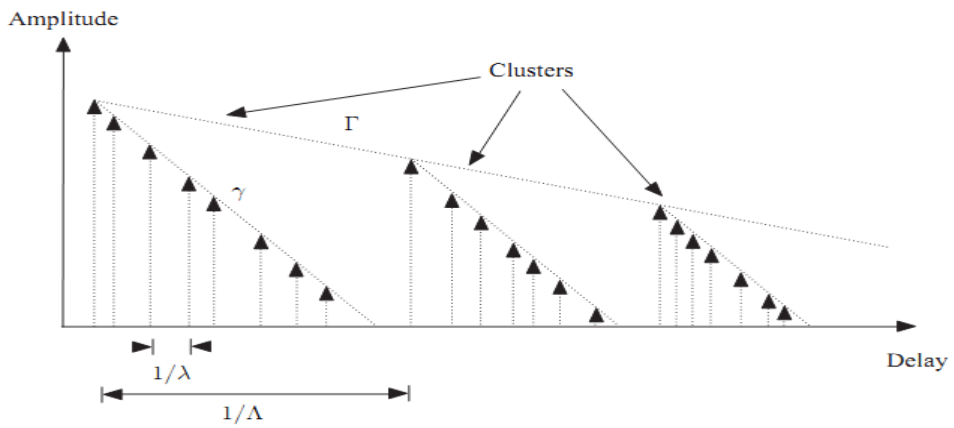

Fig. 2.3 Principle of Saleh-Valenzuela model.

The Saleh-Valenzuela model is a tapped-delay line model given by

$$h(t) = \sum_{c=0}^{C} \sum_{l=0}^{L} \alpha_{c,l} \delta(t - \tau_c - \tau_{c,l}) \qquad (2.27)$$

where: $\alpha_{c,l}$ denotes the gain of the l^{th} multipath component in the C^{th} cluster, C is the total number of cluster, and L is the total number of rays within each cluster. The time duration τ_c represents the delay of the C^{th}cluster, and $\tau_{c,l}$ is the delay of the l^{th} path in theC^{th} cluster relative to the cluster arrival time. The cluster arrivals and the path arrivals within each cluster are modeled by Poisson processes

$$P(\tau_c/\tau_{c-1}) = \Lambda \exp\left[-\Lambda(\tau_c - \tau_{c-1})\right], \qquad l > 0 \qquad (2.28)$$

$$P\left(\tau_{c,l}/\tau_{(c-1),l-1}\right) = \lambda \exp\left[-\lambda(\tau_{c,l} - \tau_{(c-1),l}\right], \quad C > 0 \qquad (2.29)$$

whereΛ the cluster arrival rate, and λ is the ray arrival rate.

In S-V-type model where multiple clusters are present, it is usually assumed that each cluster is exponentially decaying, so that

$$\mathrm{E}\left[\left|\alpha_{c,l}\right|^2\right] = \Omega_0 \exp\left(-\frac{\tau_c}{\Gamma}\right) \exp\left(\frac{\tau_{c,l}}{\gamma}\right) \qquad 2.30$$

Where Ω_0 is the mean energy of the first path of the first cluster, Γ is the cluster decay factor, andγ is the ray decay factor; this reflects the exponential decay of each cluster, as well as the

decay of the total cluster power with delay.

2.3.4 The Standard IEEE 802.15.3a Channel Model

The working group IEEE 802.15 request contributions in order to provide a unique channel model to test various UWB system proposals. Two statistical models were defined: the IEEE 802.15.4a for the long range low data rate applications and the IEEE 802.15.3a for high data rate short range wireless communication systems (indoor environment) applications. The main features of this channel model are described in detail as follows.

Based on this clustering phenomenon observed in several channel measurements, this channel model derived from the Saleh-Valenzuela model [4, 6] with a couple of slight modifications. Experimental observations show that the lognormal distribution seems to better fit the measurement data.A lognormal rather than a Rayleigh multipath gain magnitude distribution is taken as a standard. In addition, independent fading is assumed for each cluster along with each ray within the cluster. Therefore, the multipath model consists of the following, discrete time impulse response:[6,47]

$$h_i(t) = X_i \sum_{c=0}^{C} \sum_{l=0}^{L} \alpha_{c,l}^{i} \delta(t - T_c^i - \tau_{c,l}^i) \qquad (2.31)$$

where $\{\alpha_{c,l}^i\}$ are the multipath gain coefficients, $\{T_c^i\}$ is the delay of the cth cluster, $\{\tau_{c,l}^i\}$ is the delay of thel^{th}multipath component relative to the c^{th} cluster arrival time (T_c^i), $\{X_i\}$ represents the log-normal shadowing, and *i* refers to the i^{th} realization.

The proposed model uses the following definitions:

τ_c= the arrival time of the first path of the *l*-th cluster;

$\tau_{c,l}$ = the delay of the l^{th}path within the c^{th}cluster relative to the first path arrival time,

Λ = cluster arrival rate;

λ = ray arrival rate, i.e., the arrival rate of path within each cluster.

By definition, we have $\tau_{0,l} = 0$. The distribution of cluster arrival time and the ray arrival time are given by

$$P(\tau_c/\tau_{c-1}) = \Lambda\exp\left[-\Lambda(\tau_c - \tau_{c-1})\right], \qquad c > 0 \tag{2.32}$$

$$P\left(\tau_{c,l}/\tau_{(c-1),l-1}\right) = \lambda\exp\left[-\lambda(\tau_{c,l} - \tau_{(c-1),l}\right], \quad l > 0 \tag{2.33}$$

The channel coefficient is log normally distributed with mean $\mu_{c,l}$ and variance $\sigma_1^2 + \sigma_2^2$ defined as follows: where σ_1^2, σ_2^2 variances correspond to the fading on each cluster and ray, respectively,

$$\alpha_{c,l} = p_{c,l}\xi_l\beta_{c,l}, \tag{2.34}$$

$20\log 10(\xi_l\beta_{c,l}) \propto \text{Normal}(\mu_{c,l}, \sigma_1^2 + \sigma_2^2)$, or

$$\left|\xi_l\beta_c\right| = 10^{(\mu_{c,l}+n_1+n_2)/20} \tag{2.35}$$

where $n_1 \propto \text{Normal}(0, \sigma_1^2)$ and $n_2 \propto \text{Normal}(0, \sigma_2^2)$ are independent and correspond to the fading on each cluster and ray, respectively,

$$E\left[\left|\xi_l\beta_{c,l}\right|^2\right] = \Omega_0 e^{-T_l/\Gamma} e^{-\tau_{c,l}/\gamma} \tag{2.36}$$

where T_l is the excess delay of bin l and Ω_0 is the mean energy of the first path of the first cluster, and $p_{c,l}$ is equiprobable +/-1 to account for signal inversion due to reflections.

The mean of the channel fading is given by $\mu_{c,l}$ is given by [6]

$$\mu_{c,l} = \frac{10\ln(\Omega_0) - 10T_l/\Gamma - 10\tau_{C,l}/\gamma}{\ln(10)} - \frac{(\sigma_1^2 + \sigma_2^2)\ln(10)}{20} \tag{2.37}$$

In the above equations, ξ_l reflects the fading associated with the cthcluster, and $\beta_{c,l}$ corresponds to the fading associated with the l^{th}ray of the cthcluster. Note that, a complex tap model was not adopted here. The complex baseband model is a natural fit for narrowband systems to capture channel behavior independently but for UWB systems a real-valued simulation at RF may be more natural.

Finally, since the log-normal shadowing of the total multipath energy is captured by the term, X_i, the total energy contained in the terms $\{\alpha_{C,l}^{i}\}$ is normalized to unity for each realization. This shadowing term is characterized by the following:

$$20\log 10(X_i) \propto \text{Normal}(0, \sigma_x^2). \tag{2.38}$$

The key parameters that define the model:

Λ = cluster arrival rate;

λ = ray arrival rate, i.e., the arrival rate of path within each cluster;

Γ = cluster decay factor;

γ = ray decay factor;

σ_1 = standard deviation of cluster lognormal fading term (dB).

σ_2 = standard deviation of ray lognormal fading term (dB).

σ_x = standard deviation of lognormal shadowing term for total multipath realization (dB).

These parameters are found by trying to match important characteristics of the channel. Since it's difficult to match all possible channel characteristics, the main characteristics of the channel that are used to derive the above model parameters were chosen to be the following:

- Mean excess delay
- RMS delay spread
- Number of multipath components (defined as the number of multipath arrivals that are within 10 dB of the peak multipath arrival)
- Power decay profile

Table 2.1: Multipath channel characteristics and corresponding model parameters [3, 6]

Target Channel	**CM 1**	**CM 2**	**CM 3**	**CM 4**
Model Parameters values				
Λ (1/nsec)	0.0233	0.4	0.0667	0.0667
λ (1/nsec)	2.5	0.5	2.1	2.1
Γ	7.1	5.5	14.00	24.00
γ	4.3	6.7	7.9	12

σ_1 (dB)	3.3941	3.3941	3.3941	3.3941
σ_2 (dB)	3.3941	3.3941	3.3941	3.3941
σ_x (dB)	3	3	3	3
Model Characteristics				
Mean excess delay (nsec) (τ_m)	5.0	9.9	15.9	30.1
RMS delay (nsec) (τ_{rms})	5	8	15	25
NP_{10dB}	12.5	15.3	24.9	41.2
NP (85%)	20.8	33.9	64.7	123.3

The IEEE 802.15.3a collected a huge number of measurements and categorized them into four band groups, representing distinct UWB WPAN operational conditions both LOS and Non LOS (NLOS). The resulting models designed CM1 t o CM4 are:

- CM 1 LOS from 0 to 4 meters, CM 2 NLOS from 0 to 4 meters
- CM 3 NLOS from 4 to 10 meters, CM 4 very high multi path

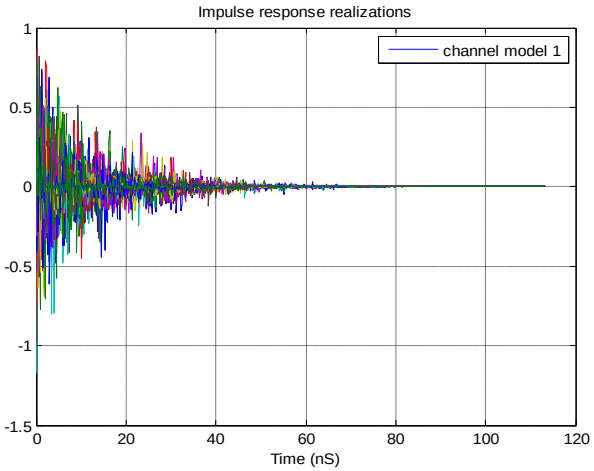

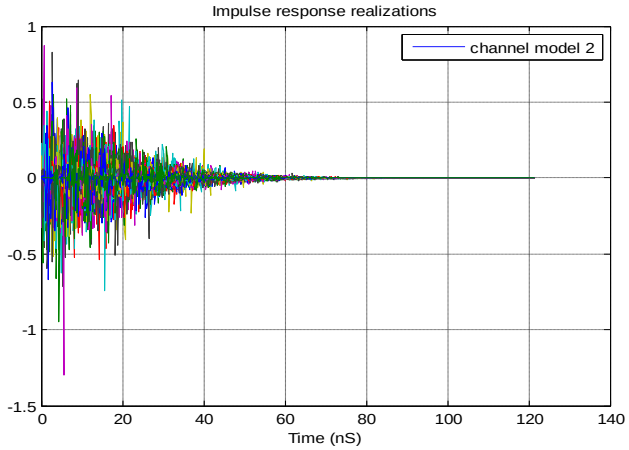

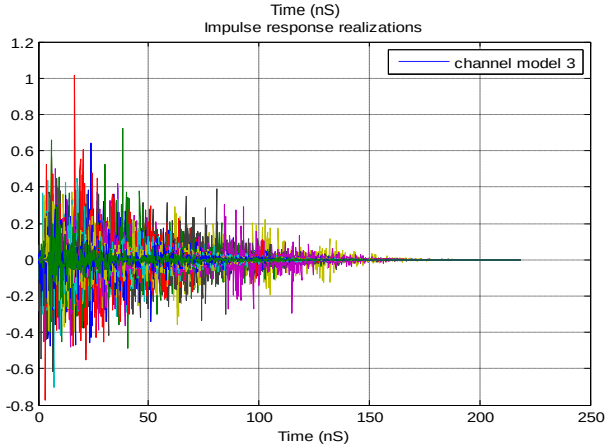

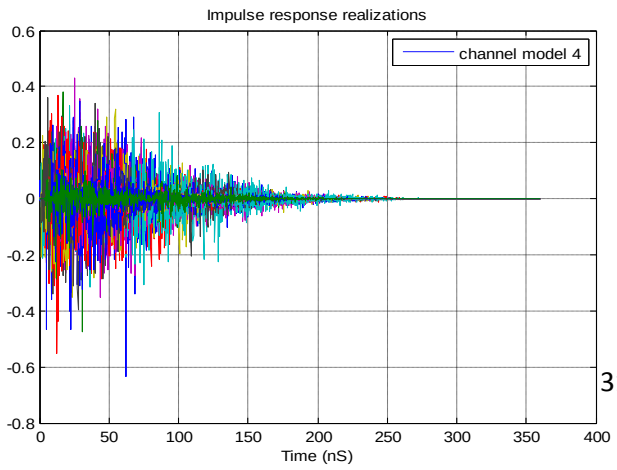

Fig.2.4 discrete time channel impulse response for the four channels

Fig. 2.4 depicts the discrete time channel impulse response for the four channel models of the Standard IEEE 802.15.3a over One hundred (100) realizations for each channel model. As it can be seen from the plot, the difference between LOS and NLOS transmissions is clearly visible between CM1 and CM2; in CM2, the group of strongest multipath components is delayed by about 5 ns in comparison with the same group in CM1. A spreading of the CIR energy amongst a larger number of multipath components compared to CM1 and CM2 is observed in channels CM3 and CM4. This is due toan increase in the distance between transmitters and a receiver and implies a reduction in the number of significant multipath components.

2.4 Received signal model

Consider a multiuser UWB system with N_u users. Theu^{th} user transmitsIR-UWB signal carrying information sequence as described in Section 2.1.3. The channel impulse response of the u^{th} user for the standard IEEE 802.15.3a channel model discussed in section 2.2.4 can be written as

$$h^u(t) = X^u \sum_{c=0}^{C-1} \sum_{l=0}^{L-1} \alpha_{c,l}\, \delta\left(t - \tau_c - \tau_{c,l}\right) \qquad (2.39)$$

The u^{th} user received signal per transmitted symbol is simply the convolution of the transmitted signal with the channel impulse responseplus an additive Gaussian noise.The general expression for the received signal from a user u can be written as

$$r(t) = s^u(t) * h^u(t) + n(t) \qquad (2.40)$$

where$s^u(t)$ is the transmitted signal format by user u as described in eqns (2.13, 2.14), $h^u(t)$ is the channel impulse response and $n(t)$ is the additive nose, which is modeled as a real additive white Gaussian noise process with zero mean and two-side power spectral density$NO/2$. Using

the channel impulse response for user u of the standard IEEE 802.15.3a channel the received signal can be simplified as

$$r(t) = X^u \sum_{u=1}^{N_u} \sum_{c=0}^{C-1} \sum_{l=0}^{L-1} \alpha_{c,l}^u \, S^u\left(t - \tau_c^u - \tau_{c,l}^u\right) + n(t) \qquad (2.41)$$

2.5 Detection schemes

In single band UWB systems there are some typical demodulators which are often used. A brief description is presentedhere.

2.5.1 Correlator receiver

The correlator is a widely employed UWB receiver. The principle behind this detection scheme is to perform the correlation of the received pulse with the pulse expected, called a reference or template signal. The receiver could also consist of a filter matched to the channel response rather than the received pulse waveform. This is equivalent to evaluating the cross-correlations between the received signal and a reference signal. A block diagram of a simple correlation receiver is shown in fig.2.5. The output from the multiplier is a function of how well the template waveform generator matches the incoming waveform in time and shape. The correlation receiver can provide the optimum detection SNR if the template waveform exactly matches the time and shape of the incoming waveform [4, 10].

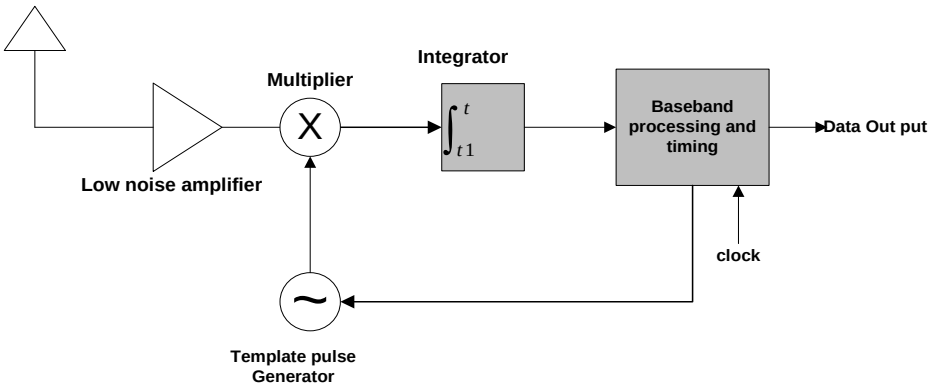

Fig 2.5 Basic Correlation Receiver

Depending on the type of modulation (PAM or PPM), the template can be a single pulse, or two opposite polarity pulses.

2.5.2 Rake receiver detector

Wireless channel suffers from multipath, where reflections and other effects of thechannel cause multiple copies of the transmitted pulse to appear at the receiver [6,10].Nevertheless, the received signal energy can be improved in a multipath channel by utilizinga time diversity technique, such as employing a Rake receiver.A Rake resceiver is a bank of correlators which could be used to exploit multipath diversity by combining constructively the monocycles received from resolvable multipath components. It also provides time diversity by combining various replicas of the signal components where each finger of the rake is synchronized to a multi-path component. A Rake receiver can be used to gather energy and to increase the strength of the received signal. A typical Rake receiver structure composed of several correlators followed by a linear combiner as shown in Fig. 2.6. Each of those correlators is known as Rake finger.

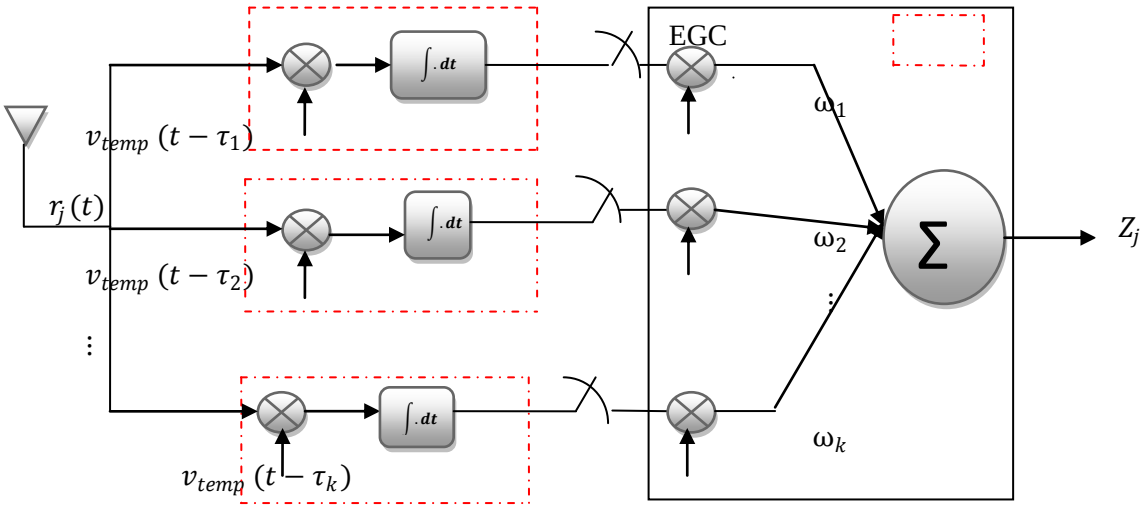

Fig.2.6 Rake receiver structure with bank of correlators and reference signals $v_{temp}\ (t)$

The signal received at the Rake receiver is correlated with delayed versions of the reference pulse. Rake receivers are three types. The All-Rake (ARake) receiver captures all most all the energy carried by a very large number of different multipath signals. To reduce the rake complexity, a partial combining (called PRake) is used as partial combining of the energy, which combines the first arriving paths out of the available resolved multipath components. Selective combining (called SRake) is suboptimum Rake receiver, which combines the energy selectively carried out by the strongest multipath components [31,37]. Rake

receivers are used in time-hopping impulse radio systems and direct sequence spread spectrum systems [36,43]. The outputs of the fingers are appropriately weighted and combined using maximal ratio combining (MRC) or equal gain combining (EGC) to reap the benefits of multipath diversity [51].WhenMaximal ratio combining (MRC) technique is used; the amplitudes of the received MPCs are estimated and used as weighing vector in each fingers. In case of equal gain combining (EGC) scheme, all the tracked MPCs are weighted with their corresponding signs and combined. In a carrier-less UWB system, determining the phase is even simpler because the phase is either 0 or π, to account for pulse inversion [51].

Assume that we have perfect knowledge of the channel, all paths are resolvable, that is, the minimum time betweenany two paths is larger than the pulse width and PRake receiver is used, the output of the k^{th} finger of thereceiver forj^{th} symbol, can be written a

$$z_{j,k} = \int_{-\infty}^{\infty} r_j(t) v_{temp}(t-\tau_k) dt \, , k = 0, 1, \ldots . K-1 \; for \; each \qquad (2.42)$$

where is$v_{temp}\ (t)$ assumed to be the normalized template signal matched tothe whole pulse sequence of j^{th} information symbol.

If there is a perfect match of the received signal with the reference signal, zero inter-frame and inter-symbol interference, then the output of k^{th} finger with $K\ (k \leq L)$ fingers, summation over N_f frames of j^{th} symbol with the diversity combining weight vector ωcan be written in discrete time as

Let $\quad g(t) = w_{tr}(t) * h(t)$

Then$z_{j,k} = \sqrt{N_f E}\,\omega_k \alpha_k \quad + \eta_{j,k}$ (2.43)

where the term$\eta_{j,k} = \int_{-\infty}^{\infty} n(t) v_{temp}(t-\tau_k) dt$is the noise at the outputof the correlator which has zero mean and varianceσ_n^2 and $\alpha(\tau_k) = \int_0^{\infty} g(t)\, v_{temp}(t-\tau_k)$.

The outputs of all the fingers (correlators) for the j^{th} symbol can be written together in vector notation as$z_j = \sqrt{N_f E}\,\omega\alpha \quad + \eta_{j,k}$ (2.44)

wherefingers of Rake use a delayed version of the template signal $v_{temp}\ (t)$, with a delay chosen from the vector $\tau\ = [\tau_0 . \cdots , \tau_{k-1}]^T$, to match itto a specific multipath component.

The approximate mean and variance of the decision statistic at the output of Rakefor a PAM modulated signal from (2.44) are evaluated as [10, 55]

$$E[z_j] = \sqrt{N_f E} \sum_{k=0}^{K-1} \omega_k \alpha_{c,l} \tag{2.45}$$

$$var[z_j] = \sigma_n^2 \sum_{k=0}^{K-1} \omega_k \alpha_{c,l} = \frac{No}{2} \sum_{k=0}^{K-1} \omega_k \alpha_{c,l} \tag{2.46}$$

Chapter 3

Coding Framework for IR-UWB-MIMO systems

As previously discussed, Ultra-wideband (UWB) has emerged as a strong candidate for a wide variety of indoor wireless applications. Most UWB applications are in rich scattering indoor environment, which provides an ideal transmission scenario for MIMO implementation. In addition, the GHz center frequency of UWB radio relaxes the requirements on the spacing between antenna array elements. Accordingly, the combination of UWB and MIMO technology might achieve the requirement for applications offuture short range wireless systems [31-35].

In this section we describe MIMO space–time-coded systems and then present brief explanation of space–time-coded UWB systems for the modulated UWB signals with multiple access schemes.

3.1 Multiple antenna systems and space time coding

MIMO space–time-coded systems are well known for their effectiveness at improving system performance under multipath scenarios. MIMO can simultaneously provide high spectral efficiency and remarkable quality improvement. Using multiple antennas at both receiver and transmitter sides to increase the capacity of the wireless channel was originally the main idea.Consequently, there was a growing interest toward the development of codes and schemes to enable the systems to approach the Shannon limit such as space time coding (STC) [25]. On

other hand works by Alamouti on space-time block coding (STBC) [26], demonstrated the prospect to obtain transmit diversity.

Single-Input Single- Output (SISO) is the usual configuration with one antenna at both ends, Single- Input Multiple- Out put (SIMO) uses a single transmitting antenna and multiple receiving antennas, Multiple- Input Single- Out put (MISO) employs multiple transmitting antennas and a single receiving antenna and Multiple- Input Multiple- Output (MIMO) systems employ multiple antennas at both receiver and transmitter.

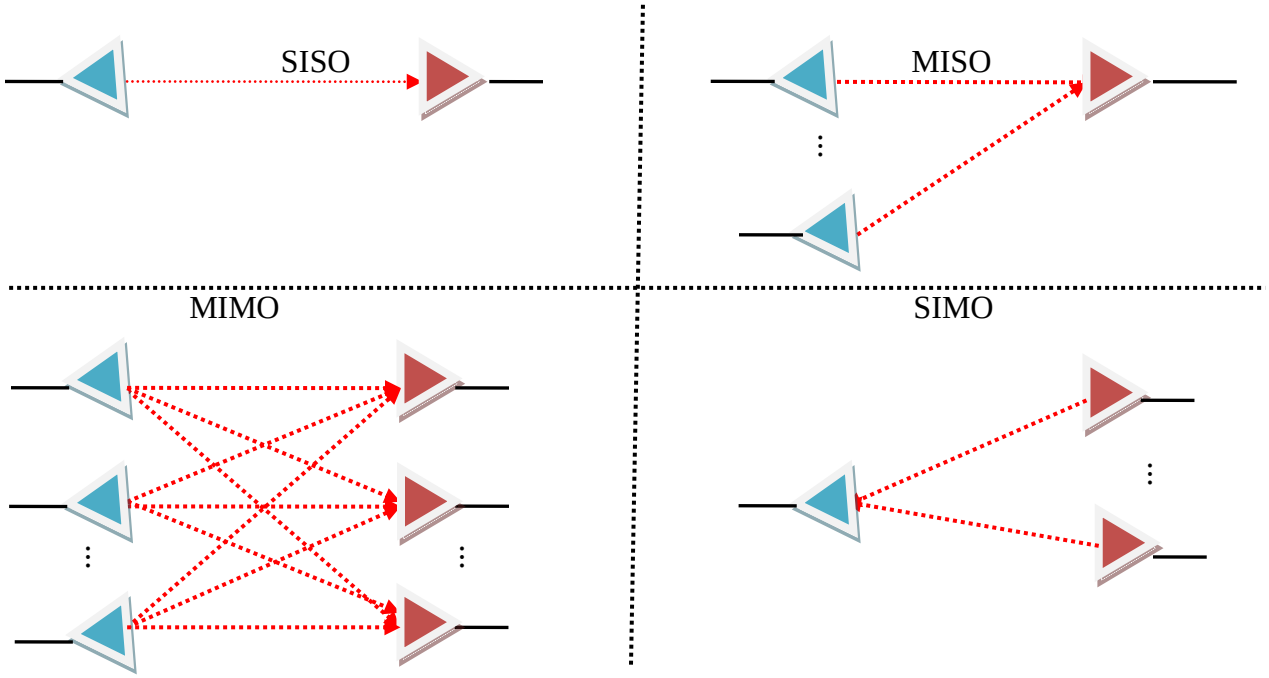

Fig 3.1 Multiple antenna configurations

3.1.1 Spatial diversity

Under most conditions, the received signal of a wireless system consists of the superposition of delayed and attenuated replicas of the transmitted signal. Transmitted signals are received through multiple paths which usually add destructively resulting in serious performance degradations. This phenomenon isnormally referred to as fading. When the received signal

power drops below some level, the channel is said to be in deep fade, or in a fading dip. Diversity techniques are applied as a means to combat fading and increase throughput by lowering the variations of the received SNR which in turn reduce the average symbol error rate (SER) [28, 34]. There are different diversity schemes:

- **Temporal Diversity:** replicas of the transmitted signal are provided across time. It is applicable when the coherence time of the channel is small compared with the interleaving symbol.
- **Frequency Diversity**: replicas of the transmitted signal are in frequency domain. It is employed when the channel coherence band width is smaller than the signal band width.
- **Spatial Diversity:** space diversity is the most common and is a relatively simple technique. It can be implemented easily by using multiple antennas at the transmitter end or at the receiver end or at both ends. Replicas of the transmitted signal are provided across different antennas. This is significant when inter antennas distance is larger than the coherence distance, to guarantee independent fades.

In MIMO systems we often talk about antenna diversity, which can be at the receiving or transmitting side.If the received signals on different antennas are independent,when one experiences a fading deep, it is very unlikely that also other paths fade.This could be achieved if combined multiple branches are ideally uncorrelated.

Diversity gain measures the decrement in error rate against the SNR and can be expressed as the slope of the error rate as a function of SNR when SNR tends to infinity as defined below [22, 25, 28]:

$$d = -\lim_{SNR \to \infty} \frac{log\big(P_e(SNR)\big)}{log(SNR)} \tag{3.1}$$

$P_e(SNR)$denotes the error rate measured at a fixed SNR value. Since the performance gain at high SNR is dictated by the SNR exponent of the error probability, the above definition somehow extracts" its exponent", which is the diversity gain we always referredto[25]..

3.1.2 Multiplexing gain

MIMO systems perform spatial multiplexing. The basic concept of spatial multiplexing is to transmit multiple data streams simultaneously by dividing (or multiplexing) the data stream into several sub streamsto be transmitted. The independentdata signals are transmitted from each transmit antenna as demonstrated by the BLAST transmission schemes [50].The receiver could distinguish between the different signals if it has channel knowledge. Thus; MIMO channel can then be seen as a number of parallel spatial SISO sub-channels. Such technique leads to an increase in the system spectral efficiency without any need neither for additional bandwidth nor for additional power allocation. It is basically ameasure of the capacity increase. The spatial multiplexing order,is expressed as [25, 38]

$$r = \lim_{SNR \to \infty} \frac{\mathrm{R(SNR)}}{log(SNR)} \tag{3.2}$$

$R(SNR)$denotes the rate of the transmission scheme as a function of the signal-to-noise ratio.The tradeoff between diversity and spatial diversity will depend on the throughput and link robustness requirements of the applications [22, 25].

3.2 UWB-MIMO System Model

The objective of this section is to give a brief explanation of UWB-MIMO system model and its components. A generalized system model is given in Fig. 3.2 where the main components of the system model are the transmitters, wireless channels and the receivers. A multiuser system model with N_u users, N transmitting and M receiving antenna elements is considered.

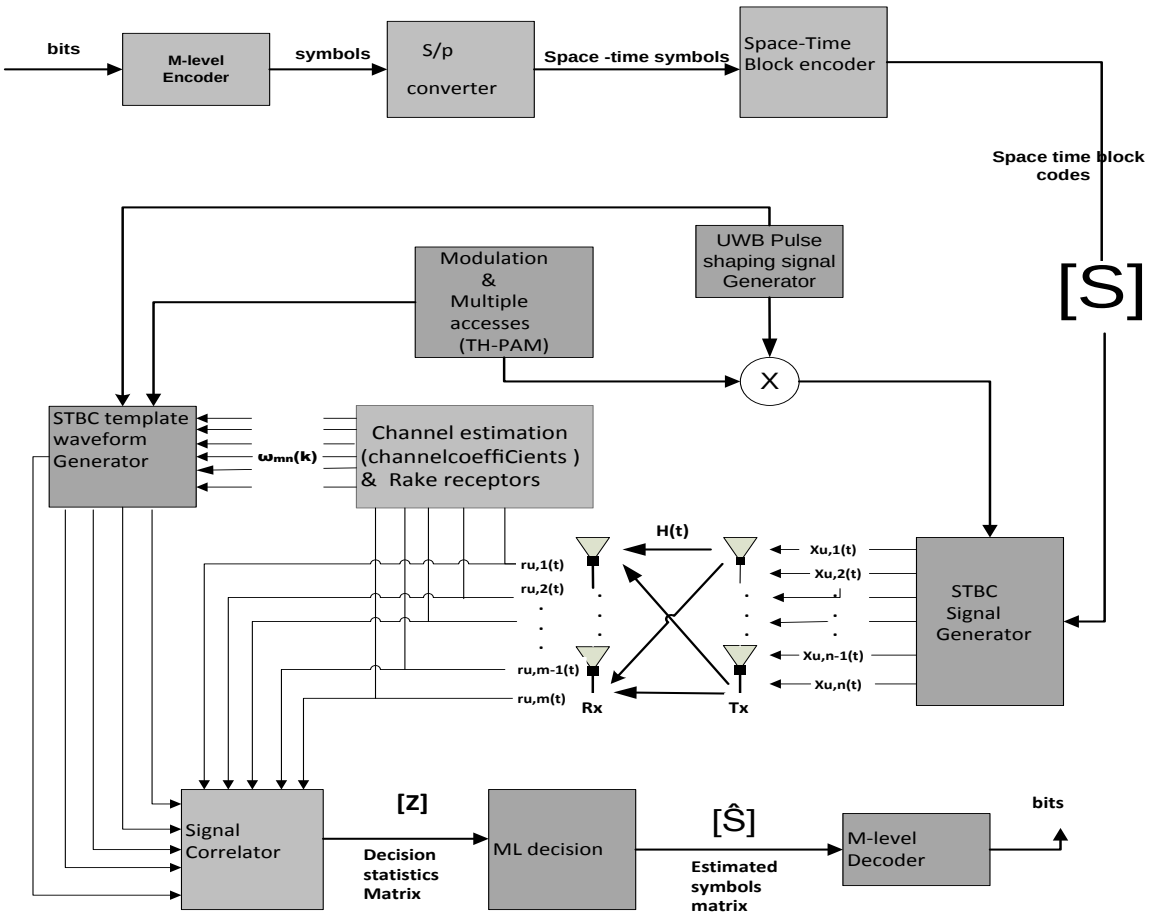

Fig.3.2 Block diagram of STBC-UWB-IR system, with N transmit and M receive antenna,

3.2.1 Transmitter description

Consider a communication system consisting of N transmit and Mreceives antennas with $N_u$users operate over a UWB channel. At any given time, for any user u, a bit stream flowstoward the input of the system and mapped into symbols. At each transmitter, the input binary symbol sequence is divided into blocks of N_b symbols. Each block is encoded into a ST Codeword to be transmitted over N transmit antennas during T time slots. Each ST Codeword matrix can then be expressed as a $N \times T$ ST block code matrix S^u whose $(T,n)^{th}$element $s_n^u(T)$,and represents the binary symbol transmitted by the u^{th}user at transmit antenna n over time slot T.The space–time codeword matrix can be expressed asan$N \times T$ matrix [4].

$$S^{u} = \begin{bmatrix} s_1^u(o)s_1^u(1) & \cdots & s_1^u(T-1) \\ s_2^u(o)s_2^u(1) & & s_2^u(T-1) \\ \vdots & \ddots & \vdots \\ s_N^u(o)s_N^u(1) & \cdots & s_N^u(T-1) \end{bmatrix} \quad (3.3)$$

Where $s_n^u(T)$ represents the binary symbol transmitted by the u^{th} user at transmitter antenna n over time slot T.

The ST Codeword $S^u(T)$ from transmitter is shaped into its corresponding UWB ST waveform matrix $X^u(t)$ whose $(T,n)^{th}$ element is the transmitted UWB signal $x_n^u(T,t)$ corresponding to the symbol $s_n^u(T)$. Finally, the N streams of waveforms are generated and distributed to N transmit antennas for simultaneous transmission as depicted in Fig. 3.2. Any transmit signal per antenna and symbol block, i.e. $s_n^u(t,i)$ is designed according to a random multiple-access technique. Every binary symbol is power loaded, pulse shaped, and transmitted repeatedly over consecutive frames[3, 36]. For TH-UWB systemsfrom equations (2.13, 2.14), the transmitted signal $x_n^u(t)$for UWB TH-PAM MIMO and UWB TH-PPM MIMO systems from the n^{th} antenna of theu^{th} user can be extended and expressed below respectively[24, 34, 35,].

$$x_n^u(t) = \sqrt{\frac{\epsilon_u}{NN_f}} \sum_{j=0}^{N_s-1} s_{n,j}^u \sum_{i=0}^{N_f-1} W_{tr}\left(t - jT_s - iT_{f-}C_{n,j,i}^u T_c\right) \quad (3.4a)$$

$$x_n^u(t) = \sqrt{\frac{\epsilon_u}{NN_f}} \sum_{j=0}^{N_s-1} \sum_{i=0}^{N_f-1} W_{tr}\left(t - jT_s - iT_{f-}C_{n,j,i}^u T_c - m_{n,j,i}^u \delta\right) \quad (3.4b)$$

Equation (3.4) describes mathematically how the encoding process is performed for each antenna and the transmitted signal vector $x^u(t)$is formed by stacking $x_n^u(t)$as follows:

$$x^u(t) = [x_1^u(t), x_2^u(t) \ldots\ldots, x_n^u(t)]^T \quad (3.5)$$

where $\sqrt{\frac{\epsilon_u}{N}}$is an energy normalization term, and $\sqrt{\frac{1}{N}}$ guarantees a total transmitted power equal to the one considered as in the case of single-antenna communication system.

$s_{n,j}^u$ and$m_{n,j}^u$correspond to the amplitude and the position of the j^{th} symbol transmitted from the n^{th}antenna of the u^{th} user respectively. δ is the separation between two consecutive modulation

positions.The monocycle pulse with duration T_w is normalized to have unit energy $\{\int_o^{T_w} w_{tr}^2(t)\,dt = 1\}$.$T_s$is the symbol duration and$T_s = N_f T_f$, $\epsilon_u$is the amplitude of different u^{th} user. N_f is the number of time-hopped pulses used to transmit one information symbol, T_f is the average separation between two consecutive pulses. Each one of these pulses is emitted during one time frame of durationT_f.

Each user is assigned a distinctive time-shift pattern $C_{n,j,i}^u$ called as TH sequence to allow the channel to be shared by many users and eliminate catastrophic collision. It takes values in $\{0,1,\ldots,N_{h-1}\}$. The frame time $T_f$and the chip time T_c are chosen to satisfy $N_h T_c \leq T_f$.The TH sequence $\{C_{n,j,i}^u\}$ are taken to be periodic with period N_f and therefore the subscript j can be dropped down. Moreover, the antennas of a given user will share the same pseudo-random TH sequence and the subscript n can be dropped down from the TH sequence [34, 35]. Equation (3.4) can be re-expressed as

$$x_n^u(t) = \sqrt{\frac{\epsilon_u}{NN_f}} \sum_{j=0}^{N_s} s_{n,j}^u \sum_{i=0}^{N_f-1} W_{tr}\left(t - jT_s - iT_{f\_}C_i^{(u)}T_c\right) (3.6a)$$

$$\mathrm{x_n^u(t)} = \sqrt{\frac{\epsilon_u}{\mathrm{NN_f}}} \sum_{\mathrm{j=0}}^{\mathrm{N_s-1}} \sum_{\mathrm{i=0}}^{\mathrm{N_f-1}} W_{tr}\left(t - jT_s - iT_{f\_}C_i^u T_c - m_i^u \delta\right) \qquad (3.6b)$$

3.2.2 Channel Model.

The wireless propagation channel (often referred to as only “the channel") is the medium linking the transmitter and receiver in a wireless system.The research field of channel modeling aims at providing the means for describing and emulating the channel in terms of certain quantities. In a UWB-MIMO system, the channel model is described by a channel impulse response (CIR) matrix. For N transmit antennas and M receives antennas the CIR matrix is adopted from the IEEE 802.15.3a single-antenna channel model and extended to $M\,x\,N$ matrix $H(t)$ formed by stacking the CIR $h_{n,m}(t)$ of each link [4]. Considering transmit–receive pairs will experience similar clustering structures, the impulse response of the UWB-MIMO channel can thus be constructed as [4]

$$H(t) = \sum_{c=}^{C} \sum_{l=1}^{L} A_{c,l}\, \delta\left(t - \tau_c - \tau_{c,l}\right) \tag{3.7}$$

where$H(t)$ is the CIR matrix of the system,$A_{c,l}$ is the amplitude fading matrix, where $\alpha_{c,l,}^{(m,n)}$denotesthe $(m,n)^{th}$entry of $A_{c,l}$ for the c^{th} cluster and l^{th}ray, and $\tau_c$and $\tau_{c,l}$have the same meaning as those in Eqn(2.27).To characterize the model for $H(t)$ completely, one needs to know the correlation functions among all the entries of each$A_{c,l}$. Since the matrices $\{A_{c,l}\}$ for different $C\ or\ l$ characterize the microwave propagations caused by different scatterers, it is reasonable to assume that the matrices $A_{c,l}$with different $C\ or\ l$ are independent of each other.Considering any of transmit – receive pairs will not experience similar clustering structures. Then, the entire channel can be described by an $M \times N$channel matrix $H(t)$ and described as

$$H(t) = \begin{bmatrix} h_{1,1}(t) & h_{2,1}(t) & ..... & h_{1,N}(t) \\ h_{2,1}(t) & h_{2,2}(t) & ..... & h_{2,N}(t) \\ .... & .... & .... & ..... \\ h_{M,1}(t) & h_{M,2}(t) & ..... & h_{M,N}(t) \end{bmatrix} \tag{3.8}$$

where $h_{m,n}\ (t)$ is the CIR of the channel from the n^{th} transmit antenna to the m^{th} receive antenna, which can be typically modeled as

$$h_{m,n} = \sum_{c=1}^{C} \sum_{l=1}^{L} \alpha_{c,l}^{m,n}\, \delta\left(t - \tau_c^{m,n} - \tau_{c,l}^{m,n}\right) \tag{3.9}$$

$\alpha_{c,l,}^{(m,n)}$is the tap gain from the n^{th}transmit antenna to the m^{th}receive antennafor thec^{th} cluster andl^{th} ray. In this case it is fair to assume that all $\{\alpha_{c,l,}^{(m,n)},\ c = 1,\dots,C, l = 1,\dots,L,\ m = 1,\dots,M,\ n = 1,\dots,N\}$ are independent of each other, and so are $\{,\tau_c^{(m,n)}\}$ and $\{,\tau_{c,l}^{(m,n)}\ \}$ respectively. Lognormal model (2.18) can be used to characterize the statistic distribution of$\left|\alpha_{c,l,}^{(m,n)}\right|$.Specifically, the statistical IR-UWB-MIMO channel model is described by MxN SISO time dispersive channel responses, [4, 31].

In indoor environmentin general,the doppler spectrum is quasi-constant. Accordingly, duration of each fading block can be very large. In other words, we assume that the channel is invariant over a block composed of a certain number of symbol durations and then the channel parameters change independently from one fading block to another.

By fact, the assumption of quasi-static fading may be considered well met when the coherence time $T_{coh}(ns)$ of the MIMO channel equates (at least) the signalling period T_s.

$$T_{coh}(ns) \geq T_s = N_f T_f \qquad (3.10)$$

typical UWB systems work at $N_f = 10$ and $T_f = 30(ns)$. the above inequality may be considered met when $T_{coh}(ns)$exceeds 250 - 300(ns) [33]. More precisely, we assume that it remains invariant over a symbol duration $N_f T_f$seconds, but it is allowed to change from symbol to symbol.

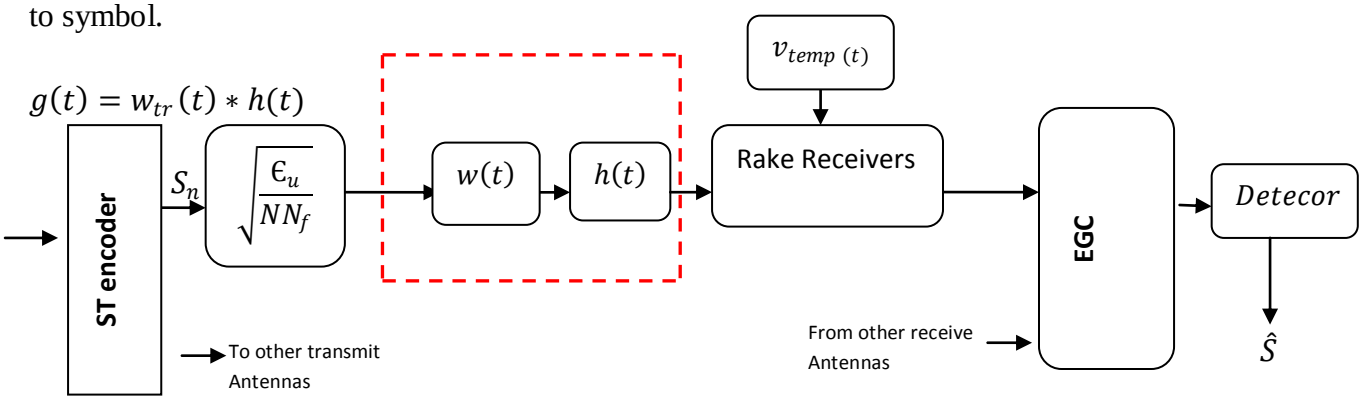

Fig 3.3 Generalized Multi antenna UWB-IR block diagram

3.2.3 Receiver processing

The signal received at each receive antenna is a superposition of the N transmitted signals. The received signals are further corrupted by AWGN; statistically independent among the m receiver antennas,across different symbol periodsand different resolvable paths of the same symbol. Here we assume perfect synchronization in the receiver, as well as perfect channel estimation.This means the Rake stages are capable to determine precisely the path delays and path amplitudes, and combine the 1stsignificant ones. At the receiver end, any element $y_m^u(t)$ of the received signal vector $Y^u(t)$ is obtained via the summation of the element-wise convolution of vectors$X^u(t)$ and matrix $H(t)$plus AWGN$N(t)$ vector with two-sided power spectral density$N_o/2$ such that

$$R^u(t) = X^u(t) * H(t) + N(t) \tag{3.11}$$

$$= [r_{u,0}(t), \ldots, r_{u,m}(t), \ldots, r_{u,M-1}(t)]$$

Designate by$h_{m,n}^{(u)}$; the impulse response of the frequency selective channel between the n^{th} transmit antenna and the m^{th} receive antennain a system comprising u interfering users: the received signal at the m^{th} receive antenna can be expressed as

$$r_m(t) = \sum_{u=0}^{N_u} \sum_{n=1}^{N} x_n^{(u)}(t) * h_{m,n}^{(u)}(t - t^{(u)} - T_{m,n}^{(u)}) + n_m(t) \tag{3.12}$$

Where * stands for convolution and $n_m(t)$ is the real AWGN noise with variance $N_o/2$at the m^{th}receive antenna.$t^{(u)}$ corresponds to the propagation delay of the u^{th} user with respect to the first user $(t^{(0)} = 0)$ where as$T_{m,n}^{(u)}$ corresponds to the arriving time of the first multi-path component of $h_{m,n}^{(u)}(t)$. In what follows: as shown in Fig. 3.3 the overall channel comprises the convolution of the pulse shaper with the physical multipath channel, and fixed as:

$$g_{m,n}^{(u)}(t) = w_{tr}(t) * h_{m,n}^{(u)}(t) \tag{3.13}$$

$$g_{m,n}^{(u)}(t) = g_{m,n}^{(u)}\left(t - t^{(u)} - jT_s - iT_{f\_}C_i^{(u)}T_c\right) \tag{3.14}$$

Following these notations and dropping the superscript u for the desired user and j for the desired symbol duration (the period during which the decision variables are collected) Eqn. (3.6a) is reduced to

$$x_n(t) = \sqrt{\frac{E_u}{NN_f}} S_n \sum_{i=0}^{N_f-1} W_{tr}\, tr\left(t - iT_{f\_}C_iT_c\right) \tag{3.15}$$

And combined Eqn. (3.12, 3. 14 and 3.15) together will result in:

$$r_m(t) = \sqrt{\frac{E_u}{NN_f}} \sum_{n=0}^{N} \sum_{i=0}^{N_f-1} S_n g_{m,n}(t - iT_{f\_}C_iT_c) + r_m^{(mui\,,MAI)} + r_m^{(isi)} + n_m(t) \tag{3.16}$$

The antennas of the same user will share the same TH sequence and hence multiple-access interference is $r_m^{(mui\,,MAI)}$ not considered in this work. Considering a single user we can also ignore the multiuser interference [24, 31]. The sum of interference produced by any transmitted symbol on the other transmitted symbols is denoted $r_m^{(isi)}$.In dealing with ISI in MIMO channels, channel equalizer can be used to mitigate the effects of ISI. However, the equalizer is much more complex in MIMO channels because the channel must be equalized over both space and time. Moreover, when the equalizer is used in conjuction with a space-time code, the nonlinear and non causal nature of the code further complicates the equalizer design[54]. Thus; to avoid Inter Symbol Interference (ISI), exceeding T_f from the UWB channel maximum delay-spread have been proposed in many papers and is of course agreeable since there is sufficient bandwidth and from the perspective complexity to apply equalizers. Inter Symbol Interference (ISI) can be thus eliminated by choosing $T_f \geq max_{m,n,u}\left(T_{m,n}^{(u)}\right) + (C_i T_C) + T_w$ where is $T_{m,n}^{(u)}$ the maximum delay spread of the channel $h_{m,n}^{(u)}(t)$ [24, 35, 36].In order to retrieve each symbol within the received signal with great accuracy and harvest the multipath diversity, a Rake receiver is employed at the receiver. In practice, only a subset of total resolved multipath components is used to take advantage of the multi-path diversity with moderate complexity [10, 51]. A simplified k^{th} order Rake receiver is assumed by choosing the finger delays as $\tau = kT_w$ for $k = 0,1,2 \ldots . K-1$ [24, 35, 36]. We assume that a suitable channel estimation algorithm is able to provide the template generator with reliable information about the delays and amplitudes of the MPC. However, for complexity reasons, it does not attempt to estimate the received waveform shape. This estimation algorithm may require the transmission of pilot symbols that would modify the structure of the transmitted signal [51].

Adopting fig.2.6 and eqn(2.42) to multiple antenna systems; at the receiver, we employ K-finger ($K \leq L$) Rake receivers,where each Rake finger is matched to a particular multipath component to combine the received multipaths coherently. In the case of PAM, the signal at each receive antenna is correlated with the following reference signal [35, 24] for the k^{th}rake finger, j^{th} symbol and i^{th}frame

$$v_{temp}(t-\tau_k) = \mathrm{V}_{m,n,i,k,j}(t) = w_{tr}\left(t - iT_s - jT_f - C_j T_c - \tau_{m,n,k}\right) \qquad (3.17)$$

Where $\tau_{m,n,k} = \tau_k = kT_w$ designates the delay of the k^{th} Rake fingers for $k = 0, \ldots, K-1$

At the m^{th} receive antenna, the output of the k^{th} Rake fingeris a decision statistic towards the decoding of the j^{th} transmitted symbol during each symbol duration. Outputs can be written in the matrix form.

$$z_{m,k} = \int_0^{iN_f} r_m(t) v_{temp}(t - \tau_k) dt$$

$$z_{m,k} = \sqrt{\frac{E_u}{NN_f}} \sum_{n=0}^{N} \sum_{i=0}^{N_f - 1} S_n \varphi_{m,n}(\tau_k) + w_{m,k} \quad (3.18)$$

$$\varphi_{m,n}(\tau) = \int_0^{T_f} g_{m,n}(t) w_{tr}(t - \tau)\, dt,$$

$$w_{m,k} = \int_o^{T_f} n_m(t)\, w_{tr}\left(t - iT_f - C_i T_c - \tau_k\right) dt \quad (3.19)$$

Given that the reference signals are different from zero only over a limited time interval (of duration T_w) and are equal to zero elsewhere, the correlation between the noise samples results in a white Gaussian noise since $w_{tr}(t)$ has unit energy [24, 34, 35].

Considering EGC, where all the tracked MPCs are weighted with their corresponding signs and combined;we limit ourselves to PRakes. It also simplifies our analysis. Assuming perfect channel estimation (the desired user's channel state information (CSI) is known at the receiver but not at the transmitter)and perfect synchronization, the template signal $v_{temp}(t)$for the desired user along with combining weight can be written as

$$v_{temp}(t) = \sum_{l \epsilon MPC} sgn\left(A_{c,l}\right) V_{m,n,i,k,j}(t) \quad (3.20)$$

Estimated combining weights are chosen as [52]

$$\omega_{m,n}(k) = \sum_{k=0}^{K-1} e^{-j\theta_{m,n,f}}\, \delta\left(t - \tau_{m,n,k}\right) \quad (3.21)$$

Decision statistic matrix towards the decoding of the j^{th} transmitted symbol for any user u is: $z =$

$$z_{m,k} * \omega_{m,n}(k) + \omega_{m,n}(k) * w_{m,k} \quad (3.22)$$

The resulting ML decision variables collected during each symbol duration corresponding to the symbol S corresponding to a given transmit antennas are then summed up over the number of receiver antennas, given by

$$\mathcal{Z} = \sqrt{\frac{E_u}{NN_f}} \sum_{i=0}^{N_f-1} \sum_{m=1}^{M} \sum_{n=1}^{N} \sum_{k=0}^{k-1} \left|\alpha_{m,n}(k) * \omega_{m,n}(k) R_w(\tau_{k,i})\right| [S_1 S_2 S_3 \dots S_N] + \eta(k) \quad (3.23)$$

Assume a perfect match of the received signal with the reference signal, inter-symbol interference, the correlation $R_w(\tau_{k,i})$ is resulted to unity. Then the output of k^{th} fingers of j^{th} symbol can be written as

$$\mathcal{Z} = \sqrt{\frac{\varepsilon}{N}} \sum_{m=1}^{M} \sum_{n=1}^{N} \sum_{k=0}^{K-1} \left|\alpha_{m,n}(k) * \omega_{m,n}(k)\right| S + \eta(l) \quad (3.24)$$

The equality (3.24) follows from the assumption that the channel is static across the N_f frames (for a given symbol of duration T_s) and can be written in matrix form as [3, 4].

$$\mathcal{Z} = \sqrt{\frac{\varepsilon}{N}} \mathcal{H} S + \mathcal{W} \quad (3.25)$$

For a N × T ST block code, $\mathcal{Z}$ and $\mathcal{W}$ are $Mk \times$T matrices corresponding to the decision variables and the noise terms, respectively and S isN × T code word symbol. $\mathcal{H}$ is $Mk \times$ N effective channel matrix which represents the energy captured by the Rake receiver with K-fingers of course log normally distributed [24, 41, 44].

Chapter 4

Diversity-Multiplexing Tradeoff analysis for Ultra Wideband-Multiple Antenna Systems (UWB-MAS)

Diversity–multiplexing gains tradeoff (DMT) presents a compact framework to compare various MIMO systems and channels in terms of the two main advantages they provide i.e. high data rate and/or low error rate. Increase in transmission reliability in a MIMO system is made possible by having an increased number of transmission data copies over the independent fading paths from each transmitter antenna to each receiver antenna. This results in a higher probability of receiving the correct data by combining all the faded copies of data at the receiver. The increase in transmission reliability (The speed that the error probability decays as SNR increases) is usually measured by the $diversity\ gain$.Roughly, the diversity gain refers to the gradient of the probability of error curve against SNR ratio. In case of slow Rayleigh fading environment with 1 transmits and m receive antennas; the transmitted signal is passed through m different paths. If the fading is independent across antenna pairs, a maximal diversity advantage of m can be achieved: the average error probability can be made to decay like $1/SNR^m$ at high SNR, in contrast to the SNR^{-1} for the single antenna fading channel. With n transmit and m receive antennas and Rayleigh fading channels, the maximal diversity gain is mn, which is the total number of fading gains that one can average over[16, 25].

Increase in transmission data rate in a MIMO system, on the other hand, is made possible by utilizing the available multiple antennas to increase number of different data streams sent over the parallel, independent fading paths (parallel spatial channels) from eachtransmitter antenna to each receiver antenna. This is beneficial through increasing the degrees offreedom available for communication and allows for a gain in the amount of data transmitted, i.e., a capacity gain, at no additional power or bandwidth requirements. Full data rate is achieved when onaverage, foreach transmitter antenna, a symbol is transmitted in each time slot. The increase in transmission data rate is usually measured by the $multiplexing\ gain$ [25] and is particularly important in the high signal-to-noise ratio (SNR) regime where the system is degree-of-freedom-limited (as opposed to energy-limited).

In [25] has shown that in the high SNRregime, the capacity of a channel with n transmit, m receive antennas and i.i.d. Rayleigh faded gains between each antenna pair is given by

$$C\ (SNR\ )\ =\ min\{m,n\}log\ SNR\ +\ O\ (1)$$

The number of degrees of freedom is thus the minimum of m and n .

However, from the fundamental limit in communication theory, increase in data transmission invariably leads to a decrease in system performance. This results in a fundamental trade-off between data rate and performance in a MIMO design [22, 25]. From the above discussion, we can see that MIMO technology allows for the improvement of data transmission rates as well as system performance. Each can be optimized according to the trade-off limit to provide superior wireless communication systems.The improvement of transmission data rate and system reliability in a MIMO system can be achieved by efficient STBC designs. Due to the fact that an increase in data rate invariably results in a loss of performance, the current optimum STBC designs aim to fix the data rate and design the code to optimize the performance measured in terms of the probability of error in the receiver.

To go over the main points, a MIMO system can grant two types of gains: diversity gain and spatial multiplexing gain. Yet, maximizing one type of gain may not necessarily maximize the other. For instance, it was observed in [38] that the coding structure from the orthogonal designs, while achieving the full diversity gain, reduces the achievable spatial multiplexing gain. Thus; higher spatial multiplexing gain comes at the price of sacrificing diversity and vice versa.Adifferent perspective: given a MIMO channel, both gains can in fact be simultaneously obtained, but there is a fundamental tradeoff between how much of each type of gain any coding scheme can extract. The tradeoff curve provides a more complete picture of the achievable performance over multiple antenna channels than the two extreme points. This able us to obtain insights to understand the overall resources provided by multiple antenna channels.

A common way to study the tradeoff is to compute the reliability function from the theory of error exponents [25]. Secondly, instead of using the machinery of the error exponent theory, one can exploit the special properties of fading channels and develop anapproach; based on the outage capacity formulation [38].

The conventional definition of multiplexing and diversity gains of a MIMO system refer to asymptotic quantities asthe SNR approaches infinity. For instance, consider a space-time system with average SNR per receive antenna γ, spectralefficiency R(bps/Hz) $R(\gamma)$, and corresponding outage probabilityP_{out} . The asymptotic multiplexing and diversity gains defined in [25, 38] are given by

$$r_{asymptotic} = \lim_{\gamma\to\infty} \frac{R(\gamma)}{log_2\gamma} \quad , \qquad d_{asymptotic} = \lim_{\gamma\to\infty} \frac{log_2 p_{out}(\gamma)}{log_2\gamma}$$

Hence; $R(\gamma) = rlog_2\gamma$ and $p_{out}(\gamma) = \gamma^{-d} = (1/SNR)^d$ (4.1)

In other words, r defines scaling of the achievable data rate $R(\gamma)$ with respect to $log_2\gamma$ whereas d defines the exponent of the corresponding outage rate.Intuitively, the multiplexing gain indicates how fast the transmission rate increases withthe SNR, γ, whereas the diversity gain represents how fast the outage probability decayswith the SNR, γ.If we let the transmission rate$R$ increase too quickly with γ, it is easy to imagine that the outage probability might notdecay very rapidly and vice-versa. In general a scheme is saidto have a spatial multiplexing gain r and a diversity advantage d in the high SNR region,if the rate of the schemescales like $r\ log\ SNR$ and the average error probability decays like$(1/SNR)^d$. This guides the diversity-multiplexing trade-offanalysis in given SNR, γ.The maximum achievable diversity gain $d(r)$ subject to a fixed multiplexing gain satisfies

$$d_{max}(r) = -\lim_{\gamma\to\infty} \frac{log_2 P\{C(\mathcal{H}, \gamma) < rlog_2\gamma\}}{log_2\gamma} \qquad 4.2$$

This thesis deals about a framework to characterize the diversity-multiplexing tradeoff of space-time codes for IR-UWB. The diversity gain at each SNR is obtained from the slope of the outage probability versus SNR curve. Significance of this definition for system design is that diversity gainat a particular operating SNR provides an indication of the additional power required to decrease the error probability by a specified amount. The multiplexing gain is measured as the ratio of the spectral efficiency of the MIMO systemto the capacity of an additive white Gaussian noise (AWGN) channel. The multiplexing gain can be interpreted in the context of rate adaptation in which the data rate is adapted as a function of SNR.For a constant multiplexing gain, the spectral efficiency increases with SNR.

4.1 Channel Capacity

Within communication theory, information theory answers two fundamental questions: what is the ultimate data compression, and what is the ultimate transmission rate of any communications system [7].We will only work out the second fundamental concept; capacity, which is usually defined as the maximum error-free data rate that a channel is ableto support.We need to abstract the physical process of communication, as it can be seen in Figure 4.1. A sequence of source symbols (denoted as message in Figure 4.1) from some finite alphabet is mapped viaan encoder on some sequence X of channel symbols, which then produces the output sequence$Y$ of the channel. The output sequence is random but has a distribution that depends on the specific input sequence. From the output sequence, we attempt to recover the transmittedmessage via a decoder.

Fig. 4.1General communication system.

Each of the possible input sequences induces a probability distribution on the output sequences.By mapping the source messages into appropriate inputsequences for the channel, we can transmit a message with very low probability of confusion(or equivalently, error) at the decoder and reconstruct the source message at the output via the decoder. The maximum rate at which this can be done is called $the\ capacity$of thechannel.

Definition 4.1 (Channel capacity): Let $x\ and\ y$ be the input and output of a discrete vectorchannel with input alphabet X and output alphabet Y , respectively. If the probability distributionof the output depends only on the input at that time, and is conditionally independent ofprevious channel inputs or outputs, then, Shannon defined the channel capacity C as the maximum mutual information $I(x,y)$ given by [7]

$$\boldsymbol{C} \triangleq \max_{p(x)} I(X;Y) \tag{4.3}$$

where; the maximum is taken over all possible input distributions $p(x)$.This allowed him to quantify the capacity per channeluse of a channel with additive white Gaussian noise (AWGN).

Finally, Shannon showed that a signal essentially limited to duration T and bandwidth Bw can be represented by approximately $2BwT$ samples (or dimensions). The capacity of a bandlimited signalcan be found to be

$$\boldsymbol{C} = BwTlog_2(1 + SNR) \tag{4.4}$$

Shannon then defined the channel capacity in [bits/s] as the capacity of the $2BwT$ samples per time T, i.e.

$$\boldsymbol{C} = \lim_{T\to\infty} \frac{BwTlog_2(1 + SNR)}{T} = Bwlog_2(1 + SNR) \tag{4.5}$$

In this thesis, the normalized channel capacity is used for notational simplicity. It is definedas the channel capacity per unit bandwidth, which simplifiesEqn(4.5) to

$$C = log_2(1 + SNR) \tag{4.6}$$

Finally, Shannon proved that anerror-free transmission rate exceeding the channel capacity is impossible. We can describe the capacity of a discrete memoryless channel as the supremum of all achievable rates. Thus, rates less than capacity yield arbitrarily small probability of error for sufficiently large block lengths.

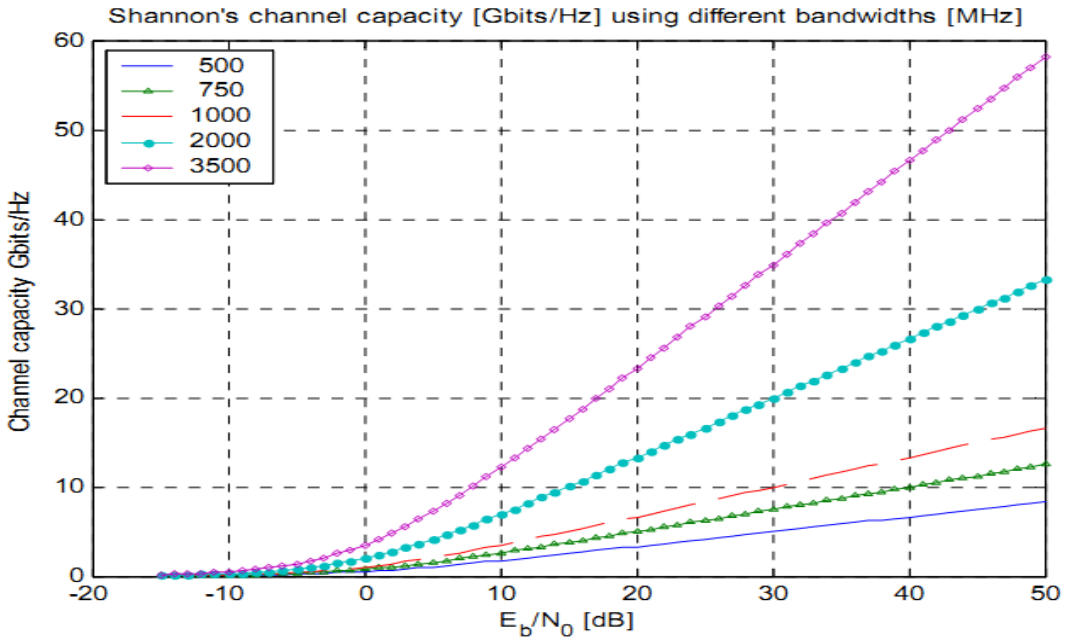

Fig.4.2. Shannon's channel capacity for different bandwidths as a function of $SNR(Eb/N0)$

4.2 Capacity of Random MIMO Channels

This section focuses on the Shannon capacity of a MIMO channel, which equals the maximum data rate that can be transmitted over the channel with arbitrarily small error probability. Communication is achieved by properly encoding the information$S$ at the transmitter spanned by n number of antennas acrossthe temporal and spatial dimensions to produce a given space-time codeword. This code-word is transmitted with average power P and received by the receiverwith $m$number of antennas which has an averagenoise power NO.The receiver performs appropriate decoding to yield an estimate $\hat{S}$of theoriginally transmitted information S.

The mutual information of a MIMO channel in the case that the channel matrix is$\mathcal{H}$ wheredeterministic could be written as [22, 25, 38]

$$I(x;y) = log\left\{det\left(I + \frac{\gamma}{N}\mathcal{H}R_{xx}\mathcal{H}^H\right)\right\} \quad [bps/hz] \tag{4.7}$$

Then we can write the capacity of the MIMO channel (within our power constraint P) as

$$C = \max_{R_{xx}:tr(R_{xx})\leq p} log\left\{det\left(I + \frac{\gamma}{N}\mathcal{H}R_{xx}\mathcal{H}^H\right)\right\} \tag{4.8}$$

R_{xx} represents the covariance of the input symbols, therefore $tr\,(R_{xx}\,) \leq P$ is bounded by$p$. When T_{coh} is much smaller than the codeword duration T , the channel is defined as fast fading. Any codeword experiences a large number of different channel realizations (at the limit, the whole channel distribution is explored) and the achievable rate is well represented by the so-called ergodic capacity. It is the ensemble average of the information rate over the statistics of the channel matrix. The effective channel matrix $\mathcal{H}$ is a random quantity and hence the associated channel capacity $C(\mathcal{H})$ is also a random variable. To deal with this circumstance, we assume the elements$\mathcal{H}$ is known to the receiver, thenergodic channel capacities (bps/Hz) of a system with N transmit and M receive antennas is given by

$$C_E = E\left\{\max_{R_{xx}:tr(R_{xx})\leq p} logdet\left(I + \frac{\gamma}{N}\mathcal{H}R_{xx}\mathcal{H}^H\right)\right\} \tag{4.9}$$

Here the expectation is with respect to the distribution on the channel matrix $\mathcal{H}$.The capacity (4.9) is obtained by averaging (4.8) over all realizations of $\mathcal{H}$.

After having identified the channel capacity in a fading MIMO environment, it remains to evaluate the optimal input power distribution, or covariance matrix R_{xx} that maximizes Equation (4.9).If the channel $\mathcal{H}$ is known to the transmitter, the transmit correlation matrix R_{xx} can bechosen to maximize the channel capacity for a given realization of the channel. The main tool for performing this maximization is commonly referred to as water-filling [16] which we will not restate here.

We chose to focus on the case of perfect CSI on the receiver side and no CSI at the transmitter. Maximization of Equation (4.9) is now morerestricted and showed that theoptimal signal covariance matrix has to be chosen according to $R_{xx} = E[XX^H] = I$. When no CSI at the transmitter, it equally divides the power among the transmit antennas; i.e. the antennas should transmit uncorrelated streams with the same average power. Thechannel capacity reduces to

$$C_E = E\left\{logdet\left(I_M + \frac{\gamma}{N}\mathcal{H}\mathcal{H}^H\right)\right\}$$

$$= E\left\{logdet\left(I_N + \frac{\gamma}{N}\mathcal{H}^H\mathcal{H}\right)\right\} \quad (4.10)$$

4.3 Outage Capacity

In contrast to an ergodic fading channel, the channel realizations of a non-ergodicchannel are randomly fixed at the beginning of the transmission and kept constant over theduration of the codeword transmission. Therefore; there is a non-zero probability that agiven transmission rate cannot be supported by the channel [25, 38]. The probabilitythat a certain communication rate can be supported by a channel can be gauged, and isreferred to as the rate outage probability.Since the MIMO channel capacity (4.10) is a random variable, it is meaningful to considerits statistical distribution. A particularly useful measure of its statistical behavior is theso-called outage capacity.

Definition 4.2(Outage MIMO channel capacity). The $q\%$ outage capacity $C_{out}\ (q)$ is definedas the information rate that is guaranteed for $(100\ -\ q\ )\%$ of the channel realizations, i.e.

$$P(C(\mathcal{H}) \leq C_{out}(q)) =\ q\ \%$$

The outage capacity is often a more relevant measure than the ergodic channel capacity, because it describes in some way the quality of the channel. Theoutage capacity measures how far the instantaneous rate supported by the channel is spread,in terms of probability. So if the rate supported by the channel is spread over a wide range, the outage capacity for a fixed probability level can get small, whereas the ergodic channel capacity may be high. This means that for any non-zero signaling rate there is always a finite probability that the channel is unable to support it.If we use very large block size and optimal coding, the packet is always decoded successfully if the channel supports the rate and is always in error otherwise. Using independent realizations of the CM2 channel model [6], we have calculated outage capacity at an outage of = 0.1 for all possible antenna formations. These results are depicted in Figure 4.2. We can see that at medium SNR, (N=2, M=2) system can provide double the data rate that can be achieved by the (N=1, M=1) system with the same bandwidth. Also, (N=1, M= 2) system has certain advantage over the (N=1, M=1)system from the capacity point of view.

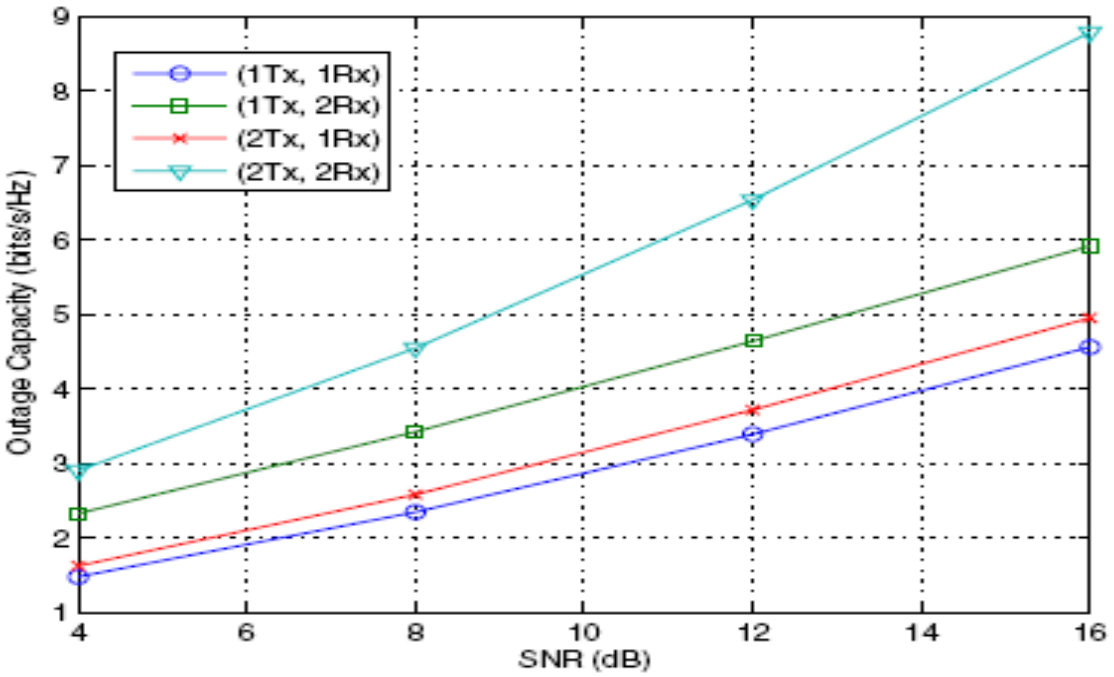

Fig. 4.3 Outage Capacity of MIMO UWB Channels

An outage is thus; defined as the event that the mutual information of this channel does not support a target data rate: [25, 38]

$$(\mathcal{H}: I\,(x;\ y/\mathcal{H} = \mathcal{H}) < R) \tag{4.11}$$

Where $X\ and\ Y$ are defined in definition 4.1

$$I\,(x;\ y/\mathcal{H} = \mathcal{H}) = log\ det(I + \frac{\gamma}{N}\mathcal{H}R_{xx}\mathcal{H}^{H}) \tag{4.12}$$

A detection error can occur as a result of the combination of the following three events: the channel matrix$\mathcal{H}$ is typically ill-conditioned, the additive noise is typically large, or some code words are typically close together. By going to the outage formulation the problem is simplified by allowing us to focus only on the bad channel event. When there is no outage, the error probability is very small [25]. Thus;

$$\begin{aligned} Pe\ (SNR)\ &\leq P\ (error\ /\ outage)\ +\ P\ (error/\ no\ outage) \\ &\leq\ Pout\ (R)\ +\ P\ (error/\ no\ outage) \end{aligned} \tag{4.13}$$

This result says that conditioned on the channel outage event, it is very likely that a detection error occurs; therefore, the outage probability is a lower bound on the error probability.

Hence; the average error probability Pecan be lower-bounded and upper-bounded as [22]

$$Pout\ (R)\ \leq Pe\ (SNR) \leq\ Pout\ (R)\ +\ P\ (error/\ no\ outage) \tag{4.14}$$

From this formulation; for a system with unity bandwidth and rate R, the probability of error can be lower bounded as

$$P\big(P_e \geq\ \ P(C(\mathcal{H}) < R)\big) = P\left(\mathcal{H}: logdet\left(I + \frac{\gamma}{N}\mathcal{H}\mathcal{H}^{H}\right) < R\right) \tag{4.15}$$

In capacity with outage; thetransmitter fixes a transmission rate R, and the outage probability associated with R is theprobability that the transmitted data will not be received correctly or, equivalently, the probability that the channel $\mathcal{H}$ has mutual information less than R.Optimizing over all input distributions, the outage probability is [22]

$$P_{out}\,(R) = P\left[\mathcal{H}: log\ det(I_M + \frac{\gamma}{N}\mathcal{H}\mathcal{H}^{'}) < R\right]$$

$$= P\left[\mathcal{H}: log\ det(I_N + \frac{\gamma}{N}\mathcal{H}^{'}\mathcal{H}) < R\right] \tag{4.16}$$

The probability is taken over the random channel matrix$\mathcal{H}$ andR could be set$r * log\ (1+\gamma)$at finite SNR and $r * log\ (\gamma)$ for high SNR.In the outage capacity formulation, we can ask a question as given a target rate R which scales with SNR as $log\ (1+\gamma)$for finite SNR, howdoes the outage probability decrease with the SNR?

4.4 Capacity of Orthogonalised MIMO Channels (OSTBC)

Closed form representations of the capacity of MIMO channels of arbitrary statistics, correlation and attenuation between the transceiver elements have proven to be difficult to derive. This is mainly because of the difficulty to find the pdf of the eigenvalues involved in representingthe power of each uncorrelated sub-channel.Fortunately, space-time block codes inherently orthogonalize the MIMO channel. Theyare known to reduce the MIMO channel into parallel SISO channels, which drasticallysimplifies analysis. Orthogonal space–time block codes (OSTBCs) are a very important sub-class of linearSTBCs. They have remarkable properties which make them extremely easy to decode,while still achieving a full-diversity at high SNR region [22].

Transmitted symbols are encoded with an orthogonal space-time coding matrix S of size NxT, where$T$the number of symbol durations required to transmit the space-time code word, and N is the number of transmit elements. At each time instant $1 \leq t \leq T$, the space-time encoded symbol $s_{t,i} \in$ Sistransmitted from the n^{th} distributed transmit element as described in chapter 3, where $n = 1, \ldots, N.$ such encodingmay come at a decrease in code rate R_s, defined as $R_s \equiv Q/T$ (Since Q symbols are transmitted per T symbol durations). There are two classes of orthogonal codes, using real symbol constellations (RealOSTBCs) or complex symbol constellations (Complex OSTBCs).Real OSTBCs with spatial multiplexing rate $R_s = 1$can be designed for any number of transmit antennas [22]. As example of real OSTBC; for three transmit and two transmit antennas ($S_3,\ S_2\ for\ N = 3, 2$), a real OSTBC expanding on four and two symbol durations ($T = 4, 2$) with a code rate equal to one is given by

$$S_3 = \frac{1}{\sqrt{3}}\begin{bmatrix} s_1 & -s_2 & -s_3 - s_4 \\ s_2 & s_1 & s_4 \quad -s_3 \\ s_3 & -s_4 & s_1 s_2 \end{bmatrix} S_2 = \frac{1}{\sqrt{2}}\begin{bmatrix} s_1 & -s_2 \\ s_2 & s_1 \end{bmatrix}$$

Symbols$s_1, s_2, s_3$and s_4 originate from a real symbol constellation. For S_3, the code is delay-optimal in the sense that $T = 4$ is the smallest delay achievable to guarantee a full-diversity real OSTBC with a code rate of one for three transmit antennas. The Alamouti code has a spatialmultiplexing (code) rate $R_s = 1$since two symbols are transmitted over two symbol durations.

To yield orthogonality, the transmission matrix $S(s_1, s_2, s_3, \ldots \ldots s_q)$ with the real orthogonal design (ROD)has to satisfy;

$$SS^H \propto \left(\sum_{i=1}^{k} |s_i|^2\right) I_N \tag{4.17}$$

OSTBCs transform the MIMO channel into equivalent SISO channels [22, 25] and the decision variable matrix is formulated as

$$Z = \sqrt{\frac{E_s T}{NK} \|\mathcal{H}\|_F^2 S} \quad + n \tag{4.18}$$

Adopting the capacity of multi antenna wireless systems over flat fading channel from Eqn (4.10)and from the representation in Eqn(4.18); the instantaneous capacityfor an arbitrary orthogonalSTBC of code rate; $R_s$is given as [22, 38]

$$C = E\left\{log\left\{det\left(I_M + \frac{\gamma}{N}\mathcal{H}\mathcal{H}^H\right)\right\}\right\}$$

$$= E\left\{R_s log_2\left(I + \frac{\gamma}{R_s N}\|\mathcal{H}\|_F^2\right)\right\} \tag{4.19}$$

The squared Frobenius norm of the effective channel $\mathcal{H}$, $\|\mathcal{H}\|_F^2$ is given by

$$\left|\left|\mathcal{H}\right|\right|_F^2) \equiv TR\ (\mathcal{H}\mathcal{H}^H) = \sum_{m=1}^{M}\sum_{n=1}^{N}\left(\hbar_{m,n}\right)^2 \tag{4.20}$$

The SNR, γ is the effective signal-to-noise ratio.Frobenius norm is interpreted as the total power gain of thechannel and it is also a random variable, whose distribution should be analyzed.The

outage properties of OSTBC could be superior to the outage obtained with optimal coding for a given transmission rate, because OSTBC fundamentally improves the link.

4.5 Diversity-Multiplexing Tradeoff (DMT) analysis for Finite SNR

Owing to the regulations imposed; the power spectral density of the transmitted UWB signal is rather limited and need to be operational in the low power region. Secondly,the DMT at asymptotic result as the signal-to-noise ratio (SNR) approaches infinity [25] suggest that the maximum diversity gain can only be achieved at very high SNR; despite wireless communication systems do not operate in thisregionin practice. Recently, several papers have noted also codes designed for maximum performance at high SNR inindependent Rayleigh fadingchannels are not optimal at low to medium SNR, especiallyin the presence of correlated fading [22].

For this thesis, rather than studying the DMT at asymptotic values of the SNR as in [25], we choose to apply the framework proposed in [38] for determining the DMT at finite values of the SNR γ. This characterizes achievable diversity and multiplexing gains for a givenspace-time code at SNR's encountered in practice.The formulation in equation (4.16) is used to characterize thediversity-multiplexing tradeoff of space-time codes as a function of SNR. The significance of this formulation for system design is that the diversity gainat a particular operating SNR provides an indication of the additional power required to decrease the error probability by a specified amount. The DMT at finite SNR is generalizations of the corresponding definition given for anasymptotic result as the signal-to-noise ratio (SNR) approachesinfinityas discussed in section 3.1.Capacity and Outage formulations are used in each block such thatthe probability that the mutual information between the transmitted and received signals is less than the target data rate. Such ablock fading model is applicable in several wireless systems.For instance, the channel in a wireless local area network is constant for the duration of a packet and varies from packetto packet. Thus, with capacity achieving codes applied to each packet, the packet error rate is determined by the outageprobability [38].

As stated in section 4.3 the non-asymptotic definitionfor the multiplexing gain r isdefined as the ratio of R to the capacity of an AWGN channelat SNR, γ [22, 38].

$$r = \frac{R(\gamma)}{log_2(1+\gamma)}\,, \qquad R(\gamma) = r * log\,(1+SNR) \tag{4.21}$$

Note that for a constant multiplexing gain r, the spectral efficiency must increase as the γ. increases. The multiplexing gain r provides an indication of the sensitivity of a rateadaptation algorithm as the γ changes. As the value of $r$increases, a more sensitive rate adaptation strategy is used inwhich a moderate change in γ can result in a significant change in the data rate.

The diversity gain $d(r,\gamma)$ of a systemwith multiplexing gain r at SNR γ is defined by the negative slope of the $log - log$ plot of outage probability versus γ for a transmission rate $R(\gamma)$[22, 38]:

$$\begin{aligned} d(r,\gamma\ ) &\triangleq\ -\frac{\partial \log\big(Pout(R)\big)}{\partial \log(\gamma)} \\ &= -\frac{\gamma}{P_{out}\,(r,\gamma)}.\frac{\partial Pout(r,\ \gamma\ )}{\partial \gamma}, \end{aligned} \tag{4.22}$$

ConsideringOSTBC schemefora given channel realization$\mathcal{H}$, the maximum mutual information (Capacity) for OSTBC with spatial code rate R_s is given by equation (4.19). Hence the outage probability equation (4.16) could be simplified as

$$\begin{aligned} P_{out}\,(r,\gamma)\ &= P(C(\mathcal{H}) < r log_2(1+\gamma\ ) \\ &= P(R_s log_2(1+\frac{\gamma}{N}||\mathcal{H}||_F^2) < r\ log_2(1+\gamma\ ) \end{aligned} \tag{4.23}$$

The random variable $||\mathcal{H}||_{\mathrm{F}}^2$represents the total energy of the channel whose distribution should be analyzed.Studying the DMT tradeoff for any numbers of antennas compels the knowledge of the jointprobability density function of the eigenvalues of the channel matrix in eqn(4.23). While this distributionis known in the case of Gaussian random matrices [22,25, 38], it is difficult to estimate the entire distributionof lognormal distributions(do not lend themselves to an analytical solution.)and no close-form expression can be found (Up to my knowledge).Wethus present a statistical approximation of thedistribution of the elements of the channel $||\mathcal{H}||_{\mathrm{F}}^2$. Thus we consider the case of $N = n\ /M = 1$ or $M = m/N = 1$;where $n\ \leq N\ and\ m \leq M$.

$$P_{out\,,M=1}(r,\gamma) = P(R_s log_2(1+\frac{\gamma}{N}\sum_{n=0}^{N}(\hbar_n)^2) < r\ log_2(1+\gamma) \tag{4.24}$$

$$= \; P(R_s log_2(1+\frac{\gamma}{N}\psi) < r\, log_2(1+\gamma) \;\Rightarrow\; P\left(\left(1+\frac{\gamma}{N}\psi\right) < (1+\gamma)^{\frac{r}{R_s}}\right)$$

$$P_{out,M=1}(r,\gamma) = P(\psi < \left(\frac{N}{\gamma}\left((1+\gamma)^{\frac{r}{R_s}}-1\right)\right) \quad (4.25a)$$

$$P_{out,N=1}(r,\gamma) = P(\psi < \left(\frac{1}{\gamma}\left((1+\gamma)^{\frac{r}{R_s}}-1\right)\right) \quad (4.25b)$$

We present a statistical approximation of the distribution of the ψ random variable describing the behavior of the independent and identically distributed variables $(\hbar_n)^2$, $(\hbar_m)^2$(power elements of the effective channel or the received energy at the receiver)for all values of transmit antenna N or Receiving antennas M. Therefore:

From the property of lognormal and standard Normal Gaussian Cumulative Distributiondelt in section 2.4eqn(2.19, 20); equ (2.25) can be reduced to

$$P_{out}(r,\gamma) = P\left(\ln(\psi) < \ln\left(\frac{N}{\gamma}\left((1+\gamma)^{\frac{r}{R_s}}-1\right)\right)\right)$$

Where $\ln(\psi)$ is normally distributed

$$P_{out,M=1}(r,\gamma) = \Phi\left(\frac{-\mu-\ln(\gamma/N)+\ln\left((1+\gamma)^{\frac{r}{R_s}}-1\right)}{\sigma}\right) (4.26a)$$

$$P_{out,N=1}(r,\gamma) = \Phi\left(\frac{-\mu-\ln(\gamma)+\ln\left((1+\gamma)^{\frac{r}{R_s}}-1\right)}{\sigma}\right) \quad (4.26b)$$

From eqn (2.21)we have;

$$\Phi(x) \triangleq \frac{1}{2\Pi}\int_{\infty}^{x} e^{\frac{-t^2}{2}}dt = \frac{1}{2}\left(1+erf\left(\frac{\ln(x)-\mu}{\sigma\sqrt{2}}\right)\right) \; and \; \frac{d}{dx}erf(x) = \frac{2}{\sqrt{\Pi}}e^{-t^2}$$

And the diversity gain $\mathrm{d}(\mathrm{r},\gamma)$for OSTBC given by eqn (4.22)as a function of SNR γ and multiplexing$r$ is given by

$$\mathrm{d}_{M=1}(\mathrm{r},\gamma) = \frac{1}{\sqrt{2\Pi}\sigma}\frac{1}{\Phi\left(\frac{-\mu-\ln(\gamma/N)+\ln\left((1+\gamma)^{\frac{r}{R_s}}-1\right)}{\sigma}\right)} e^{-\frac{1}{2}\left(\frac{-\mu-\ln(\gamma/N)+\ln\left((1+\gamma)^{\frac{r}{R_s}}-1\right)}{\sigma}\right)^2}\left(-1+\gamma\frac{\mathrm{r}}{\mathrm{r_s}}\left(\frac{(1+\gamma)^{\frac{r}{R_s}-1}}{\left[(1+\gamma)^{\frac{r}{R_s}}-1\right]}\right)\right) (4.27a)$$

$$d_{N=1}(r,\gamma\ ) = \frac{1}{\sqrt{2\Pi}\sigma}\frac{1}{\Phi\left(\frac{-\mu-\ln(\gamma)+\ln\left((1+\gamma)^{\frac{r}{R_s}}-1\right)}{\sigma}\right)} e^{-\frac{1}{2}\left(\frac{-\mu-\ln(\gamma)+\ln\left((1+\gamma)^{\frac{r}{R_s}}-1\right)}{\sigma}\right)^2}\left(-1+\gamma\frac{r}{r_s}\left(\frac{(1+\gamma)^{\frac{r}{R_s}-1}}{\left[(1+\gamma)^{\frac{r}{R_s}}-1\right]}\right)\right) \quad (4.27b)$$

The mean and Standard deviation of the$\ln(\psi)$in equations above have to be determined. But to estimate the entire sum of lognormal distributions ψ, there is no known exact result for the statistics of the sum of several lognormal signal components but approximations [40, 43]. The common feature of these log-normal sum approximations is that they model the sum distribution being lognormal. Several approximationsfor probability distribution of a sum of independent lognormal RV's have been derived andreported for this purpose, including Wilkinson's, Schwartz-Yeh's, and Farley's methods [40]. Formostcommunicationapplications*Fenton-Wilkinson (FW) approximation*is widely used.We considerthis widely used approximation presented below.

The sum of N lognormal random variables $L_n$can be represented by the expression

$$L = \sum_{n=0}^{N} L_n = \sum_{N=0}^{N} e^{y_n} = e^{z} \quad (4.28)$$

Where, y_n and z are normal Gaussian random variable

Fenton-Wilkinson (F-W) method computes $\mu_z$andσ_z^2 by exactly matching the first and second central moments ofnormal Gaussian random variable *z*of the both sides of equation (4.28).
If the first moment of is denoted $(L_1 + L_2 + L_3 + \cdots L_n)$ by μ_1, it can be derived to be

$$\mu_1 = E[L] = [e^z] = \sum_{i=0}^{N} e^{m_{yi}+\sigma_{yi}^2/2} \quad (4.29)$$

The second moment μ_2, as well can be obtained as

$$\mu_2 = E[L^2] = [e^{2z}] = \sum_{i=0}^{N} e^{2m_{yi}+4\sigma_{yi}^2/2} + 2\sum_{i=1}^{N-1}\sum_{j=i+1}^{N}\left(e^{m_{yi}+m_{yj}+\frac{1}{2}(\sigma_{yi}^2+\sigma_{yj}^2)}\right) \quad (4.30)$$

Generally, the k^{th}moment of the lognormal random variable is given

$$E[L^k] = \exp\left(km_{yi} + k^2\sigma_{yi}^2/2\right) \quad (4.31)$$

From equ (41 and 42) [44]:

$$\mu_z = 2\ln \mu_1 - \frac{1}{2}\ln\mu_2 \quad (4.32)$$

$$\sigma_z^2 = ln\mu_2 - 2\ln \mu_1 \quad (4.33)$$

These equations are helpful in determining the moments for multiple antennas.

Thus we can find the distribution of the parameters $\mu, \sigma$of the function $\Phi(.)$, where the parameter $\psi = \sum_{n=0}^{N}(\hbar_n)^2)$ or $\psi = \sum_{m=0}^{M}(\hbar_m)^2)$ is the sum of the random variables, given that $(\hbar_1)^2, (\hbar_2)^2, \ldots\ldots (\hbar_N)^2$or $(\hbar_1)^2, (\hbar_2)^2, \ldots\ldots (\hbar_M)^2$are lognormal random variables, where their sum can be well approximated by a lognormal random process. Moreover they have the same parameters μ_z and σ_z^2[44]. The first and second moments of $|\alpha_{c,l}|$ aregiven by [53]

$$E\left[\left|\alpha_{c,l}\right|\right] = \exp\left(\frac{\ln(10)}{20}\mu_{c,l} + \frac{1}{2}\left(\frac{\ln(10)}{20}\right)^2 {\sigma^2}_{eff}\right) \quad (4.34)$$

$$E\left[\left|{\alpha_{c,l}}^2\right|\right] = \exp\left(\frac{\ln(10)}{10}\mu_{c,l} + \frac{(\ln(10))^2}{200}\ {\sigma^2}_{eff}\right) \quad (4.35)$$

Where $\mu_{c,l}$ is given in eqn (2.33), then substitute for eqns (4.29 and 4.30).

Chapter 5

Simulation Results and Discussion

Finite-SNR DMT provides useful insight for UWB channels under realistic propagation conditions.This section provides some numerical results on the outage probabilities and diversity-multiplexing tradeoff curves, and comparison with asymptotic results.Simulation results for multiple antenna systems (SIMO/MISO) and Rake receivers under different channel models have been illustrated. All The simulation results are obtained by considering any channel model scenario of the full CIR generated by the Matlabprogram. Analysis and comparison for each result is discussed in detail. The basic simulation parameters and their corresponding values are given Table 5.1.

. Some of these basic assumptions include:

- Channel estimation is assumed to be perfect at the receiver side when acoherent reception technique is applied, i.e., EGC.
- Channel State Information (CSI) is known at the receiver but not at the transmitter
- Synchronization at the receiver side is assumed to be perfect.
- Each link of the channel $(n, m)$is considered to be spatially and mutually uncorrelated from the others.
- Results are averaged over 100 independent realizations of the CIR for all channel models CM1, CM2, CM3 and CM4 using the relevant channel parameters given in Table 2.1.
- For sake of brevity one or more of the channel models might be considered for each scenario.

Table 5.1 basic simulation parameters

System	UWB Multi-antenna system
UWB Multi-antenna system	UWB-IR-MISO/SIMO
# transmit antenna	1-4
# transmit antenna	1-4
Channel model	Standard IEEE 802.15.3a channel (CM1, CM2, CM3, CM4,) or ch-1-ch-4
Noise at the receiver	AWGN
Modulation & multiple access	PAM-TH
Receiver	Rake receiver
# Rake fingers	2-20
SNR range	0-50dB
Extra Channel coding	No

5.1 Outage probabilities Vs SNR for different multiplexing gains r

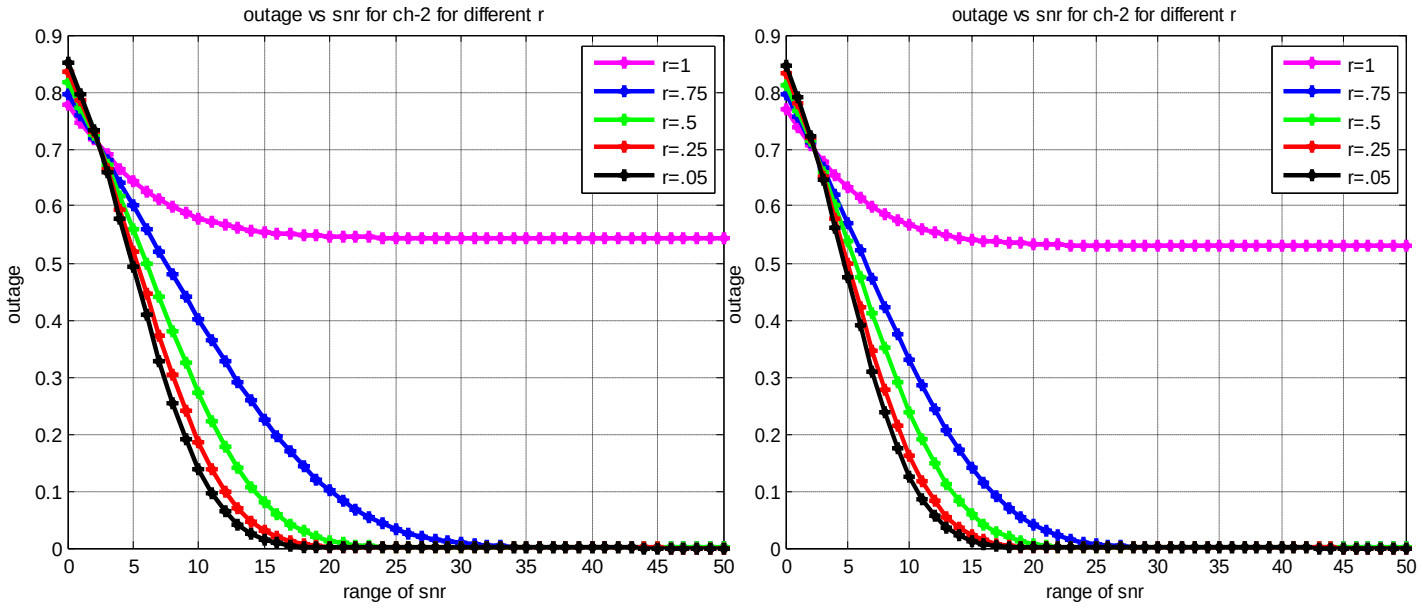

Fig.5.10 Outage probability of OSTBC for different multiplexing gains $r, CM2,$ SISO system (a) $k = 2, (b)$ $k = 5$

Outage probability curves provide a measure of system performancefor a particular sensitivity of the rate adaptation approachrepresented by the multiplexing gain r. With reference to Fig.5.10, we show the relationship between SNR, r and outage probability plotted P_{out} as functions of SNR and r.The outage probability of OSTBC UWB decreases significantly even for moderate sensitivities($e.g., r = 0.5$). This is for the reason thatOSTBC depends on the Frobenius norm of the channel rather than the channel singular values. If we spend all the SNR on the reduction of P_{out} and keep the rate constant, we can get increased the ordersof magnitude inP_{out} reduction for every additional SNR values. Taking($e.g., r = 0.25$) in Fig.5.10 for every additional 5 dB in SNR P_{out} decreases rapidly.

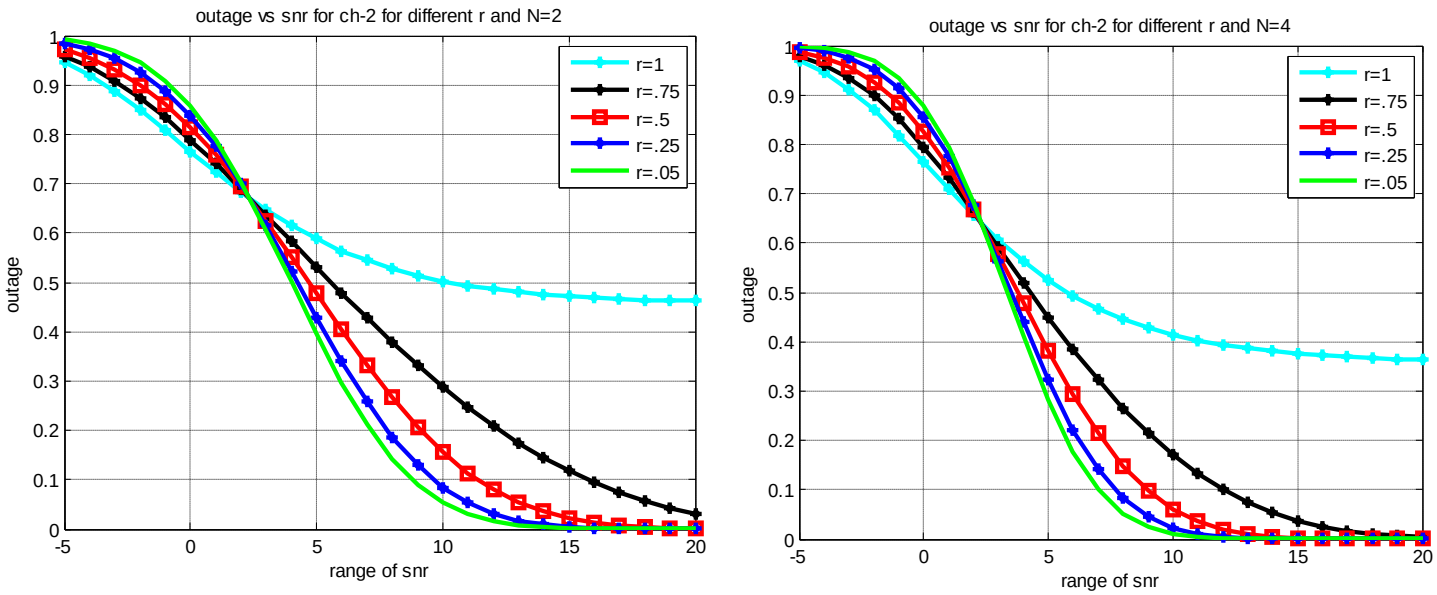

(a) (b)

Fig. 5.11 Outage probability of OSTBC for different multiplexing gains r,CM2 (a) $2x1$ (b), $4x1$

It can be stated further, for a required low outage probability, i.e. high communication reliability, the usage of all transmitting antenna elements is beneficial as shown in figs 5.11.The reliability can be influenced by adjusting the number of utilized antennas only if the communication rate and SNR are fixed. Similar results have been observed over all channel models and number of transmitting antennas as shown in Fig 5.12. Moreover, the performance difference between the various channel scenarios slightly increases the outage probability for a given SNR and spatial diversity, r from CM1 to CM4 correspondingly as shown in Fig.5.12.

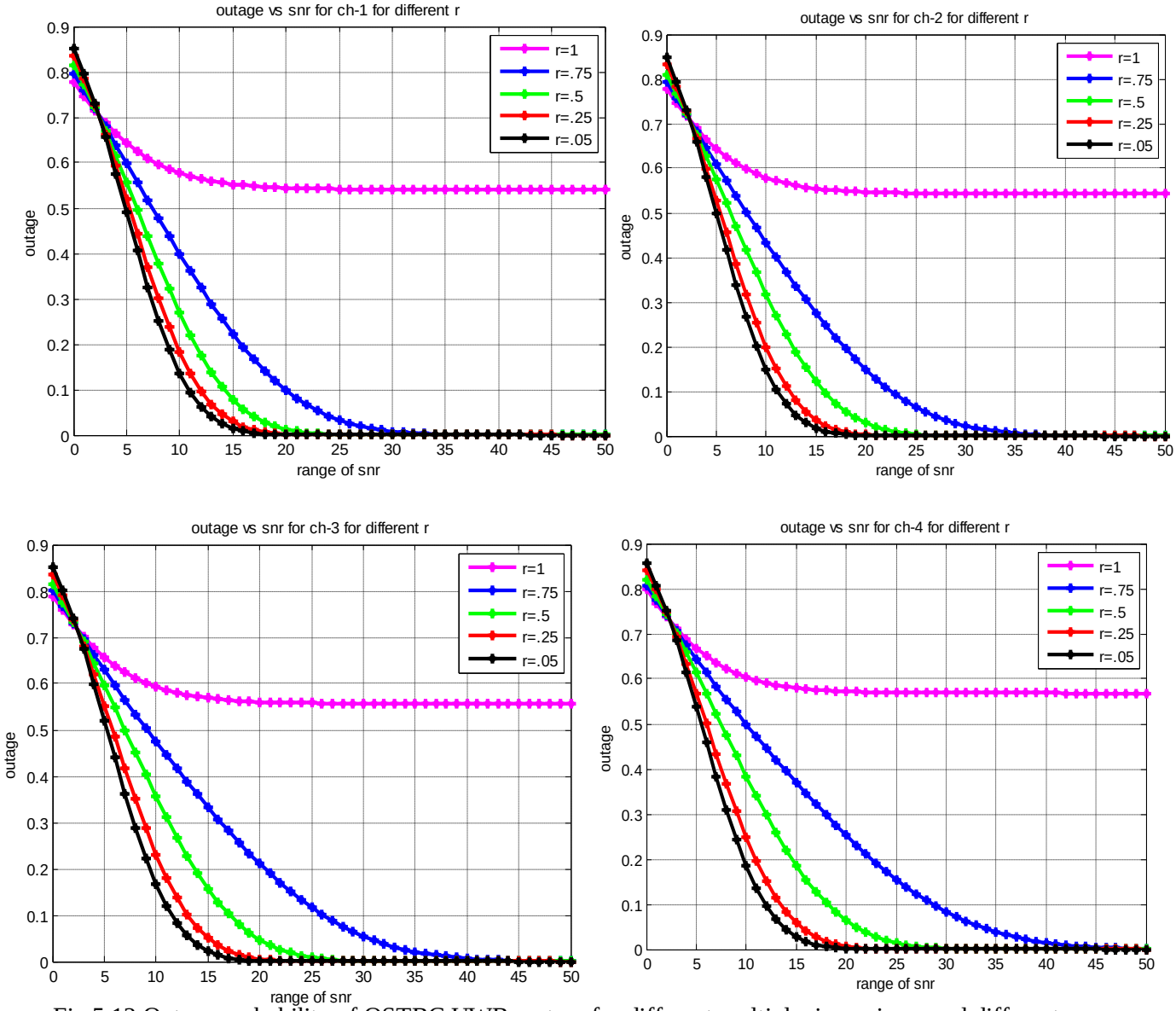

Fig.5.12 Outage probability of OSTBC UWB system for different multiplexing gains r and different channel models with k=2.

5.2 Outage evaluation of multiple antenna systems

5.2.1 Outage evaluation of MISO systems

Outage probability can be used to estimate the diversity gain as a function of SNR and multiplexing gain as described in section 5.1.Fig. 5.20 (a) depicts the outage probability$P_{out}\,(\gamma, r)$versus the $SNR\gamma$in$[dB]$in the UWB channel for a desired multiplexing gain of$r = .25$. The cases where$N = 1,2,3,4$are compared.The curves intersect, indicating that a different number oftransmit antennas should be used dependent upon the SNR so as to minimize

the outageprobability.If a high SNR is availablefor communication, then all elements should be utilized to minimize the outage probability,whereas for low SNR only one element should be used. This indicates transmit diversity gain is only beneficial in the high SNR regimefor improving the outage performance even in UWB. When the SNR of a system is too low, it isbetterto use less transmit antennas.

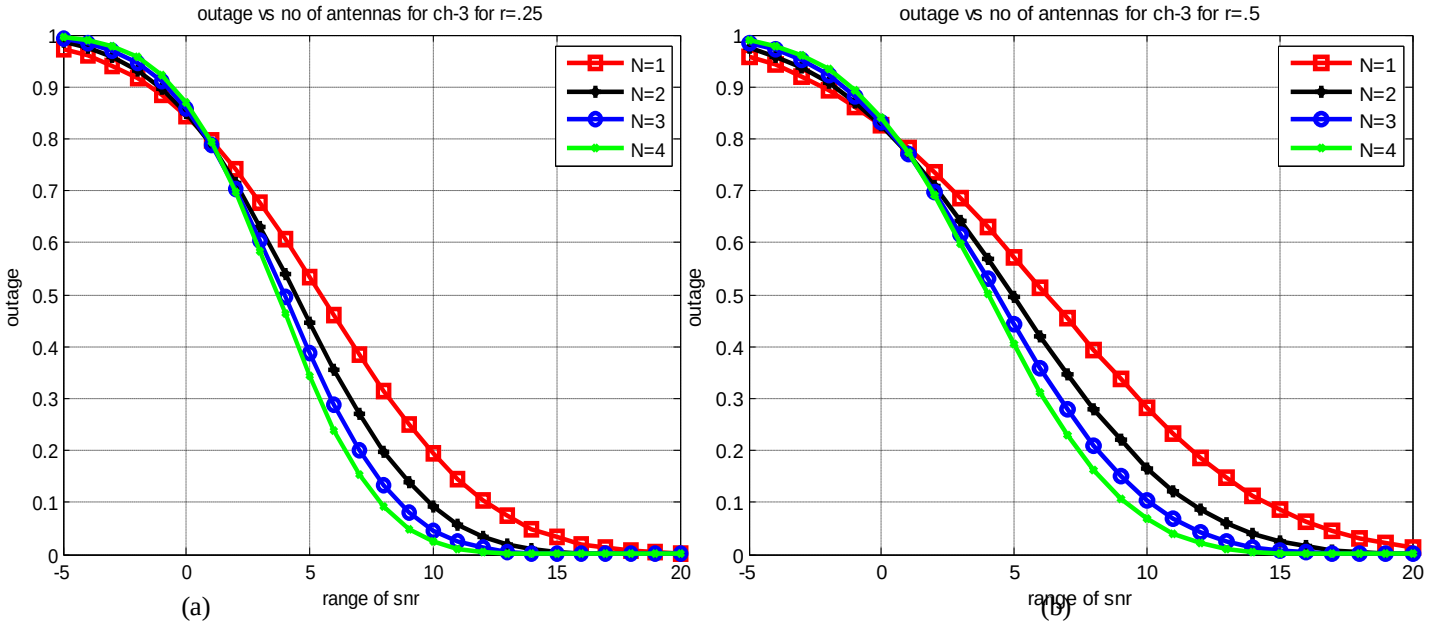

Fig.5.20 Outage probability of MISO systems for CM3 with k=2, $r = 0.25$ and $r = 0.5$

Forinstance, where $r = .25$an available SNR of 10dB yields an outage probability of $(20, 10, 5, 1.5)$ % for $N = (1, 2, 3, 4)$.Moreover, these results show increasingthe number of transmit antennae slightly improves performance; a performance thatdecreases as the number of transmits antennae increase.If, however, the available SNR is only0.25dB, then the behavior of theoutage probability is reversed as depicted in Fig.20(a).It is also illustrated in Fig.5.20 (b),.increasing the multiplexing gain decreases the reliability of the system. An available SNR of 5dB with four transmitting antennas yields outage probability of 40% for multiplexing gain of $r = .5$ while 32% for $r = .25$, 8% and 2% for $SNR = 10dB$ respectively. Therefore we can conclude that there is risein outage probability of OSTBC UWB for a given number of antennas for moderate increment in sensitivity($e.g., r = 0.25\ to\ r = .5$).

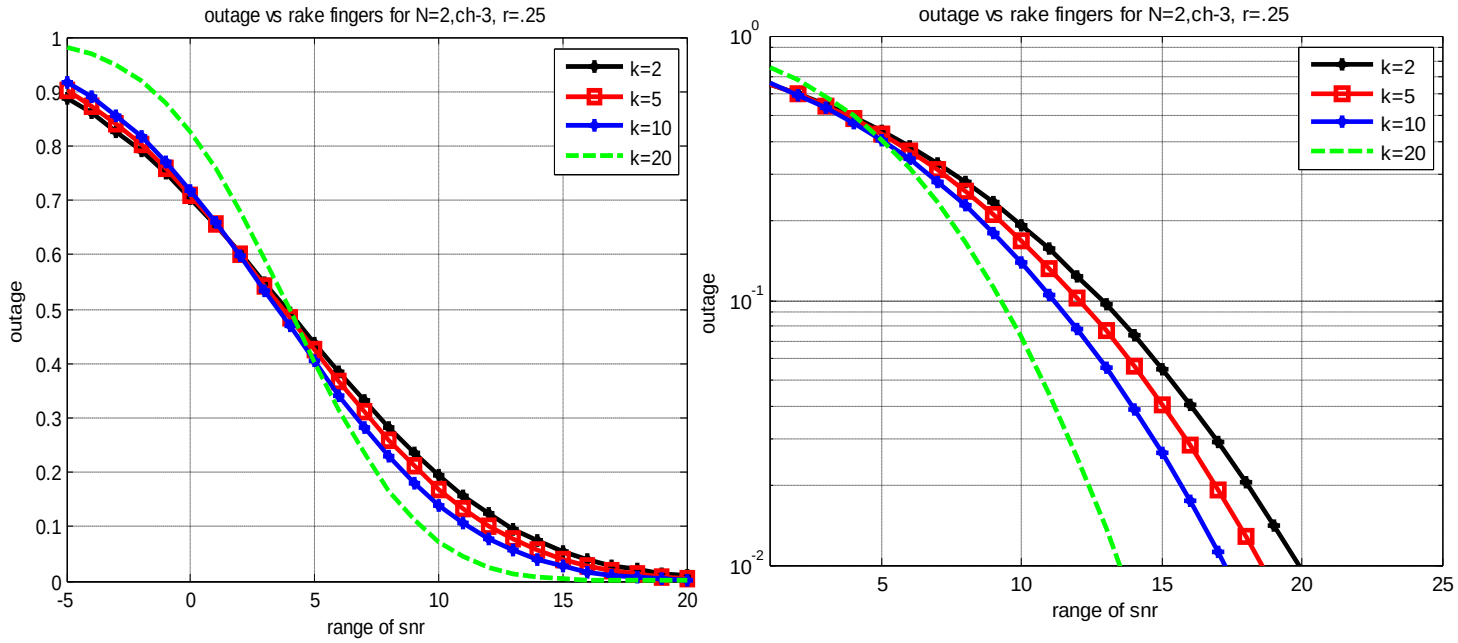

Fig.5.21 Outage of $2X1$system with multiplexing gain $r = 0.25$ and different, No of k for CM3

Results also show that increasing the number of rake fingers decreases the level of SNR per user required to transmit at a given outage. For instance, at an outage of 1%, increasing the number of fingers from 2 to 20, decreases the required SNR by about 13 dB referredin Fig 5.21.

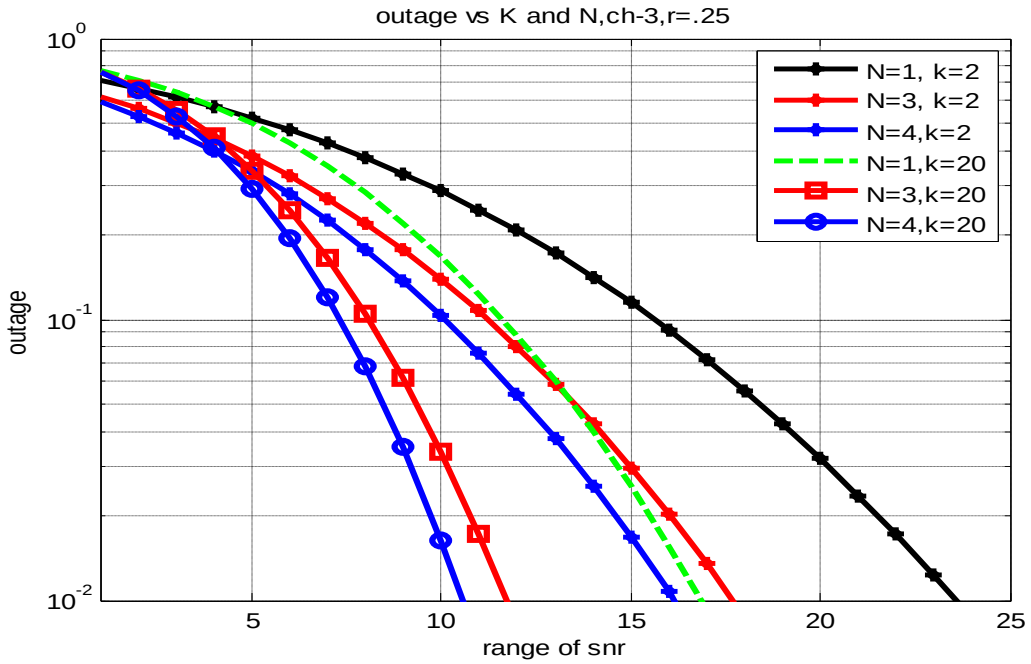

Fig. 5.22 Transmit diversity versus multi-path diversity over CM3

Fig.5.22 above compares 1 × 1 and 3x1and 4x1 systems having thesame overall multiplexing gain.Results show that, despite the inducedrate losses, applying the proposed coding scheme results inimportant performance gains even with systems that profitfrom a high multi-path diversity order $(k = 20)$. Therefore,applying the MIMO techniques can be beneficial in increasingthe diversity advantage of the system.Resultsalso depict that exploiting multi-path diversity by increasing thenumber of Rake fingers is more beneficial at low SNRs. Inthis case, performance is dominated by noise and the energycapture is enhanced by high-order Rakes resulting in betterperformance. For high SNRs, performance is dominated byfading and transmit diversity becomes more beneficial eventhough it does not increase the energy capture. This follows from the fact that consecutive multi-path components of the same sub-channel can be simultaneously faded because of cluster and channel shadowing.

5.2.2 Outage evaluation of SIMO systems

Figs.5.23 below demonstrate the outage probability $P_{out}(\gamma, r)$versus theSNR in $[dB]$ for a desired multiplexing gain of $r = .25$. The cases where $M = (1, 2, 3, 4)$ are compared. Clearly, increasing the number of receive antennas drastically decreases the outage probability of channel for a given SNR.Forinstance, with an SNR of $5dB$, a single receive antenna supports only rates smaller than a rate with $r = .25$ in54% of all cases, whereas four receive antennas support in virtually$\approx 2\%$of allcases only rates smaller than a rate with same spatial multiplexing gain. A reliable communication system is traditionallydesigned to yield an outage probability of less than 10%, i.e. for an SNR of$5dB$ four or three receive antennas suffice.In SIMO channel, increasing the number of receive antennasalways yields performance benefits and for a fixed rate, increasing the number of receiveantennas always decreases the outage, independent of the SNR. Results also show that Even increasing the number of transmit antennae slightly improve performance; a performance thatdecreases as the number of transmit antennae increase, However, increasing thenumber of receive antennae greatly improves performance.

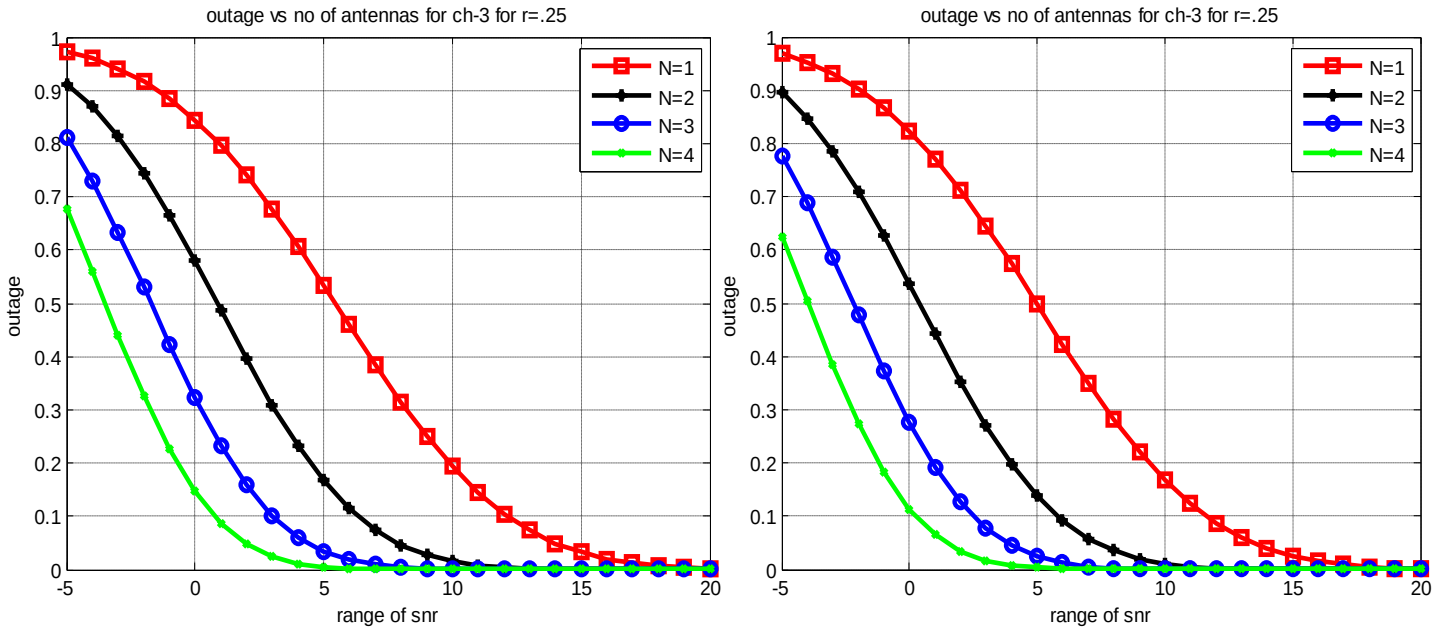

(a) (b)

Fig.5.23 Outage probability of SIMO systems for CM3 with (a) $k = 2$ (b) $k = 5$

The result can further imply that for the same system assumptions, the outage probability is much lower for a SIMO than MISO system withthe same number of antenna elements. From the given plots, in fig.5.20 (a) and 5.23 (a), at an outage of 10%, Alamouti scheme (2x1) is 3.5 dB worsedue to the fact thatthe power radiated from each transmit antenna in theAlamouti scheme is half of that radiated from thesingle antenna and sent to two receive antennas$(1x2)$That can clearly be attributed to the additional noise samples of a SIMO system.

5.3 DMT evaluation of multi antenna systems

For the scalar channelEqn(4.18), with OSTBC scheme, Fig.5.30 describes DMTperformance improvement and comparison of MISO and SIMO systems. DMT as a function of multiplexing gain, and SNR curves are plotted over CM3 with 2 fingersand $\gamma = 15dB$. These tradeoffs can beunderstood in theperspective of rate adaptation in which the data rate is adapted asa function of the SNR, stated in section 5.1.In particular, we compare the DMT of single-antenna systems with that of OSTB coded multi-antenna systems for N = 1, 2, 3 and 4.The result confirms the additional diversity advantages of coded multi-antenna systems with respect to single antenna systems have been observed.

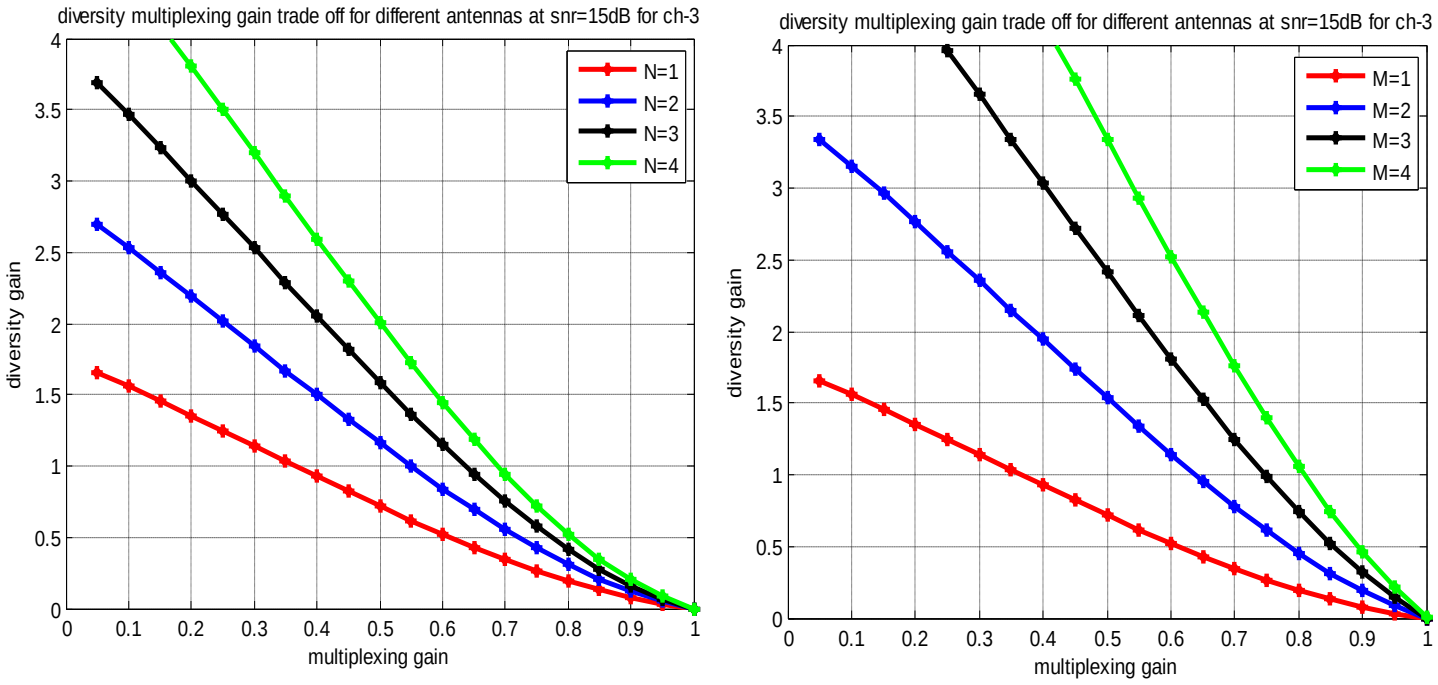

(a) (b)

Fig 5.30 DMT for (a) $N = 1,2,3,4$ and (b) $M = 1,2,3,4$ systems for CM3 and $\gamma = 15dB$

For instance, for 2, 3 and 4 transmit antennas system have a much better DMT tradeoff than a single antenna system with the same number of fingers, k=2.

$d(r,\gamma) = d(0.30,15dB)$ yieldsdiversity order of1.3, 1.8, 2.5 and 3.35 for 1,2,3,4 antennas respectively. This means 38.5% and 92.3% increments of diversity order for 1, 2 additional transmitting antennas while 157.7% increment in diversity order of the system for additional 3 transmitting antennaswith respect to the single antennas.We also confirmedthese tradeoff curves bridges the two extremes: full multiplexing gain and diversity gain as stated in theory.

In Fig.5.30 it is also observed that SIMO systems over performs MISO systems. The performance of Alamouti scheme $(2x1)$ and $3x1$ systems are worse with an order of 0.5, and 1.0 from $1x2$and $1x3$for $r = 0.4$and $\gamma = 15dB$.

An important property of the finite-SNR diversity gain is the limiting behavior asmultiplexing gain approaches zero. This region is most important for diversity gain since at low multiplexing gains, the rate adaptation strategy is not very sensitive to changes in SNR. With this motivation the achievable diversity gain from Eqn (4.27) for r $\rightarrow$ 0 /1 as a function of SNR is given by

$$\lim_{r\to 0} \mathrm{d}(\mathrm{r},\gamma\ ) = \infty \qquad (5.1)$$

$$\lim_{r\to 1} \mathrm{d}(\mathrm{r},\gamma\ ) \approx 0 \qquad (5.2)$$

All UWB systems could attain an infinite diversity order for $r = 0$and the maximal spatial multiplexing gain achieved is just $r = 1$ as depicted abovein Fig.5.30 over CM3. This shows the potential of a multiple antenna channel to support higher degrees of freedom is not also fully exploited by the orthogonal designs in UWB technology because we could attain a multiplexing gain greater than 1.0 for a reliable coding scheme.

The asymptote of the tradeoff curves to the limit as $SNR \to \infty$ of the diversity gain,as a function of SNR from Eqn(4.27) is given by

$$\lim_{\gamma\to\infty} \mathrm{d}(\mathrm{r},\gamma\ ) = \lim_{\gamma\to\infty} \ln(\gamma) = \infty \qquad (5.3)$$

This implies that the asymptotic behavior is reached at very high SNRs but differently performs as $ln(\gamma)$ while asymptotic diversity gain under Rayleigh flat fading wireless channel and Selective-Rayleigh Fading MIMO Channels are $d_{max}(r) = (M - r)(N - r)$and $d_{max}(r) = (LP - r)(Q - r)$where $P = max(M, N), Q = min(M, N)$respectively.This implies that the asymptotic behavior is reached at very high SNRs. However, these SNRs cannot be obtained in practical systems implyingthat the asymptotic regime can never be reached insome situations.

Fig.5.31 below illustrate the DMT of single antenna systems and OSTBC coded multiple antenna systems with N= 1, 2, 3 and M=1, 2, 3 and 2 Rake finger over CM1 for different SNR to give emphasis to results at high SNR region. Theseresults confirm that the diversity gains even for $\gamma = 50\ dB$, equivalently $ln(\gamma) = 10.612\ dB$, does not reach a maximum diversity gain. However this could result an asymptotic behavior over the Rayleigh fading channel [38]. It can also be seen from the tradeoff curves that the available diversity is significantly lower than the high-SNR theoretical limit for practical values of SNR. Of course results from Fig. 5.32 show 3x1 system at SNR 30dB out performs 1x1 at SNR of 50dB indicating the advantage of the multi-antenna systems is evidentespecially at high SNR.

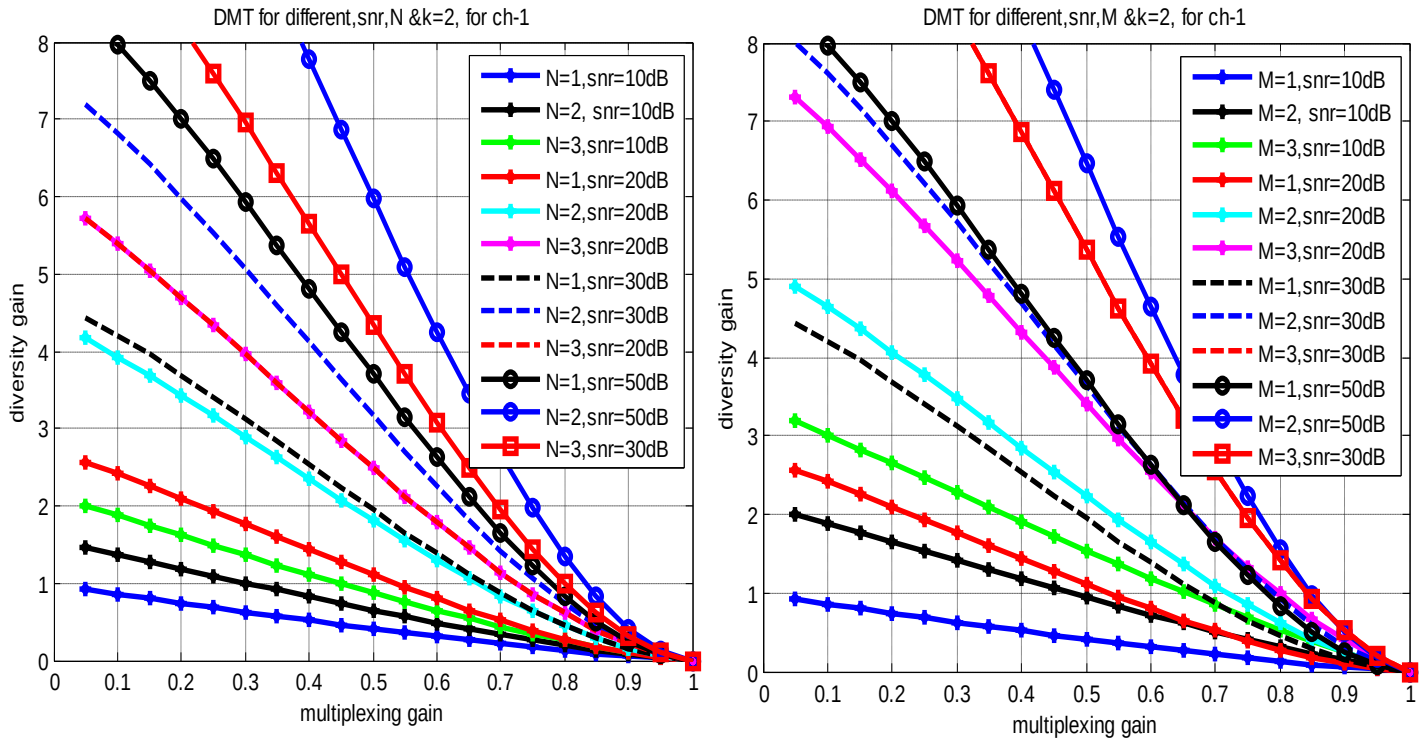

(a) (b)

Fig.5.31 DMT of single antenna systems and OSTBC coded multiple antenna systems with $N = 1, 2, 3$ (b) $M = 1, 2, 3$ over $CM1$ for $k = 2$ and differentSNR.

For system design purposes, it is useful to study:

$$\lim_{\gamma \in SNR < \infty, r > 0} d(r, \gamma) => sub - optimal \qquad (5.4)$$

This point out that maximum diversity gain is achieved, but falls below the optimum tradeoff curve for positive values of r.Therefore; the available diversity is significantly lower than the high-SNR theoretical limit for practical values of SNR. This manifests these codes that are not optimal over the Rayleigh fading channels [38] are also not optimal over the UWB channels.Obviously there is no importance in profiting from the spatial diversity at high SNR by the use of space-time coding techniques. Results shown in Fig. 5.32 (a) and (b) below plotted over CM1 for different $N$and M antennas and SNR confirms non asymptotic behavior for some controlled SNR, say $= 30dB$ .However, the advantage of the multi-antenna systems is againapparent.

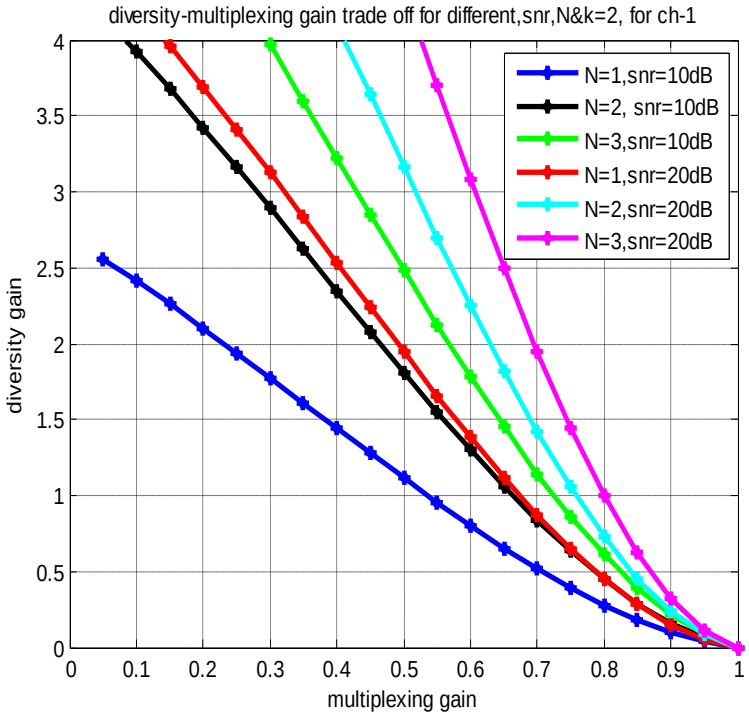

(a)

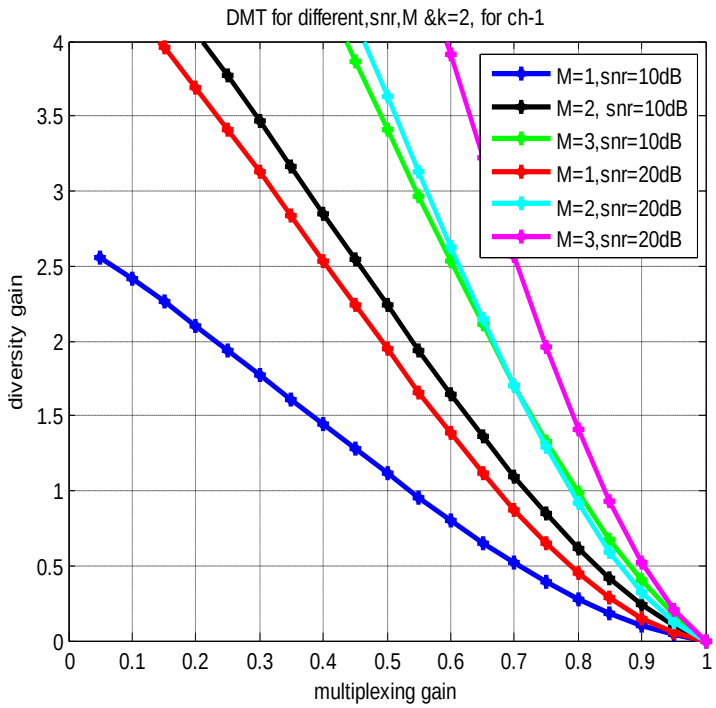

(b)

Fig.5.32$DMT\ for\ (a)\ N = 1, 2, 3\ \ (b)\ M = 1, 2, 3$ over $CM1$ for different SNR

Even increasing Rake fingers have a much better DMT tradeoff than a single antenna system, increasing the numberof transmit antennas can be more beneficial than increasing thenumber of Rake fingers. This is depicted in Fig.5.33. The DMT is superior for 2x1 with 5 fingers compared to 1x1 with10 fingers. Notice also that the benefit provided by the diversity order does not increase proportionally with the tap number k due to the exponentially decaying power delay profile in UWB channels.Similar results are obtained over CM1, CM2, CM3 and CM4 in each scenario.

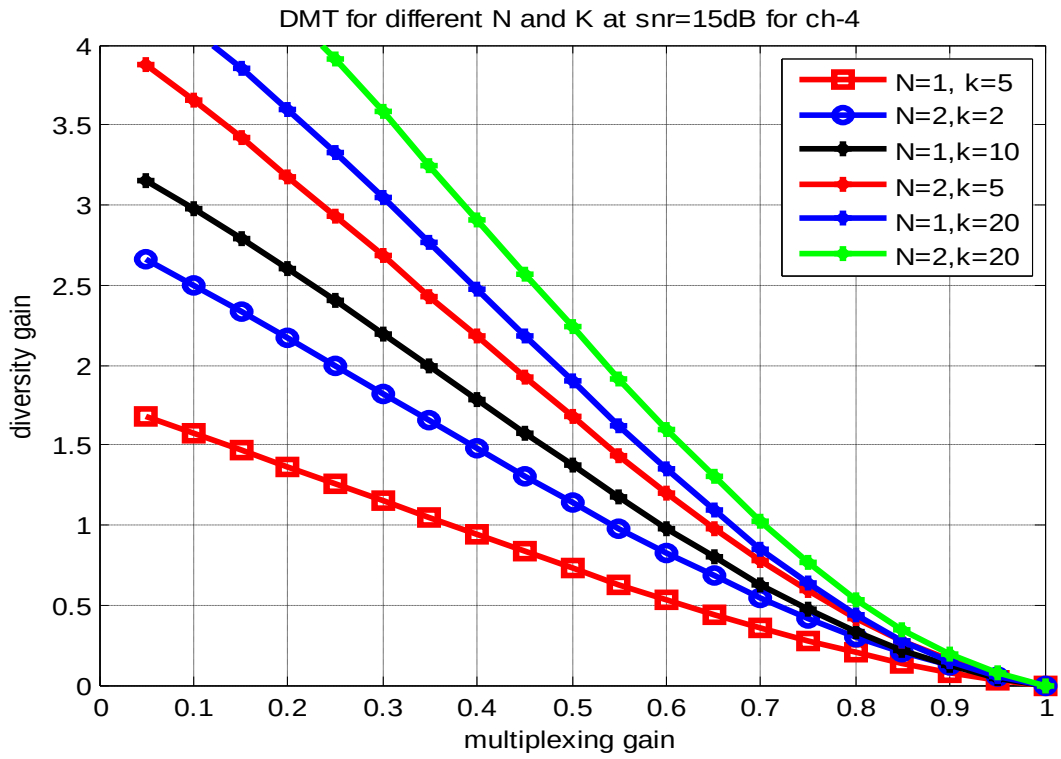

Fig. 5.33DMT Transmit antennas versus multi-path over CM4

Chapter 6

Conclusions and recommendation

6.1 conclusions

Ultra-wideband (UWB) communication is an emerging technology for wireless transmission inthe 3.1-10.6 GHz unlicensed band with signal bandwidth of 500 MHz or greater.Ultra-wideband (UWB) is one of the emerging technologies that can fulfill next generation network requirements. The enormous bandwidths available, the potential for the data rate, and the potential for very low cost operation makes UWB technology a viable candidate for current and future wireless applications.Having this all, the combination of ultra-wideband (UWB) spectrum with Multiple-Input Multiple-Output (MIMO) system techniques show great promise for developing very high bandwidth and reliable next generation wireless networks such as wireless personal area networks (WPANs).

Previous research on multiple antennas channels, especially the design of the coding schemes, such STBC and BLAST families is split into two different branches, focusing either on extracting the maximal diversity gain or the maximum spatial multiplexing gainrespectively.But recently a new point-of-view for a given multiple antenna system; both the diversity gain and the multiplexing gain can be simultaneously achieved,but there is a fundamental tradeoff between how much of each type of gain any coding scheme can achieve.The diversity-multiplexing tradeoff can be used as a new performance metric tocompare different schemes. The tradeoff curve provides a more complete view of the problem than just looking at themaximal diversity gain or the maximal spatial multiplexing gain.

A general design approach for the STBC of IR-based UWB systems with arbitrary numbers of transmit and receive antennas is presented. This designapproach (STC scheme) is based on the concept of ROD proposed in[22].A nonasymptotic framework is presented to analyzethe diversity–multiplexing tradeoff of a multiple-antenna systems (SIMO/MISO) wireless system with OSTBC scheme at finite signal-to-noiseratios (SNRs). The target data rate at each SNR is proportional tothe capacity of an additive white Gaussian noise (AWGN) channel. The proportionality constant, which can beinterpreted as a finite-SNR spatial multiplexing gain, dictates thesensitivity of the rate adaptation policy to SNR. The diversity gainas a function of

SNR for a fixed multiplexing gain is defined bythe negative slope of the outage probability versus SNR curve on alog-log scale.

Based on these definitions, diversity gains arecomputed as functions of set of the multiplexing gain for OSTBC. The diversity-multiplexing tradeoff analysis showsthat achievable diversity gains are significantly lower at operational SNR's than the conventional asymptotic values for SNR,$\gamma \to \infty$. This finite-SNR analysis provides insight todesign space-time codes optimized for realistic operating SNR andchannel conditions particularly for UWB systems which are required to operate in the low SNRrange.We found that these tradeoffs areunlikefrom those achieved over the Rayleigh fading channel. Inparticular, an infinite diversity order can be achieved even withsingle-antenna systems. The diversity advantages or outage probabilityvarywith $ln(\gamma)$, for very large values of theSNR implying that the asymptotical regime can be neverreached in practical systems while the UWB systems are required to operate in the low SNRrange. Consequently, the superiority ofthe multiple antennas in UWB systems was revealed for the controlled valuesof the SNR. For instance, 3x1 systems at SNR 30dB, 20dB outperform 1x1 at SNR of 50dB, 30dB respectively.

It is also illustrated that increasing the number of transmit antennae slightly improve performance; a performance thatdecreases as the number of transmit antennae increase. However, increasing thenumber of receive antennae greatly improves performance. If the available SNRis too low, then it is better to concentrate the available power on a single antenna or asingle symbol to transmit the information data than to distribute the power across multipleantennas or symbols to gain the diversity; while multiple antennas at the receiver.The reason behind this fundamental compromise can be deduced from an extreme casewhere the available SNR is so low that we cannot correctly receive one single bit in agiven period if we distribute the low energy across multiple antennas or symbols, whilewe can correctly receive several bits in the given period if we use only one antenna orspend the whole power on one single symbol to transmit.

For a given diversity order, increasing the numberof transmit/receive antennas can be more beneficial than increasing thenumber of Rake fingers. We can also conclude finite SNRs are important in analyzing the diversity–multiplexing tradeoff of MAS in realistic environments even in UWB.

OSTBCs have a much smaller spatial multiplexing rate than Spatial Multiplexing schemes. But since UWB has large bandwidth OSTBCsmight be critical scheme to improve the quality of the system for a given high data rate.

6.2 Recommendations for Future Work

The promising results of this thesis work led to expanding the thesis limits and widening the scope of the simulation to include the following possible approaches for future development. In this research, many important issues have not been dealt with, or have been considered tosimplified assumptions. Hence, there are some areas in which the work of this thesis can be extended.

- *Impact of channel estimation and time synchronization:* In this thesis, simulations have been carried out assuming that the receiver has perfect channel knowledge and perfect time synchronization between the transmitter and receiver which deviates from the practical.Thus, the impact of channel estimation and time synchronization errors on the system performance is another research area that needs further study.
- *Equalizers and computational complexity:* In this thesis, outage and DMT performance of multiple antenna systems for Rake receivers is evaluated for different system parameters without considering equalizers at the receivers.we avoid Inter-Frame Interference (IFI),and therefore Inter Symbol Interference (ISI), exceeding T_f from the UWB channel maximum delay-spread.Hence, analysis for outage and DMT implementatingchannel equalizer which need be equalized over both space and time, can be used to mitigate the effects of ISIat the receivers could be another research area.
- *Evaluation of Existing Schemes:*The diversity-multiplexing tradeoff can be used as a new performance metric to compare different schemes. Using the tradeoff curve to evaluate the performance of several well-known space-time schemes such as Space-time Trellis Coding (STTC), V-BLAST, and D-BLAST could be another research area.

Reference

[1]T. W. Barrett \History of UltraWideband (UWB) radar and communications: Pioneers and innovators," Proc. of Progress in Electromagnetics Symposium ,Cambridge, MA, Jul. 5-14, 2000.

[2] Federal Communications Commission Rep ort \Revision of Part 15 of the Commission's Rules Regarding Ultra-Wideband Transmission Systems, First Rep ort and Order ", Federal Communications Commission, Washington DC, ET-Docket 98-153, Feb. 2002.

[3] Thomas Kaiser, Ian Oppermann, et.al, UWB Communication Systems A Comprehensive Overview, EURASIP Book Series on Signal Processing and Communications, Volume 5,Hindawi Publishing Corporation ,2006,

[4]K. J. Ray Liu, et.al, Ultra-Wideband Communications Systems Multiband OFDM Approach, A john wiley& sons, inc., publication, 2008.

[5],Boris Lembrikov et.al,Ultra Wideband, Sciyo, Janeza Trdine9, 51000 Rijeka, CroatiaSeptember 2010.

[6] IEEE 802.15.SG3a for use as a method to evaluate the physical layer performance of proposals submitted to the IEEE 802.15.3a task group

[7] J. G. Proakis, Digital Communications, 4th Ed., McGraw-Hill, New York, 2001.

[8] A. J. Paulraj, et.al An overview of MIMO communications a key to gigabit wireless. Proc. IEEE , 92: 198 – 218, 2004

[9]EWC. HT PHY specification, Enhanced Wireless Consortium publication, 2005. version V1.27, Avail-able: http://www.enhancedwirelessconsortium.org/home/EWC MAC spec V124.pdf.

[10]Jeffrey H. Reed, An Introduction to Ultra Wideband Communication Systems, Prentice Hall PTR , April 05, 2005.

[11] H. KhaleghiBizaki et.al, MIMO Systems, Theory and Applications,JanezaTrdine 9, 51000 Rijeka, Croatia,2011.

[12] Xuemin (Sherman) Shen .et.al, Ultrawide band wireless communication and networks,John Wiley & Sons Ltd,2006.

[13]SavoGlisic,Advanced Wireless Communications 4G Technologies, University of Oulu, Finland, John Wiley & Sons Ltd, 2004.

[14] Maria-Gabriella Di Benedetto, GuerinoGiancola understanding ultra wide bands radio fundamentals, Prentice Hall PTR, 2004.

[15] James D. Taylor, P.E.et.al, Ultra wide band Radar Technology, CRC Press LLC, 2001

[16] Tolga M. Duman, Ali Ghrayeb , Coding for MIMO Communication Systems, John Wiley & Sons Ltd, 2007.

[17]M. Ghavami, L. B. Michael, R. Kohno Ultra Wideband Signals and Systems in Communication Engineering, John Wiley & Sons, Ltd, 2004.

[18] C. Holland. Europe approves UWB regulations. EE Times Europe, 3 May 2007. http://eetimes.eu/showArticle.jhtml?articleID = 197800214.

[19] C.-C. Chong,et.al, Potential of UWB technology for the next generation wireless communications. 2006 IEEE 9th Int. Symp. on Spread Spectrum Techniques and Applications , Amazon, Brazil, 28 – 31 Aug. 2006

[20] HomayounNikookar, Ramjee Prasad, Introduction to Ultra Wideband for Wireless Communications, Springer Science and Business Media B.V., 2009

[21] EUWB consortium, Ultra-Wideband: Past, Present and Future, White Paper, 2011-10-10

[22] Claude Oestges and Bruno Clerckx, MIMO wireless communications, from real-world propagation to space–time code design, Elsevier Ltd, 2007.

[23] David Tse, PramodViswanath, Fundamentals of Wireless Communication, 290-425, Cambridge University Press ,2005

[24]L.Yang and G. B. Giannakis, “Analog space-time coding for multi-antenna ultra-wideband transmissions,” IEEE Trans.

[25] LizhongZheng and David N. C. Tse, “Diversity and Multiplexing: A Fundamental Tradeoff in Multiple-Antenna Channels”, IEEE Transac-tions On Information Theory, Vol. 49, No. 5, May 2003.

[26] S. M. Alamouti, "A simple transmit diversity technique for wireless communications," IEEE J. Sel. Areas in Comm., vol. 16, no. 8, pp. 1451 – 1458, Oct. 1998

[27] V. Tarokh, N. Seshadri, and A. R. Calderbank, "Space-time codes for high data rate wireless communication: Performance criterion and code construction," IEEE Trans. Inf. Th., vol. 44, no. 2, pp. 744–765, March 1998

[28] David Gesbert et.al, From Theory to Practice: An Overview of MIMO Space–Time Coded Wireless Systems, IEEE journal on selected areas in communications, vol. 21, no. 3, april 2003.

[29] BrankaVucetic, Jinhong Yuan , Space-Time Coding, John Wiley & Sons Ltd, 2003.

[30]S. Cherry. Edholm's law of bandwidth. IEEE Spectrum, 41(7): 58 – 60, 2004.

[31] EnzoBaccarelli et.al, Optimal MIMO UWB-IR Transceiver for Nakagami-fading and Poisson-Arrivals, journal of communications, vol. 3, no. 1, january 2008.

[32] Thomas Kaiser, FengZheng, Emil Dimitrov: "An overview of ultra-wide-band systems with

MIMO", Proceedings IEEE, vol. 3 (2), pp. 285–312, Feb. 2009.

[33]EnzoBaccarelli et.al,Optimal MIMO UWB-IR Transceiver for Nakagami-fading and Poisson-Arrivals,journal of communications, vol. 3, no. 1, January 2008.

[34]ChadiAbou-Rjeily,Norbert Daniele et.al,Space–Time Coding for Multiuser Ultra-Wideband Communications,ieee transactions on communications, vol. 54, no. 11, November 2006.

[35] ChadiAbou-Rjeily, Jean-Claude Belfiore, On Space–Time Coding With Pulse Position and Amplitude Modulations for Time-Hopping Ultra-Wideband Systems,ieee transactions on information theory, vol. 53, no. 7, july 2007

[36] W. Pam Siriwongpairat et.al , Performance Analysis of Time Hopping and Direct Sequence UWB Space-Time Systems,University of Maryland, College Park, MD 20742, USA.

[37] Muhammad Gufran Khan.et.al, Performance Evaluation of RAKE Receiver for UWB Systems using Measured Channels in Industrial Environments, Blekinge Institute of Technology, SE-372 25 Ronneby, Sweden

[38] Ravi Narasimhan et.al, Finite-SNR Diversity-Multiplexing Tradeoff of Space-Time Codes,IEEE, 2005.

[39]A. Papoulis, Probability, Random Variables and Stochastic Processes", New York: McGraw-Hill, 1991.

[40] Jingxian Wu et.al, A Flexible Lognormal Sum Approximation Method, Mitsubishi Electric Research Laboratories, Inc., 2005.

[41] Huaping Liu, Error Performance of a Pulse Amplitude and Position Modulated Ultra-Wideband System Over Lognormal Fading Channels,ieee communications letters, vol. 7, no. 11, november 2003.

[42] Sebastian S.et.al, Fitting the Modified–Power–Lognormal to the Sum of Independent Lognormals Distribution,Ottawa, Ontario, Canada.

[43] J. Zhang, R. A. Kennedy, T. D. Abhayapala, Performance of RAKE Reception for Ultra Wideband Signals in a Lognormal-fading Channel,Australian National University, Canberra ACT 0200, Australia.

[44] J. R. Foerster, "The performance of a direct-sequence spread ultra-wideband system in the presence of multipath, narrowband interference, and multiuser interference," IEEE Conference on Ultra Wideband Systems and Technologies, May 2002

[45] M. Z. Win and R. A. Scholtz, "Impulse radio: how it works," IEEE Communications Letters, Vol. 2, No. 1, pp. 10-12, January 1998.

[46] S.Ali Ghorashi.et.al, An over view of MB-UWB OFDM, center of telecommunication research, King's college, London,2004.

[47]HomayounNikookar, Ramjee Prasad, Introduction to Ultra Wideband for Wireless Communications,Springer Science + Business Media B.V, 2009

[48] C. Tellambura, D. Senaratne, Accurate Computation of the MGF of the Lognormal Distribution and its Application to Sum of Lognormals. ieee transactions on communications, vol. 58, no. 5, may 2010

[49]Li-Chun Wang, and Wei-Cheng Liu, Bit Error Rate Analysis in IEEE 802.15.3a UWB Channels, ieee transactions on wireless communications, vol. 9, no. 5, may 2010 [lognormal recei energy]

[50] G. J. Foschini, Layered space-time architecture for wireless communication in a fading environment when using multi-element antennas," Bell Labs Technical Journal, pp. 41-59, 1996

[51] Muhammad Gufran Khan, et.al, Performance Evaluation of RAKE Receiver for UWB Systems using Measured Channels in Industrial Environments, Blekinge Institute of Technology, Sweden, May 26, 2008.

[52] Comparison between Coherent and Non-coherent Receivers for UWB Communications, EURASIP Journal on Applied Signal Processing 2005

[53]J. Zhang et.al,International Journal of Wireless Information Networks, Vol. 10, No. 4, October 2004

[54] Andrea Goldsmith, WirelessCommunications,Cambridge University Press, 2005

[55]John D.et.al., Performance of Ultra-Wideband Communicationswith Suboptimal Receivers in Multipath Channels,ieee journal on selected areas in communications, vol. 20, no. 9, december 2002.

[56] Pedro Coronel and Helmut Bolcskei, Communication Technology Laboratory, ETH Zurich, 8092 Zurich, Switzerland, Diversity-Multiplexing Tradeoff in Selective-Fading MIMO Channels.

[57]JunshengLiu,.et.al Ben Allen and Wasim Malik, Diversity Analysis of Multi-antenna UWB Impulse Radio Systems with Correlated Propagation Channels, University of Oxford Parks Road Oxford, UK, 2006